MULTIFACETED STUDY OF AN AREA OF MAINLY DIORITIC ROCKS IN THE SOUTHERN CAPE BRETON HIGHLANDS, NOVA SCOTIA

KEITH A. JOHNSTON

Honours Thesis
Department of Geology
Dalhousie University
March 1984

DALHOUSIE UNIVERSITY
Department of Geology
Halifax, N.S. Canada B3H 3J5 Telephone (902) 424-2358 Telex: 019-21863

DALHOUSIE UNIVERSITY, DEPARTMENT OF GEOLOGY

B.Sc. HONOURS THESIS

Author: Keith A. Johnston

Title: Multifaced Study of an Area of Mainly Dioritic Rocks in the Southern Cape Breton Highlands, Nova Scotia.

Signature of author

Date: April 19/84

Department of Geology
Dalhousie University
Halifax, N. S.

Distribution License

DalSpace requires agreement to this non-exclusive distribution license before your item can appear on DalSpace.

NON-EXCLUSIVE DISTRIBUTION LICENSE

You (the author(s) or copyright owner) grant to Dalhousie University the non-exclusive right to reproduce and distribute your submission worldwide in any medium.

You agree that Dalhousie University may, without changing the content, reformat the submission for the purpose of preservation.

You also agree that Dalhousie University may keep more than one copy of this submission for purposes of security, back-up and preservation.

You agree that the submission is your original work, and that you have the right to grant the rights contained in this license. You also agree that your submission does not, to the best of your knowledge, infringe upon anyone's copyright.

If the submission contains material for which you do not hold copyright, you agree that you have obtained the unrestricted permission of the copyright owner to grant Dalhousie University the rights required by this license, and that such third-party owned material is clearly identified and acknowledged within the text or content of the submission.

If the submission is based upon work that has been sponsored or supported by an agency or organization other than Dalhousie University, you assert that you have fulfilled any right of review or other obligations required by such contract or agreement.

Dalhousie University will clearly identify your name(s) as the author(s) or owner(s) of the submission, and will not make any alteration to the content of the files that you have submitted.

If you have questions regarding this license please contact the repository manager at dalspace@dal.ca.

Grant the distribution license by signing and dating below.

_____ _____

Name of signatory Date

TABLE OF CONTENTS

CHAPTER 1

INTRODUCTION

Regional Geology

The geology of the Cape Breton Highlands is complex and generally poorly understood. However, recent work by Jamieson (1981), Jamieson and Craw (1983) and Jamieson and Doucet (1983) has resulted in a summary of the general geology. Precambrian rock units include deformed plutonic rocks (granitic to ultramafic), paragneisses and orthogneisses, metasedimentary and metavolcanic rocks. Younger rock units include undeformed granitic rocks, volcanics, sedimentary rocks of the Horton and Windsor groups and miscellaneous granitic to dioritic rocks (Figure 1.1).

In the southern Highlands, there seem to be two main phases of tectonic activity, the first in the late Proterozoic and the second in the Devonian to Carboniferous (Jamieson, in press). The first episode is expressed by metamorphism resulting in gneisses and intrusion of diorites. Gneisses occur over much of the Highlands and include orthogneiss and paragneiss varieties. Ages of 701 $\pm$ 66 Ma (Olszewski et al., 1981) for the Kelly's Mountain gneiss complex and 752 $\pm$ 26 (Jamieson, in press) for the Baddeck Lakes diorites, from Rb-Sr dating, represent a metamorphic age and an igneous age respectively, for events associated with this tectonism (Figure 1.2). Evidence of this activity is also apparent in George River Group metasedimentary and metavolcanic rocks (Milligan, 1970). The second episode of tectonic activity important here is that of the Acadian orogeny.

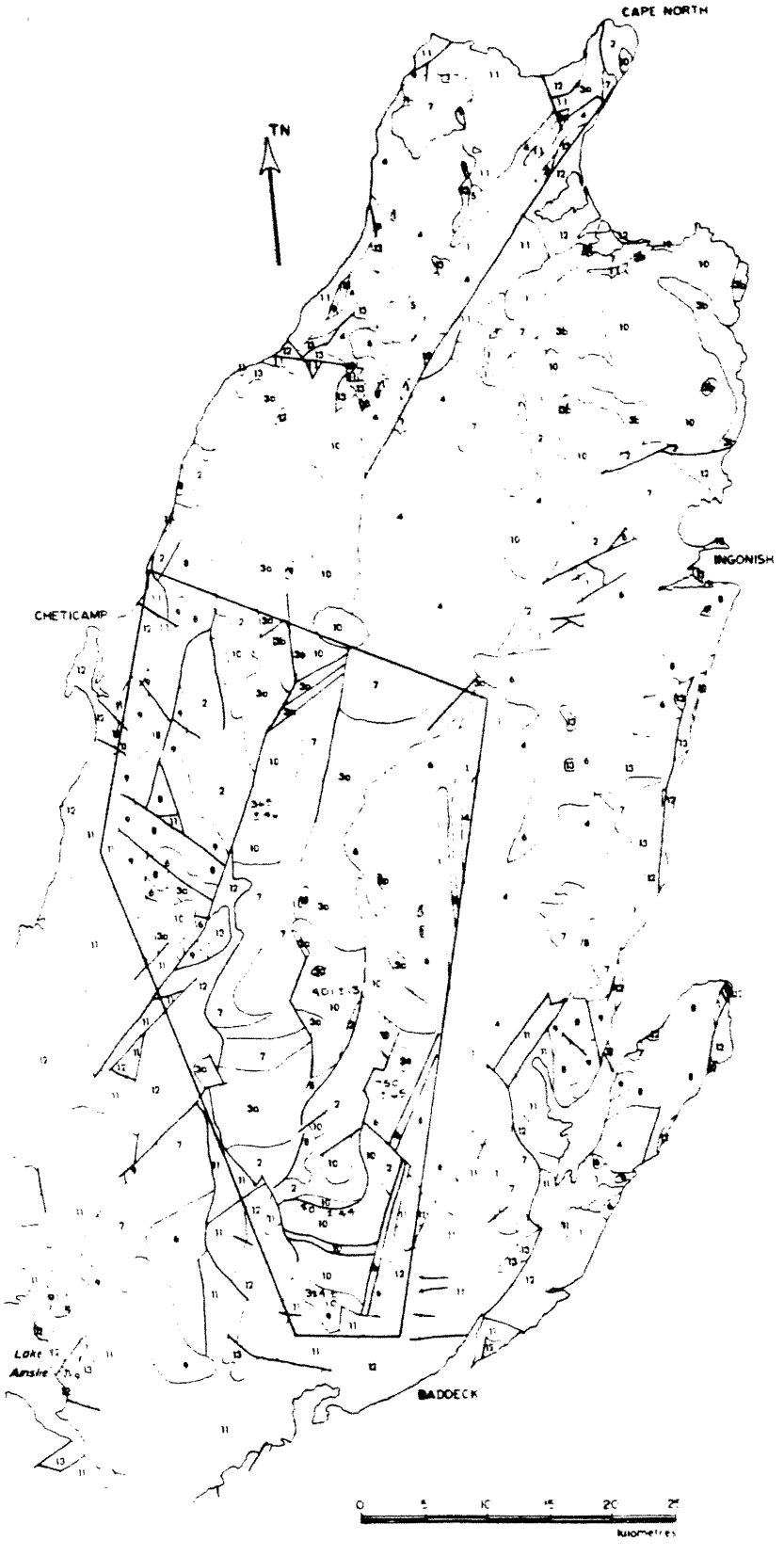

LEGEND

UNKNOWN AGE

13. Miscellaneous granitic to dioritic rocks.

CARBONIFEROUS

12. Undifferentiated younger sedimentary rocks, including Windsor Group.

11. Horton Group and its Lower Mississippian equivalents.

DEVONIAN – CARBONIFEROUS

10. Undeformed granitic rocks, locally associated with gabbro and diorite.

9. Fisset Brook Formation and its equivalents.

LOWER PALEOZOIC (CAMBRIAN – SILURIAN)

8. Unfoliated granitic rocks.

LATE PRECAMBRIAN

7. Foliated granitic rocks.

6. Variable deformed dioritic and gabbroic rocks, including minor ultramafic rocks.

5. Anorthosite.

4. Undivided gneisses, possibly equivalent to or older than unit 3.

3. Gneiss complex, high grade equivalent of unit 2.

   3a – paragneiss

   3b – orthogneiss

2. Unnamed meta-igneous and meta-sedimentary complex.

1. George River Group metasedimentary rocks.

Figure 1.1 Geology of the Cape Breton Highlands after Keppie (1979), modified by Jamieson and Craw (1983). Modifications based on data from Jamieson (unpublished), Jamieson and Doucet (1983), Blanchard (1982), Barr and Macdonald (1982) and dates from Jamieson (in press).

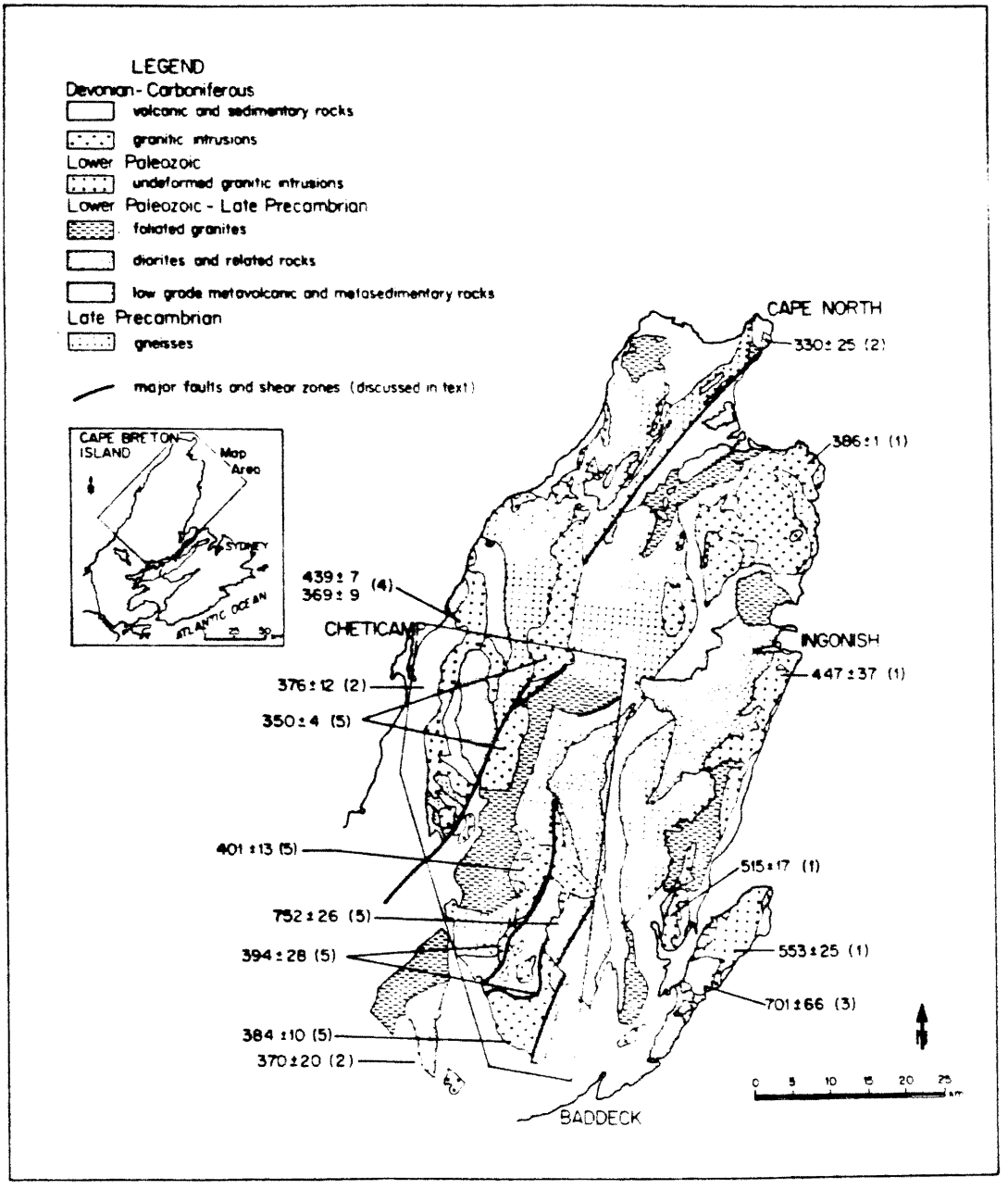

Figure 1.2 General geology of the Cape Breton Highlands after Jamieson (in press), modified from Keppie (1979) and Jamieson and Craw (1983), showing recently obtained radiometric dates. Sources: (1)Recalculated by Keppie and Smith (1979) from Cormier (1972); (2)Keppie (1979) and Keppie and Smith (1978); (3)Olszewski et al. (1981); (4)Currie et al. (1982); (5)Jamieson (in press).

Intrusion of the North River Monzogranite (401 ± 13 Ma) and formation of the Muskrat Brook/Sarach Brook mylonite zones (394 ± 28 Ma, Jamieson, in press) are manifestations (Figure 1.2). An Acadian overprint can be identified on many older rocks and it has been proposed (Jamieson, in press) that the mylonite zone represents the southernmost extent of this overprint.

Subsequent tectonic activity has resulted in extensive faulting, granitic intrusion and various volcanic activity. Ages younger than that of the Acadian orogeny have been acquired and appear on Figure 2. There are numerous rock bodies that have yet to be dated so the picture is far from complete. Also, much interpretation of existing ages, in terms of tectonism, is lacking.

When an age is acquired, the problem remains to interpret its meaning. An age only indicates the time since measurable radiogenic isotopes last began to accumulate in the rock. A metamorphic disturbance can start the process over again and an age determination of highly metamorphosed rocks will be the time since metamorphism. For igneous rocks, it must be determined how major a factor metamorphism has been and whether an obtained age is representing igneous crystallization or metamorphism. Therefore, if an igneous age is desired, the most undeformed, unmetamorphosed samples must be chosen for dating. It is also necessary to avoid alteration in rocks chosen, for anything that changes the chemistry subsequent to crystllization can alter the age determination.

It was decided that a region of mainly dioritic rocks centered nine kilometers north of the Baddeck Lakes would be the focus of this

study. The diorites to tonalites are in contact with older units of gneiss and quartzite to the west and east, respectively. Minor felsic pegmatites also exist in the area. This diorite intrusion has been tentatively linked to the Baddeck Lakes Diorite further south which has been dated by Jamieson (in press)(Figure 2). The age (752 ± 26 Ma) has been interpreted as an igneous age.

Purpose of Study

The area chosen for multifaceted study was outlined to adequately represent the diorite intrusion of interest (Figure 2). Although shown as a northern extension of the Baddeck Lakes Diorite on most maps, the relationship is not known with certainty. It is hoped that with this study, the relationship will be better understood. The Baddeck Lakes Diorite have been studied by Jamieson (1979-1983) and samples, thin sections and data are available for comparison.

A further contribution of this study is an age determination connected with the dioritic rocks. This may aid in the comparison of the two regions of diorite as well as being a contribution to the collective age dating of the Cape Breton Highlands, and therefore an aid in regional tectonic interpretation.

Detailed study of this area serves as an account available for reference and, added to efforts of other workers, aids in an understanding of its place in the tectonic evolution of the region.

Approach

Samples were collected and notes made concerning lithologies and contact relations, in several days of field work. A complete petrographic study was undertaken using thin sections from these samples in addition to several previously available from the study area (Jamieson, 1981-1982). A microscope stage mounted point counter was used to determine modal mineral percentages. Mineral analysis was performed using the Electron Microprobe and with the assistance of R. MacKay, computer programs were used to perform recalculations from oxide percentages to unit formula atomic proportions.

Geochronologicial work was done for argon-argon dating with a mass spectrometer operated by K. Taylor, who also is the creator of the computer program that performed the calculations necessary for age determination and drew the plots that are represented here.

CHAPTER 2

FIELD WORK

Introduction

An area approximately eight by ten kilometers was chosen based on access and coverage considerations. Major, well travelled, logging roads provide access and branch roads, less well maintained, provide relatively even coverage, although constrained by topography (Figure 2.1). The region consists of highlands of less than 1500 meters elevation, cut by numerous steep stream valleys. The general trend of major stream valleys has an azimuth of slightly west of north. A number of highland lakes occur in the eastern half of the study area, the largest being Timber Lake.

The study area was known to contain predominantly diorite in close proximity to gneisses and quartzites providing the opportunity to determine the relationship of the diorite to these metasedimentary rock units.

The highland area is heavily vegetated with secondary growth of raspberry and other low level shrubs among dead tree remains left from extensive logging operations (Photo 2.1). The steep stream valleys are thickly vegetated with a variety of taller trees and ground flora. Exposure is, therefore, very poor in the valleys with outcrops existing only in steep portions of streams. More accessible outcrops occur infrequently along the logging roads, where bedrock is cut. To provide better representation pseudo-outcrops, fractured loose rock probably in place, were treated, with reservation, as

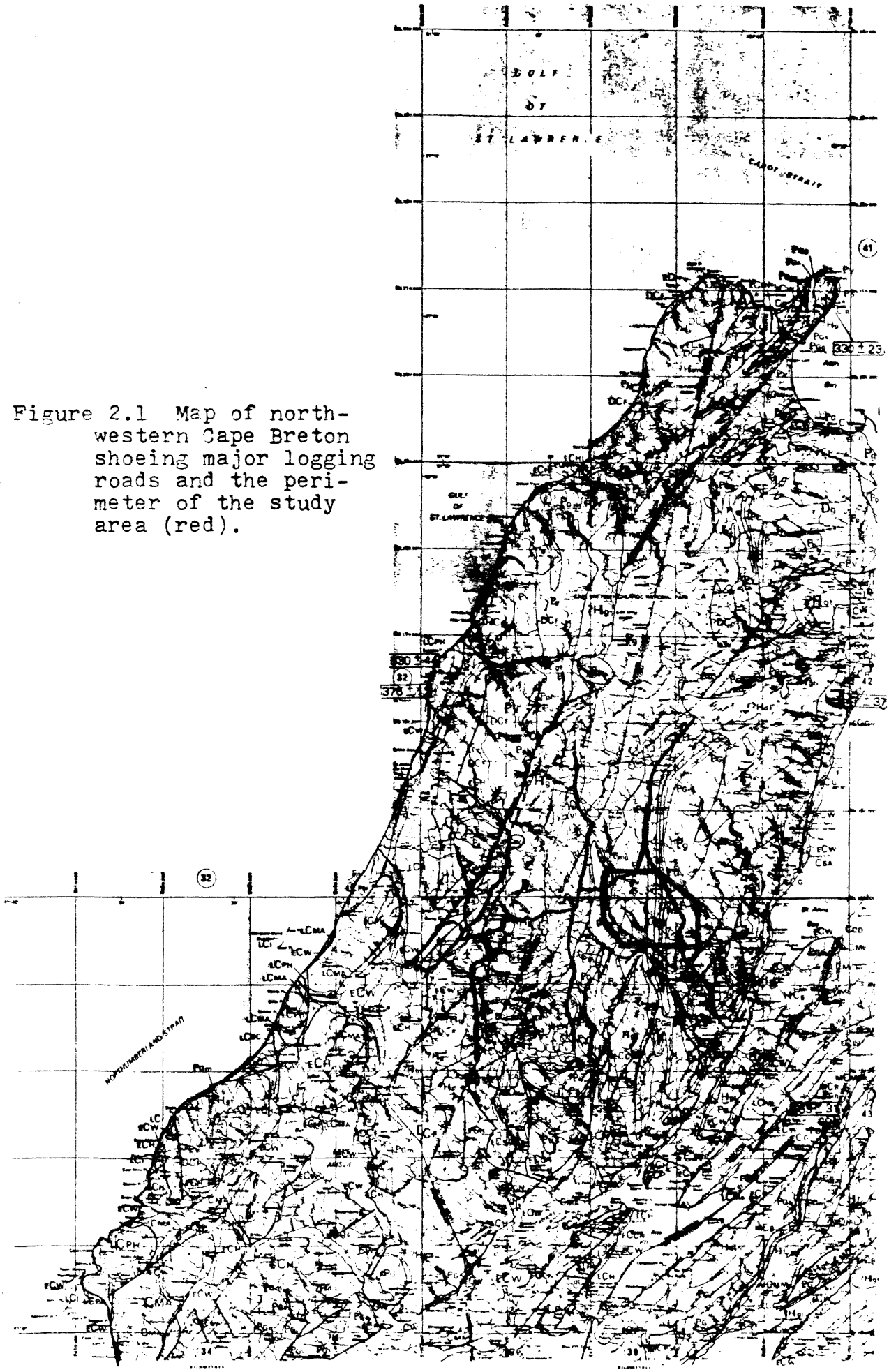

Figure 2.1 Map of north-western Cape Breton shoeing major logging roads and the peri-meter of the study area (red).

outcrops. Float from road construction can be considered a reasonable indication of underlying bedrock, and contacts are approximately expressed by changes in float lithology.

Field work was completed in two and a half days in middle August 1983. Road work was done by rented car in a manner maximizing coverage in the time available. A 1.4 kilometer section of John MacLeods Brook near the intersection with East Branch North River was worked to provide a high resolution control on lithologic variation. This section of stream showed considerable outcrop and provided a southernmost representation within the study area. The great majority of stream in the area, however, showed little promise for enough outcrop to make investigation worthwhile. In the time provided, thirty-six samples were taken from fifty nine outcrop localities (Figure 2.2).

The rest of this chapter is devoted to field relations and descriptions categorized into dioritic/tonalitic rocks, quartzites, gneisses and others. A comparison with tonalitic samples from the Baddeck Lakes region, collected by Jamieson (1979-1983), concludes this chapter.

Gneisses

Gneisses occur as a major rock type in the thesis area. Gneissic layering is expressed by alternating leucocratic layers (leucosome) and melanocratic layers (melanosome). The former consists mainly of quartz and plagioclase and the latter of micas and plagioclase. Banding varies with degree of mineral segregation, and

Figure 2.2 Map of thesis area with outcrop rock types, sample numbers and structural information indicared (scale: 1:25,000). See pocket inside front cover.

plagioclase porphyroclasts and quartz pods are common. The amount of mica varies, with some gneisses being almost schistose and others more equigranular in texture.

Folding varies from very complex and convoluted with indeterminable fold axes at some localities (Photo 2.2) to almost indistinguishable elsewhere. Epidote veinlets of approximately one millimeter thick showing no regular orientation or pattern cut some of the gneisses observed.

The majority of gneiss observations (Figure 2.2) occur on the west side of the study area consistant with the placement of a major gneissic unit west of the thesis area (Jamieson, 1983). However, several outrops occur further east on West Mariana Road.

Quartzites

Quartzites are generally well fractured, iron stained, granular textured metasediments. Quartz dominates with minor amounts of plagioclase and micas. Several outcrops showed a definite green colouration.

Foliation is defined by micas in the rock and varies in degree depending on the amount of mica present. Remnant bedding is revealed by slight colouration variations, in several outcrops.

One outcrop on West Mariana Road had a semi-pelitic lithology with a schistosity and crenulations due to abundant micas. It will not be treated as a separate rock type here because it is an individual example, interbedded with typical quartzite.

Quartzite outcrops are located in the eastern potion of the study area on Mariana Road and West Mariana Road (Figure 2.2). This is consistent with the placement of a major metasedimentary and metavolcanic unit east of the study area (Milligan, 1970). One outcrop of quartzite is an exception to this trend, located in John MacLeods Brook, further west, with an unusually high feldspar content (KJ10).

Field Relations with Diorite

Direct, observable, field relations between gneiss and diorite are almost non-existant. However, it is clear that gneisses are older than diorites due to the complex folding which occurs in gneiss outcrops only several hundred meters from relatively undeformed diorites. Also, an outcrop on southern Mariana Road exhibits gneiss xenoliths within a diorite several meters from a larger isolated body of gneiss, probably a large xenolith.

Quartzite-diorite contacts were also not observed but alternating outcrops of diorite and quartzite occur on West Mariana Road. Where quartzite appears near diorite, a more recrystallized, granular, texture exists, an effect of diorite intrusion. In John MacLeods Brook, an outcrop of quartzite with veins and pods of diorite cutting it exists surrounded by outcrops of diorite. The quartzite is probably part of a large xenolith.

No contacts or field relations of any kind were observed between quartzite and gneiss.

Diorite

The dominant rock type observed in the field is a diorite to tonalite which has intruded the previous gneiss and quartzite. Mineralogy is generally plagioclase and hornblende with varying amounts of quartz. According to the IUGS classification, a quartz percentage of greater than 5% indicates a quartz diorite and greater than 20% indicates a tonalite. Although determination is very difficult in hand samples, most outcrops appeared to be diorite or quartz diorite with quartz percentages less than 20%. Other minerals present are biotite, generally either a major constituent or absent, and opaques.

Texturally, diorites are holocrystalline, phaneritic, generally equigranular with respect to major constituents, and range from fine to coarse grained, with intermediate varieties less common. In fact most observed diorites seem to fall into one of two distinct populations, a fine grained melanocratic version and a coarse grained leucocratic version.

Population I diorites (the former) have an apparent mafic proportions of nearly 50% (KJ05, KJ09, KJ11, KJ22, GONS-146) and population II diorites and quartz diorites (the latter) are dominantly plagioclase (KJ01, KJ03A, KJ03B, KJ08, KJ23, KJ24, KJ28, KJ30, KJ34, KJ35,MR81-481, GONS-145, GONS-147, GONS-148, GONS-149). It is a general trend that the coarser the diorite, the more leucocratic, but exceptions do exist. Coarse melanocratic diorites were observed (KJ16, KJ20) and one was almost entirely very coarse hornblende crystals up to 4 cm long (KJ20) and should more appropriately be

termed a hornblendite. In addition, medium to fine grained leucocratic diorites were observed (KJ07, KJ14, KJ19).

It must be remembered that the partitioning of all diorites into two populations is arbitrary, since much of the range between extremes is represented and no exact criterion for classification is wholly adequate. The samples with considerable biotite are medium to coarse grained and contain less hornblende than most others.

Metamorphic foliation varies from apparently absent to very strong. Some samples taken could arguably be termed amphibolite (KJ22, KJ36). Foliation azimuths vary, but trend slightly west of north (Figure 2.2), a trend exhibited by stream directions. Dips are steep in west or east directions.

Several outcrops show distinct recrystallization textures. Shear zones exist in the area (Figure 2.2) evidenced by mylonitized rocks. Generally, foliation and recrystallization texture becomes more distinct in proximity to shear zones and some sheared diorites exhibited plagioclase porphyroclasts. Most shear zones are tiny on the scale of centimeters, existing within strongly foliated diorite, many showing slickensides (Photo 2.3). However, a one meter wide shear zone of well developed mylonite with plagioclase porphyclasts (KJ04) occurs on East Kathy Road. Shear is sinistral and diorite appears quite undeformed only several meters from the mylonite. A line of shear can be placed on the map trending somewhat west of north (Figure 2.2).

Tiny, one millimeter thick, epidote veins, exhibiting no regular pattern or orientation, are associated with almost all

diorite. Many veinlets show a sheath of pinkened or whitened grains of variable thickness around epidote veins due to extreme alteration. A general alteration to epidote was noticeable at several localities (KJ20). Trondjhemite and quartz veins also appear but with less frequency.

There doesn't seem to be a relationship between grain size or composition and location in the study area, with an even and wide distribution of all diorites. In fact, many outcrop locations, scattered evenly over the area, show diorites of both populations in close proximity or in contact, indicating a complex intrusion history with respect to different phases. However, it can be stated that most of the exceptionally leucocratic phases observed, occur on the east side of the study area, specifically on East Mariana Road.

Field Relations between Diorites

Despite poor exposure, thus limited expected observable field relations, many outcrop areas do, in fact, show more than one diorite phase, some exhibiting actual contacts.

Contacts observed (KJ05) are sharp but show no chilled margin or other texturally variant zone, on a visible scale. More revealing are the numerous xenoliths which are, in all cases, a more melanocratic fine grained diorite than the host. In most cases, distinct population I xenoliths are included in distinct population I hosts (Photo 2.3), although on East Mariana Road an outcrop of an extremely leucrocratic phase has population II xenoliths. In most cases xenolith contacts are sharp showing no signs of assimilation.

However, on East Mariana Road, dark grey patches with large feldspar growth coexist with coarse hornblende patches as possible xenoliths showing assimilation within a medium grained intermediate to mafic diorite. These dark grey xenoliths may be volcanic, possibly not associated with the diorite, because of a similar looking outcrop of what appears to be volcanic rock (KJ33) nearby. The large feldspars only present in the xenoliths may be due to assimilation processes.

Preliminary field indications are that leucocratic diorites were intruded subsequent to intrusion of melanocratic diorite and perhaps several or more phases of increasingly leucocratic diorite intrusion occurred.

Intrusion mechanisms and crystallization patterns may be varied and complex over the study area. An outcrop on Mariana Road (KJ26)(Photos 2.4, 2.5) shows an igneous layering defined by layers up to 20 centimeters across, showing distinctly different textures and modal compositions. Many grain sizes are represented including a pegmatitic phase. Features such as flow banding exist suggesting crystallization from magmatic currents. These are layers which have border zones consisting of elongate amphiboles extending normal to contacts. Called crescumulates (Wager and Brown, 1968), they are indicative of in-situ crystallization as opposed to crystallization in flowing magma. They are thought to result from supercooling of local pockets of liquid possibly due to sudden loss of water (Donaldson, 1974). It is clear that more than one mechanism of crystallization is responsible locally. Sample KJ26 shows that minor sulphide mineralization has occurred along layer contacts.

Other Rock Types

Other less commonly observed rock types occur in the study area. Intrusive granitic pegmatite occurs in outcrops scattered over the area (Figure 2.2). It is typically very coarse grained with quartz, plagioclase, alkali-feldspar, muscovite mineralogy (KJ12, KJ17). Phases with and without huge muscovite books (KJ18) occur, suggesting different sources or processs.

Aplite dykes are numerous in the eastern portion of the study area. Equigranular and unfoliated, they are dominantly plagioclase, quartz, potassium feldspar and micas (KJ32B). Also, in the eastern portion, are several individual very leucocratic phases, mentioned here because of their anomalous nature, although they may be technically quartz diorite or tonalite (KJ24, KJ34). All have a coarse grain size.

At the base of East Mariana Road, is a curious red aphanitic volcanic rock with numerous tiny prismatic amphibole and plagioclase phenocrysts (KJ29). The phenocrysts have a slight indication of a lineation, possibly a result of flow. As mentioned in the last section, another volcanic rock is present on the same road. It lacks the red colour and is coarser grained but contains plagioclase and hornblende phenocrysts.

Field Relation with Diorites and Metasediments

Undeformed granitic pegmatite veins are seen intruding diorite and quartzite in several locations (Photo 2.6). An outcrop on North Kathy Road shows a diorite/pegmatite contact with inclusions of the former within the latter (KJ18). Coarse undeformed pegmatite is located close to complexly folded gneiss on West Kathy Road. These field relations indicate a younger age of the pegmatite than all of the three major rock types and its undeformed nature suggests that it is also younger than the deformation of the diorite.

Aplite was observed cutting several phases of diorite and the quartzite and is therefore considered younger. Although in close proximity with pegmatite in many cases, a cross cutting relationship was not observed and therefore an age relationship cannot be drawn between them.

Volcanic rock outcrops showed no contacts but the inclusion of possible volcanic xenoliths within a diorite makes them (or that one volcanic) older. They may be part of the same metasedimentary and metavolcanic group as the quartzites.

Lastly, it can be stated that epidote, trondjhemite and quartz veinlets cutting all phases of diorite are younger than the diorite.

Conclusion

Field work done in August 1983, combined with some previous work, show that multi-phase diorites of the defined study area intrude what are now complexly folded biotite gneisses to the west and fractured quartzites to the east. Most diorites can be arbitrarily categorized as fine grained melanocratic or coarse grained leucocratic, but intermediates and exceptions exist. Leucocratic phases seem to be generally younger, although intrusion history is complex. The whole area was deformed resulting in a general foliation and subsequent mylonitization in a zone and later intruded by one or more phases of pegmatite and aplite. Minor veinlets of eipdote, trondjhemite and quartz infiltrated the diorites some time after deformation contributing to an alteration of the mineralogy.

Comparison with Baddeck Lakes Diorite

A group of samples were collected from the Baddeck Lakes region, approximately 9 kilometers south of the study area, by Jamieson (1979-1983). Hand sample inspection showed compatibility within the mineralogical and textural range described for the thesis diorites. Both populations were represented with a greater emphasis on population II rocks and fewer intermediates. Foliation is variable, including nearly mylonitic versions.

Leucocratic rocks of the Baddeck Lakes samples are generally more leucocratic than those of the thesis area, with higher quartz contents and a significant amount of alkali feldspar in some samples, making them tonalites. Also, biotite was a major mineral in more of

these.

The Baddeck Lakes samples lacked epidote veinlets, a feature very prominent in thesis rocks, although one sample did have probable epidote grains. Diabase dykes are numerous in this region seen to be intruding leucocratic diorite. They are not represented in the study area. These differences may not be very significant due to poor representation numerically, possible collection bias and the wide mineralogical and textural range observed.

Photo 2.1 General vegetation coverage of the Cape Breton Highlands. (taken by R.A. Jamieson).

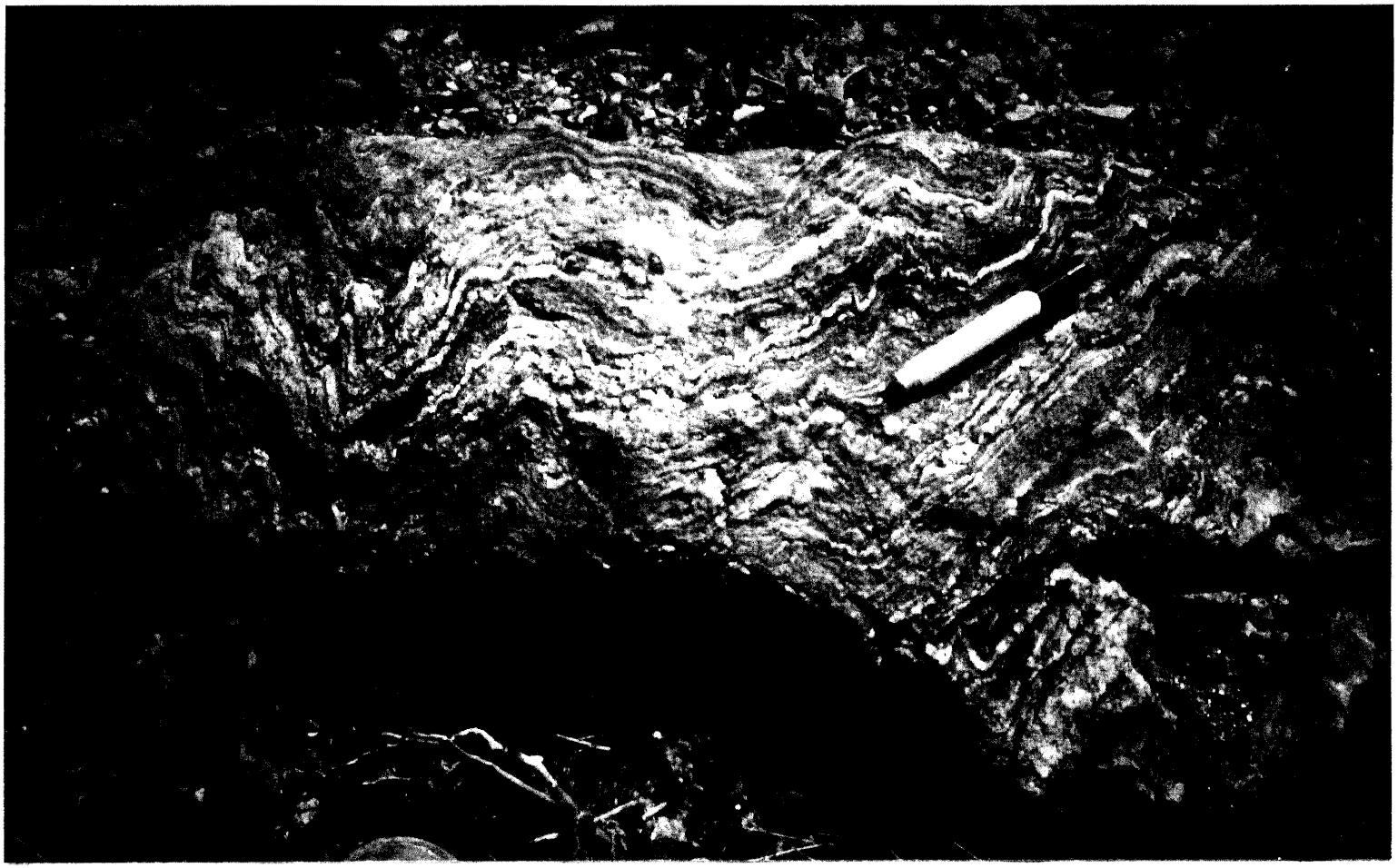

Photo 2.2 Complexly folded gneiss typical of outcrops in the study area (taken from outside the study area by R.A. Jamieson).

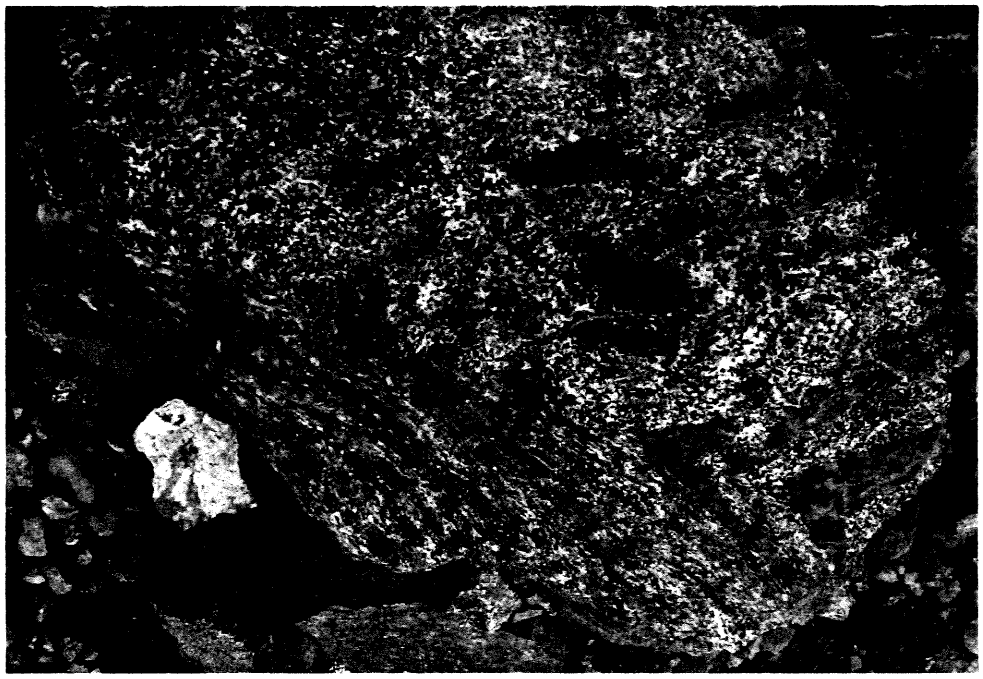

Photo 2.3 Boulder showing fine grained melanocratic xenocrysts included in coarse grained leucocratic diorite. Small shear zone appears at lower left.

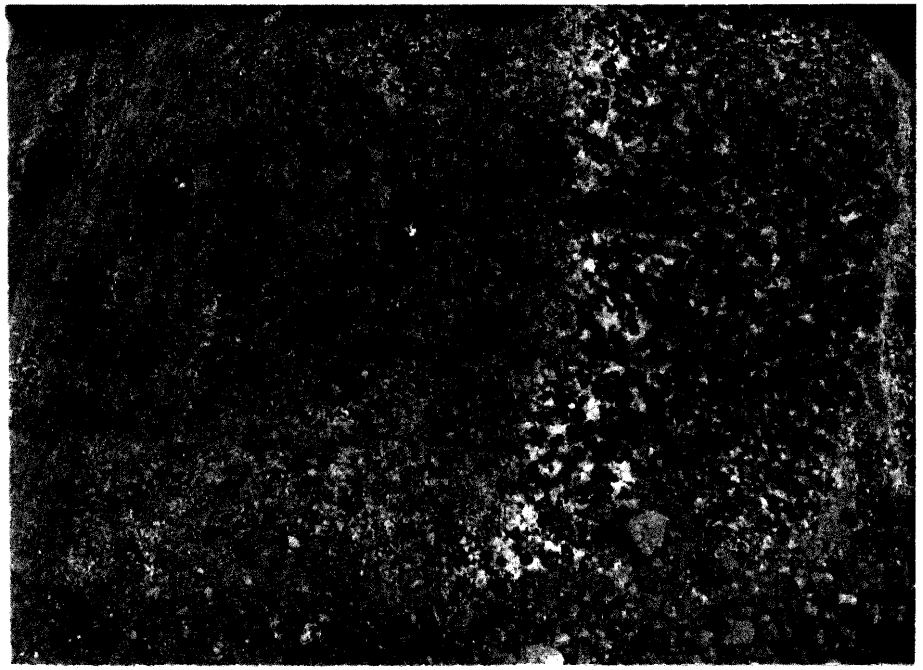

Photos 2.4 / 2.5 Outcrop showing complex intrusion pattern with a variety of textures.

Photo 2.6 Boulder showing pegmatite intruding several phases of diorite.

CHAPTER 3

PETROGRAPHY

Introduction

From field samples taken in addition to some collected previously by Jamieson (1981-1983), 38 representative samples were chosen for detailed petrographic study, and cut for thin sections. A better understanding of the diversity involved, specifically between phases of dioritic rocks, and the degree of metamorphism was sought. Also desired was a precise classification of dioritic rocks and some indication of the degree of alteration. Table 3.1 lists these samples with their determined rock type, grain size and approximate location. Following is a rock type by rock type general description and a comparison with thin sections from the Baddeck Lakes Diorites.

Dioritic Rocks

Dioritic rocks make up the majority of outcrops in the study area. Petrograpahic examination showed that many samples collected were quartz diorites and some were tonalites. Table 3.2 gives detailed descriptions of mineralogy and texture of each slide in order of decreasing mafic content. Whether samples are diorites, quartz diorites or tonalites is indicated and a note about degree and type of alteration is included. Quartz proportions are generally less than 10% and potassium feldspar is almost nonexistent, so they are mostly diorite or quartz diorite. Mineral modal proportions were either determined by point count or by estimation. Turbid, patchy,

Sample #	Rock Type	Grain Size	Map Location
KJ01	Diorite	Coarse	Kelly Road, west side
KJ02	Gneiss	Medium	Kelly Road, near Miners Road
KJ03A	Tonalite	Coarse	East Kathy Road
KJ03B	Diorite	Coarse	" " "
KJ04	Qtz Diorite	Medium	" " "
KJ05	Contact	Fine/Coarse	" " "
KJ07	Diorite	Medium	John MacLeod Brook
KJ08	Diorite	Coarse	" " "
KJ09	Contact	Fine/Medium	" " "
KJ10	Quartzite	Fine	" " "
KJ11	Diorite	Fine	West Kathy Road
KJ12	Pegmatite	Very Coarse	" " "
KJ13	Gneiss	Medium	" " "
KJ14	Qtz Diorite	Medium	" " "
KJ15	Pegmatite	Very Coarse	Intersection East Kathy/West Kathy Roads
KJ16	Qtz Diorite	Coarse	North Kathy Road
KJ19	Qtz Diorite	Medium	" " "
KJ20	Hornblendite	Very Coarse	Intersection Mariana/West Mariana Roads
KJ21	Quartzite	Fine	West Mariana Road
KJ22	Diorite	Fine	" " "
KJ23	Qtz Diorite	Coarse	" " "
KJ24	Contact	Med/V.Coarse	" " "
KJ26	Contact	Variable	Mariana Road, southern end
KJ27	Qtz Diorite	Medium	" " " "
KJ29	Volcanic	Fine	East Mariana Road
KJ30	Qtz Diorite	Coarse	" " "
KJ31	Qtz Diorite	Medium	" " "
KJ32A	Diorite	Fine	" " "
KJ32B	Aplite	Medium	" " "
KJ33	Volcanic	Fine	" " "
KJ34	Qtz Diorite	Coarse	" " "
MR81-481	Qtz Diorite	Very Coarse	West Kathy Road
MR82-579	Quartzite	Fine	North Kathy Road
GONS-145	Diorite	Coarse	West Kathy Road
GONS-146	Diorite	Fine	" " "
GONS-147	Qtz Diorite	Coarse	East Kathy Road
GONS-148	Diorite	Coarse	" " "
GONS-149	Qtz Diorite	Coarse	" " "

Table 3.1 List of samples used in petrographic study, with their classification, grain size and map location (see Figure 2.2)

alteration products, sericite and saussurite (with possible other related minerals; kaolinite), were not counted separately but were included within percentages of the associated parent mineral. Epidote, whether turbid or as distinct grains, was counted separately.

In an attempt to group dioritic rocks into population, each sample was plotted on a graph with plagioclase plus quartz on the abscissa and mafics on the ordinate (Figure 3.1). Clearly, no obvious separation exists. The majority of samples plot near the equal proportion region of the graph with fewer points in either direction. Hollow point markers represent the four biotite rich slides with biotite proportions subtracted from the ordinate scale. An alternate view of the same criterion is presented in Figure 3.2 and 3.3 which are histograms for mafics and plagioclase/quartz respectively. Despite the low number of data points, this presentation shows fairly continuous variation in the colour index.

Grain sizes vary from fine to very coarse and each sample has been assigned one of four grain size names (Table 3.1). Divisions are arbitrary and grain size are gradational over them (especially between medium and coarse). In Figure 3.1 each sample number is represented by a point marker corresponding to its grain size. The only consistant trend between modal proportions and grain size is that fine grained samples tend to be rather mafic. Another consistancy observed is that the four slides which feature considerable biotite are all quite leucocratic, meaning small proportions of hornblende.

For purposes of description, discussion will be divided into categories based on composition and grain size.

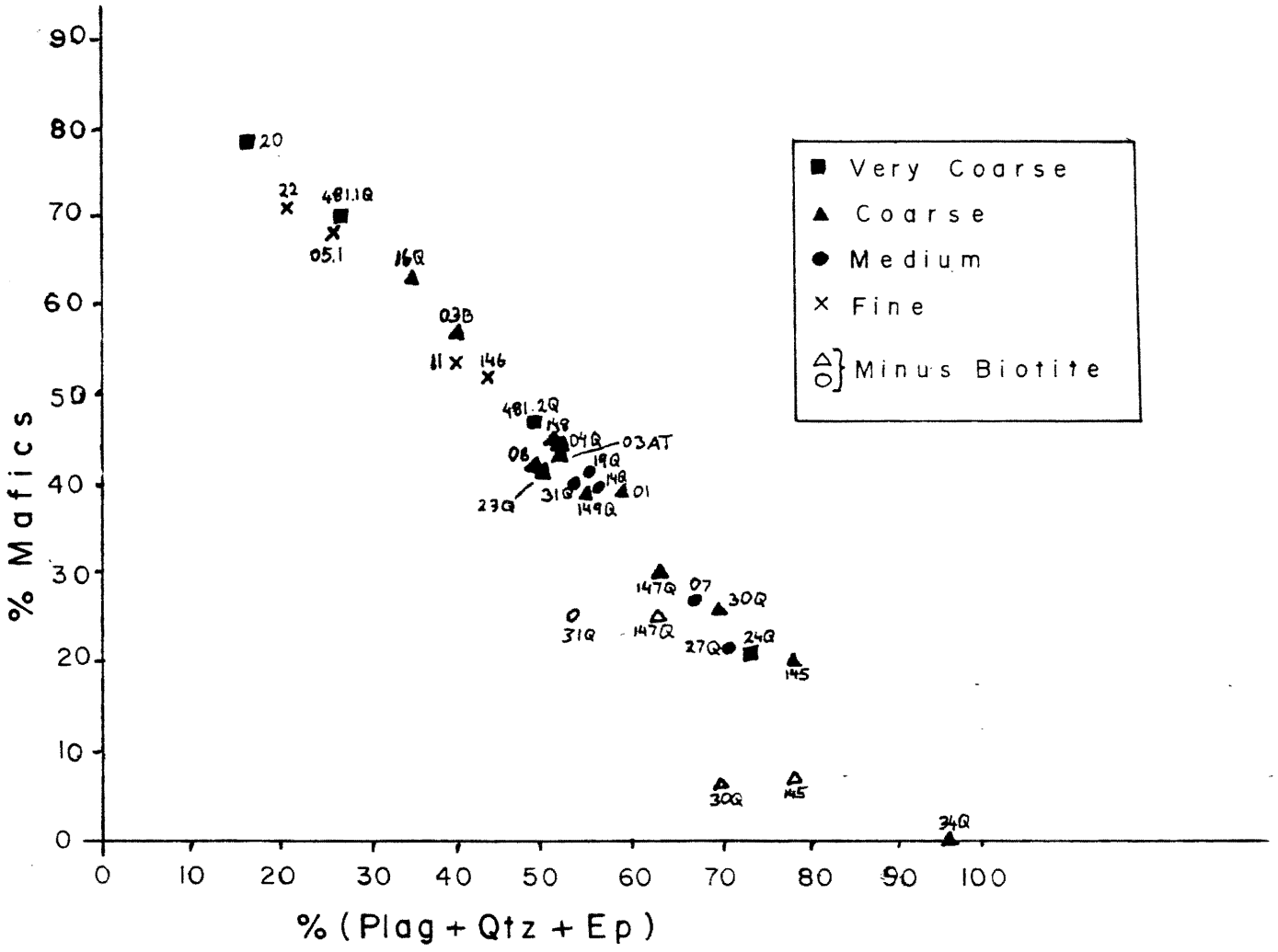

Figure 3.1 Plot of quartz plus plagioclase (plus epidote if considerable) versus mafic minerals (modal per centages) for thin sectionsstudied. Numbers are thin section numbers. "Q"-quartz diorites,"T"-tonalites, others are diorites.

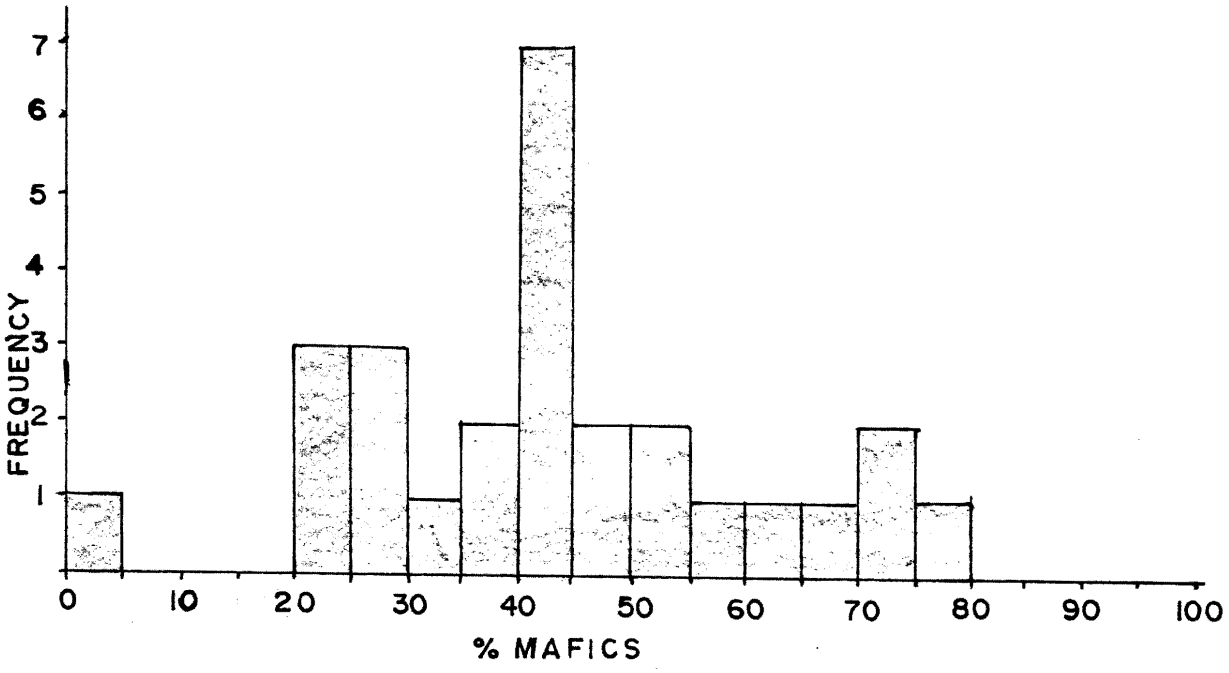

Figure 3.2 Histogram for mafic proportions of thin sections studied.

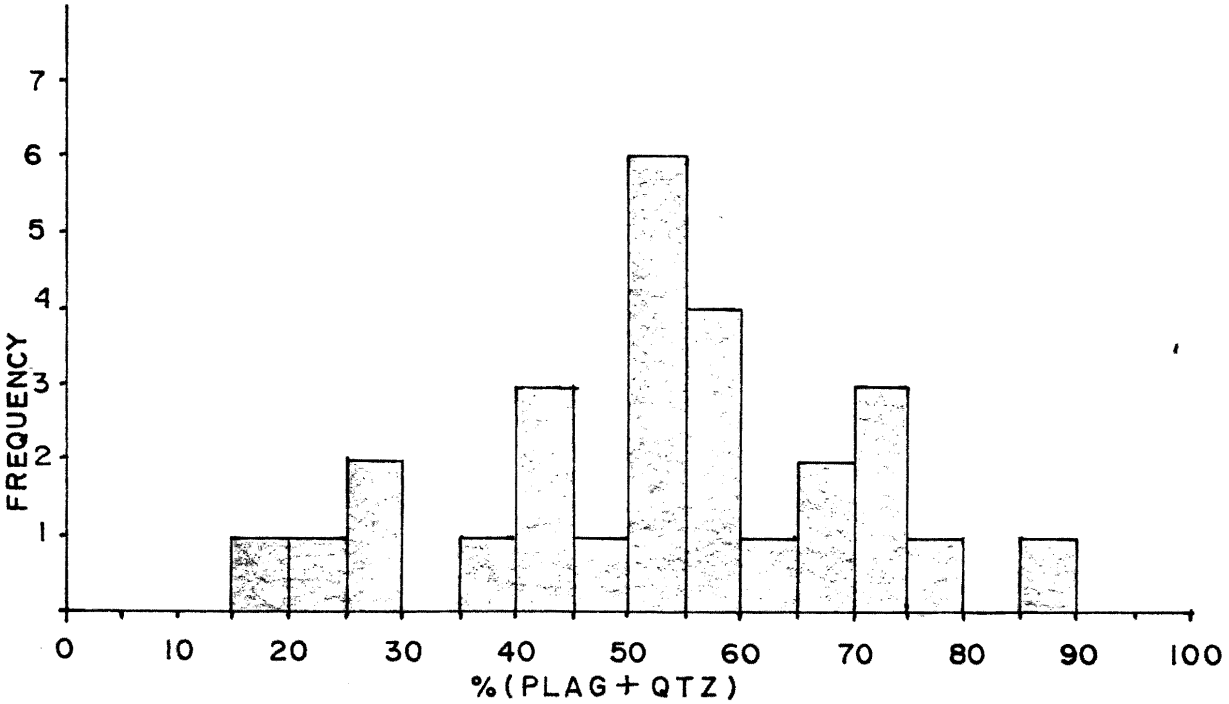

Figure 3.3 Histogram for plagioclase plus quartz proportions of thin sections studied.

(a) Typical Diorite and Quartz Diorite

Typical diorites dominate the study area being medium to coarse grained with plagioclase, hornblende and quartz (may be absent) as major minerals.

Hornblende (22%-63%) occurs as slightly to extremely poikilitic, mostly anhedral grains. Inclusions are quartz, plagioclase, euhedral apatite, zircon (with halos) and opaques and are so numerous in some examples that grains appear disintegrated. Many grains show tiny opaque inclusions lined up in hornblende cleavage planes, as a result of ilmenite exsolution. Generally slides show some degree of recrystallization, from very few indistinct patches, to total overgrowth of idioblastic polygonal aggregates. In many cases of considerable recrystallization, elongate grains have grown with a preferred orientation in response to stress, resulting in a noticeable foliation. The recrystallized aggregate acts as a pseudomorph of the original hornblende grain.

Hornblende grains exist in three forms, either relict igneous, prograde replacement or recrystallized. Relict igneous grains are signified by extreme ilmenite exsolution (a metamorphic process) resulting in a depletion of titanium, but are not very poikilitic. They also show good cleavage, and are commonly well fractured and twinned (Photos 3.1, 3.2). Extremely poikilitic hornblende suggests prograde replacement, probably mainly of igneous hornblende, and these grains commonly have a slight idioblastic form. Most replacement is of igneous hornblende but some may be of pyroxene, evidenced by possible hornblende pseudomorphs. Ilmenite exsolution has also

occurred in these replacement grains, creating the possibility of confusion, but generally to a lesser degree. Recrystallization has accompanied the replacement causing a reduction in hornblende grain size. Ilmenite inclusions have apparently coalesced into large ilmenite grains within polygonized inclusion free hornblende aggregates. Hornblende is also free of twinning and signs of deformation (Photos 3.3, 3.4). In most cases, two or more grain types co-exist.

All slides showed a small amount (<5%) of retrograde alteration of hornblende to biotite and/or chlorite along cleavage planes and grain edges. Igneous grains are more affected than metamorphic grains.

Plagioclase is present in a variety of textures in all slides. Anorthite contents were determined where grain condition allowed, and most were andesine with some as calcic as labradorite. Grains are coarse, with well developed twinning and zoning (Photo 3.5). Various signs of strain are apparent, from deformation twinning and kinking to sub-grain development to recrystallization (Photos, 3.4, 3.5, 3.6, 3.7). Recrystallized plagioclase grains are smaller and more equidimensional than hornblende.

Recrystallized grains are undoubtedly metamorphic but the nature of the coarser grains is not obvious. Visible zoning and well developed twinning suggests an igneous nature but some of this zoning may be metamorphic and it is possible that plagioclase has acted as a replacement mineral also. Perhaps larger grains lacking twinning features are metamorphic replacements. Nevertheless, several forms

co-exist in many slides. It is common for plagioclase porphyroclasts (igneous) to be surrounded and overgrown with recrystallized aggregates. In many cases, a whole range of grain sizes are represented (seriate texture). Non-recrystallized plagioclase may be slightly poikilitic but inclusions are usually alteration products or plagioclase relicts possibly indicating that the grain is metamorphic.

Plagioclase is commonly significantly altered by varying amounts up to 100%. Retrograde products include sericite, saussurite (possibly including kaolinite or other clays) and epidote. Sericite and saussurite occur as turbid, patchy material obscuring the plagioclase (Photos 3.7a, 3.8). Epidote occurs similarly with sericite and saussurite or as monomineralic patches, in some cases well developed enough to form cores of distinct solid grains (Photo 3.9). Hematite traces appear as a stain often associated with fractures. Generally, alteration increases in the proximity of veinlets of epidote or chlorite. Also, samples that are near the shear zone determined in the field have distinctly higher alteration of plagioclase associated with more numerous veinlets and fractures.

Quartz uniformly shows undulose extinction as a result of strain, and occurs in primary and recrystallized forms. Primary grains are fine to coarse, anhedral, equidimensional and often irregularly shaped, occurring in pockets of several grains together or as small grains between larger plagioclase or hornblende grains. Quartz is easily recrystallized, so commonly exists in fine grained recrystallized form. In a recrystllized matrix, quartz is difficult to distinguish from plagioclase, so percentages are rough estimates.

Epidote occurs in four distinct forms. Most common is the turbid, patchy retrograde form, present in almost all thin sections. Next most common are the tiny idioblastic to sub-idioblastic grains often embedded in hornblende, or plagioclase. These grains are in reasonable equilibrium with their surroundings and are probably due to a different stage of retrograde metamorphism. Some of the larger of these grains have cores of allanite, a yellow-brown mineral of the epidote group, possibly an alteration product of epidote. In KJ04, allanite also occurs as large grains separate from epidote. The third form of epidote is vein fill, in which grains are distinct but not idioblastic. Lastly, epidote occurs in several slides, as coarse distinct, non-idioblastic grains approximating textural equilibrium and therefore probably due to prograde metamorphism.

In the typical diorites, biotite occurs solely as retrograde alteration of igneous and to a lesser extent replacement hornblende. Grains are poorly developed, only existing along cleavage planes and grain edges, as brown coloured sections. Hornblende is rarely more than several percent gone to biotite. Chlorite exists also as retrograde alteration of hornblende, often replacing retrograde biotite, and in the same form (Photo 3.5). In some veinlets, chlorite exists in the penninite variety. Wispy grain aggregates and large patches of chlorite may be an indication of igneous biotite, since replaced.

Opaques are present in a variety of shapes and sizes, but usually small in relation to other grains. Usually equidimensional, they are evenly scattered throughout thin sections. They commonly

occur as inclusions, especially of hornblende; as discussed previously, and are therefore probably exsolved ilmenite taking titanium from the hornblende. Some opaques are encircled by hematite and are interpreted, therefore, as magnetite. Opaques may be igneous, or in the case of exsolved ilmenite (some coalesced into larger grains), metamorphic. Other oxides may make up part of the opaque portion as well.

Sphene is common, as small rounded or oval grains, often associated with opaques and commonly mantling them. Since sphene is a titanium mineral, the associated opaques are likely ilmenite. Although not abundant, sphene grains tend to clump together in contact or in close proximity. Sphene is a metamorhic mineral, forming at the expense of ilmenite.

Apatite occurs only as tiny euhedral inclusions in hornblende. They are not abundant but occur in most sections. Of similar nature is zircon, which exhibits radioactivity halos of disturbed crystal lattice structure. Hematite is present in trace amounts in nearly all sections, usually as a stain associated with fractures or as a mantle of magnetite. Rutile was found in MR81-481 as a rounded or oval variety found in clumps much like sphene. Lastly, tourmaline was found in several highly altered sections as a low grade alteration product associated with other retrograde alteration products.

The presence of replacement hornblende, prograde epidote and andesine (if of metamorphic origin) places these diorites in the lower amphibolite metamorphic facies.

(b) Fine Grained Melanocratic Variety

Four slides are distinctly finer grained than the typical diorite of the study area. They are KJ11, KJ23, KJ05.1 and GONS-146 and are on the melanocratic end of the range (Figure 3.1).

The mineralogy is generally the same as the typical diorites and quartz diorites, but proportions are sightly different. Mafics (52%-71%) are more dominant and quartz is less than 3%, making them diorites by composition. Anorthite content was determinable only in KJ11 being 39% (andesine).

Hornblende grains are not as easily categorized, since they are all close to the same size (Photo 3.10). It appears that recrystallized grains make up a higher proportion but ilmenite exsolution is present, suggesting that igneous grains may remain. Grains are only slightly poikilitic but many are idioblastic, possibly indicating a replacement nature. Recrystallized grains exhibit a preferred orientation resulting in a slight foliation.

Plagioclase is irregularly shaped, filling in spaces between hornblende grains and does not appear to be significantly recrystallized. Idioblastic epidote grains occur as do scattered opaques.

Alteration is of the same nature and amount as typical diorite and quartz diorites with turbid sericite, saussurite and epidote occurring. GONS-146 showed epidote and chlorite filled veinlets.

(c) Leucocratic, Biotite-Rich Variety

Four slides (KJ30, KJ31, GONS-145, GONS-147) are considered here because of their high biotite content (5%-20%). They also happen

to be rather low in overall mafics (Figure 3.1) and therefore very low in hornblende (6%-25%). The amount of quartz varies from 5% to 15% making them all quartz-diorites. Plagioclase (43%-73%) was determined as andesine (An_{42}) in GONS-145. Other mineralogy is consistent with typical quartz diorites with the exception of the presence of potassium feldspar. Distinct grains with cross hatched twinning (microcline) appear in proportions of 2% in KJ30. Possible potassium feldspar may exist in GONS-145 as well, but distinction from plagioclase is not certain.

What differs texturally in these slides is in the case of biotite. In addition to retrograde biotite from hornblende, it occurs as well developed grains showing good cleavage and features of deformation such as bends and kinks (Photo 3.11). Zircons with halos are included in these irregularly shaped grains which are often in contact with hornblende, suggesting that hornblende has replaced it to some degree. This biotite, then, is interpreted as igneous with some hornblende being metamorphic. All hornblende in KJ30 appears to be of this origin, and most in GONS-145, but the others also exhibit considerable poikilitic hornblende (probable replacement of igneous hornblende) and small amounts of possible igneous hornblende, typical of other diorites in the study area. They also have a proportion recrystallized to aggregates with a slight preferred orientation. It is somewhat questionable whether GONS-147 contains any igneous biotite (only 5%), it may all be unusually well developed retrograde biotite. Plagioclase is quite coarse showing zoning, strain and no recrystallization.

The presence of igneous biotite as well as potassium feldspar and relatively low proportions of hornblende suggest that these sections are from rocks more differentiated than the typical diorite or quartz diorite. Greater differentiation is characterized by increased K_2O and SiO_2 and the mineralogies reflect this. Also characteristic are more sodic igneous plagioclase compositions and although the An content is less for GONS-145 than most, the effect of metamorphism on this composition is uncertain. All things considered, KJ30 is the most differentiated, followed by GONS-145 and the other two are considerably less so. It is possible that many of the typical dioritic samples contained igneous biotite at one time that has been replaced since by hornblende, but no indications of such remain.

(d) Anomalous and Unusual Dioritic Rocks

There are a number of individual samples that are texturally or compositionally unusual and they will be briefly described here.

KJ04 was taken from the meter wide shear zone described in Chapter 2. Mineralogicial contents and proportions are typical (Table 3.2) but textures indicate mylonitization with plagioclase porphyroclasts sheared out in an intergranular matrix of recrystallized plagioclase and quartz. Hornblende is somewhat recrystllized into a preferred orientation and is concentrated in bands, creating a mylonitic foliation.

KJ20 is a very coarse grained hornblendite (75% hornblende) with grains being igneous showing ilmenite exsolution with slight recrystallization around grain boundaries (Photo 3.12). Intergranular plagioclase has almost entirely gone to epidote and less abundant

sericite and saussurite. Some retrograde chlorite exists at the expense of hornblende. This sample may represent a pegmatitic phase associated with magmatic fluid movement.

KJ34 has anomalously high plagioclase (88%) and no mafics (Photo 3.13). Plagioclase appears euhedral and possibly igneous but is almost completely altered to mostly saussurite with patches of sericite, epidote and penninite.

(e) Contact Zones

Four thin sections were made across contacts between two diorites of different grain sizes. A brief description of each may help to understand the relationships between phases of diorite.

Slide KJ05.2 shows a contact between a typical fine grained melanocratic diorite with highly recrystallized preferentially oriented hornblende and a typical coarse grained quartz diorite with less recrystallized hornblende. Alteration is 10% of the former and 90% of the latter (with epidote veinlets running parallel to the contact). A narrow contact zone is characterized by elongate hornblendes lined up parallel to the contact and by coarse equidimensional plagioclase and opaques.

Another contact between medium and fine grained diorites is represented by KJ09. The medium grained version has somewhat recrystallized hornblende, exhibiting no foliation while the fine grained version, although identical mineralogically, exhibits a very strong foliation defined by preferentially aligned elongate hornblende and plagioclase (Photos 3.14 and 3.15). Alteration is greater in the fine grained diorite. A narrow contact zone, parallel to the

foliation, is mineralogically and texturally equivalent to the fine grained phase, but is highly altered and contains a series of subparallel (along contact) sericite veinlets. The veinlets continue into the fine grained side but with greatly reduced concentration and associated alteration.

Slide KJ24.2 shows an extremely coarse, plagioclase dominant diorite in contact with a typical medium grained quartz diorite. Alteration is increased in the medium grained version but there doesn't seem to be a recognizable contact zone showing a chilled margin, just a sudden sharp change in grain size. Foliation and recrystallization are not factors in this section. Epidote is unusually abundant in the coarse phase (Photo 3.16).

Slide KJ26 shows a complex intrusion pattern involving several textures of dioritic rocks (see Chapter 2). Three zones are represented in this section. Zone A is characterized by very coarse elongate hornblendes, extending perpendicular to the contact as well as high alteration of plagioclase (80%)(Photo 3.17). Zone B may be a contact zone (5-8 mm wide) with enormous opaques running parallel to the contact in a matrix of fine grained equigranular plagioclase, biotite (igneous looking) and hornblende (Photo 3.18). Zone C is medium grained and is the most leucocratic (no biotite)(Photo 3.19). No foliation occurs and high proportions of opaques exist throughout.

The latter two cases discussed are unusual cases. KJ24 is from a boulder of typical quartz diorite with a pegmatitic, plagioclase-rich vein running through it. The coarse phase is therefore younger. KJ26 is more difficult to interpret. The

hornblendes perpendicular to the contact suggest a younger age for zone A. Zone B could be a contact zone and the huge opaques due to huydrothermal activity but contacts are not sharp, so the relationship is not clear. Zone B could, in fact, be a separately intruded unit. Because of the presence of probable igneous biotite and the fine grain size, we can postulate that it represents a later, more differentiated version of the diorite intruding the others.

The coarse nature of the contact zone in KJ05.2 and the parallel grains suggests that the coarser phase intruded the finer phase. However, the contact zone in KJ09 is equivalent to the finer grained phase indicating fine grined intrusion. The strong foliation is due to flow in the intruding magma is this explains why it doesn't exist in the coarser phase. This contradiction emphasizes the complexity of the diorite intrusion history of the study area.

Gneisses

Based on two slides (Table 3.3), gneiss mineralogy consists mainly of biotite, quartz and plagioclase. One sample contains 10% muscovite while in the others it is lacking. Anorthite contents are 38% and 47% for KJ02 and KJ13 respectively, both values indicating andesine. Minor mineralogy consists of epidote, opaques, garnet, retrograde chlorite, hematite and zircon inclusions.

Medium grained micas are elongate and define a foliation by being aligned between equigranular, medium grained quartz and plagioclase which exhibit considerable sub-grain development and recrystallization. In KJ13 large aggregates of quartz are encircled

by swirling biotite. Epidote occurs mainly as idioblastic grains, some with allanite cores. Minor amounts of turbid, patchy epidote also occur. Garnets are few, quite small, and well fractured. Opaques are medium to fine grained, equidimensional, and equally scattered throughout. Zircons exist as inclusions in biotite with radioactivity halos (Photo 3.20).

Chlorite occurs as retrograde alteration products of biotite along cleavage planes and grain edges and plagioclase is slightly altered to sericite, saussurite and epidote. A small amount of hematite stain was observed in KJ13, associated with opaques.

Alteration in gneisses may be due to fluids introduced by intrusion of the diorite but no other evidence of contact metamorphism exists.

Quartzites

Based on three thin sections (Table 3.4) mineralogy is dominated by quartz and feldspar, with minor biotite, muscovite, chlorite, epidote, opaques, hematite and garnet. Mineralogies vary slightly from slide to slide with not all minor minerals represented in each.

Texturally, they are porphyroclastic with medium grained partly recrystallized feldspar porphroclasts (KJ21 has some quartz porphyroclasts) in a fine grained matrix of completely recrystallized granoblastic quartz and feldspar. Matrix proportions are difficult to estimate. Fine grained micas are aligned, with hematite stain, in a thin anastomosing pattern around matrix grains or with sub-parallel

fractures to form a foliation. Epidote exists as turbid retrograde alteration of feldspar and in veinlets with chlorite. Rounded garnets (MR82-579 only) are fine grained and scattered throughout the matrix, and opaques are tiny and few.

Feldspar is altered (30-40%) mainly to saussurite. Section MR82-579 shows well developed muscovite inclusions along cleavage planes of feldspar porphyroclasts forming a crossed pattern. In KJ10 micas have all gone to chlorite, which also exists in veinlets.

Feldspar porphroclasts in KJ10 are somewhat squeezed out into a direction parallel to fractures containing muscovite and chlorite. This is indicative of shear and the other sample is from a location near the shear zone delineated on the map.

The granoblastic nature of the texture may be due, in part, to contact metamorphism since it produces this type of grain size reduction. The existance of micas along fractures in quartzite might be due to fluids associated with diorite intrusion. The garnets in MR82-579 may be products of contact metamorphism also.

Other Rock Types

Two slides of felsic pegmatite, intruding the dioritic rocks, show a dominant feldspar and quartz mineralogy. However, KJ15 also has a tiny grain of hornblende, and therefore, may not be related to the felsic pegmatite. No signs of metamorphism exist, though, so it is not related to the diorites either.

Two sections of volcanic rocks, of uncertain origin, exhibit euhedral, medium grained hornblende and plagioclase phenocrysts in a fine grained matrix of mostly plagioclase and acicular hornblende. Alteration is extreme in both cases but KJ29 has been wholly hematite altered to a distinct red colour (Photos 3.22, 3.23).

Aplite (Photo 3.24) is equigranular with plagioclase, quartz and potassium feldspar dominating one thin section. It is unmetamorphosed so intrudes the diorite but its relationship with the pegmatite is not determined.

Table 3.5 gives full mineralogical and textural details concerning the rocks mentioned in this section.

Comparison with Baddeck Lakes Diorites

Seventeen slides from the Baddeck Lakes region were observed for comparison with the thesis dioritic thin sections. Due to diversity in mineralogical modal proportions and grain sizes, and the limited number of sections available, differences are inevitable, but a maintained trend may be significant.

The Baddeck Lakes Diorites are generally less varied with a coarse, very leucocratic phase dominating. Quartz proportions make them actually quartz diorites and tonalites. Hornblende is less dominant and biotite exists as igneous grains as well as an alteration of hornblende (with chlorite).

Several very fine grained, melanocratic versions are represented but intermediates are not included. They are similar mineralogically to the fine grained thesis diorites but are even finer

grained and are from younger dykes.

By criteria discussed earlier, the tonalites appear to be more differentiated versions of diorite, much like KJ30 of the thesis samples. The hornblende in these rocks may, in fact, be metamorphic minerals replacing biotite. The fine grained melanocratic diorite dyke rock has been called diabase (Jamieson, 1981-1983) and is not related to the fine grained phase in the thesis area.

TABLE 3.2(A)

Petrographic Descriptions of Typical Diorite and Quartz Diorite

lide & ock Type	Mineralogy (Percentage)	Texture	Alteration	Notes
81-481 orite	Hornblende (70), Plagioclase 27), Opaques (2), Epidote (1), Quartz (1), Apatite (<1) (percentages estimated)	Very coarse grained, hornblende slightly poikilitic with considerable ilmenite exsolution 60% recrystallized; plagioclase 15% recrystallized. Other minerals finer grained and scattered.	Plagioclase 20% altered to saussurite and epidote	Prepared for microprobe photo 3.8
J16 uartz iorite J03B iorite	Hornblende, Plagioclase (An_{48} for KJ03B), Quartz, Epidote, Retrograde Biotite, Chlorite and Hematite Sphene, Apatite, Zircon inclusions	Coarse grained, hornblende almost completely recrystallized but slightly poikilitic; plagioclase (less coarse) strained with subgrain development. Foliation (only in KJ16) defined by preferred orientation of recrystallized hornblende.	Hornblende shows retrograde alteration to biotite/chlorite (mainly on non-recrystallized grains), plagioclase 5-10% altered to sericite/saussurite/ epidote	KJ16 has more quartz than KJ03B. KJ16 prepared for microprobe KJ03B photos 3.7 a, b
)NS-148 orite	Plagioclase (49), Hornblende (42), Retrograde Biotite (3), Opaques (3), Epidote (<1), Retrograde Hematite (<1), Apatite (<1), Quartz (2) (percentages estimated)	Medium grained, hornblende extremely poikilitic with ilmenite exsolution, 50% recrystallized, plagioclase seriate, strained and partially zoned.	Hornblende slightly gone to biotite, plagioclase has very little sericite (muscovite) and saussurite	Prepared for microprobe photo 3.4

ıble 3.2(A) - Page 2

lide & ɔck Type	Mineralogy (Percentage)	Texture	Alteration	Notes
)03A ɔnalite	Hornblende (40), Quartz (28), Plagioclase (24), Opaques (3), Retrograde Biotite (2.5), Epidote (1.5), Sphene (<1), Retrograde Chlorite (<1) and Hematite (<1), Apatite (<1) (percentages from point count)	Coarse grained, hornblende poikilitic with ilmenite exsolution and 32% recrystallized Plagioclase xenoblastic, quartz in fine grained polygonal aggregates. Slight foliation due to preferred orientation of recrystallized hornblende.	Hornblende slightly altered to biotite/ chlorite, plagioclase 5% altered to sericite/ saussurite	
)08 iorite	Plagioclase (>45), Hornblende (35), Retrograde Chlorite (7), Opaques (5), Epidote (2), Quartz (<5), Retrograde Hematite (<1), Apatite (<1) (percentages estimated)	Coarse grained, hornblende extremely poikilitic with ilmenite exsolution, 70% recrystallized by various degrees, plagioclase elongate, zoned, strained, overgrown by fine grained plagioclase and quartz polygonal recrystallized aggregates.	Hornblende considerably gone to chlorite, plagioclase 15% altered to sericite/saussurite/ epidote	Prepared for microprobe phote 3.6
)23 ıartz iorite)19 ıartz iorite	Plagioclase ($An_{59}$for KJ19), Hornblende, Quartz, Retrograde Chlorite, Epidote Sphene, Opaques, Retrograde Hematite, Apatite, Zircon inclusions	Medium-coarse grained, extremely poikilitic with ilmenite exsolution but recrystallized (KJ19 almost completely). Quartz shows sub-grain development. Epidote veinlets in KJ23	Hornblende slightly gone to chlorite, plagioclase considerably altered to epidote/sericite/ saussurite. KJ23 shows extreme alteration near veinlets	KJ23 prepared for microprobe KJ23 photo 3.1 KJ19 photo 3.3

ıble 3.2(A) - Page 3

lide & ɔck Type	Mineralogy (Percentage)	Texture	Alteration	Notes
)NS-149 ıartz iorite	Plagioclase (An_{50})(47), Hornblende (38), Quartz (8), Epidote (3), Opaques (2), Retrograde Biotite/Chlorite (1), Retrograde Hematite (<1), Apatite (<1)(percentages estimated)	Coarse grained, hornblende poikilitic with ilmenite exsolution, 5% recrystallized, plagioclase seriate, strained and zoned, quartz in polygonal aggregates, foliation apparent macroscopicly.	Hornblende shows very little alteration to biotite/chlorite Plagioclase 5% altered to epidote/sericite/ saussurite (locally up to 95%)	
)01 iorite	Plagioclase (59), Hornblende (37), Retrograde Chlorite (penninite)(2), Opaques (1), Epidote (<1), Quartz (1), Retrograde Hematite (<1) (percentages from point count)	Coarse grained, hornblende poikilitic, little ilmenite exsolution, 35% recrystallized, plagioclase strained partially overgrown by recrystallized aggregates (also intergranular) of plagioclase and quartz. Penninite veinlets crosscut.	Hornblende slightly gone to chlorite, plagioclase 40% altered to sericite/ saussurite	
)14 ıartz orite)07 iorite)27 ıartz iorite	Plagioclase (An_{43} for KJ14), Hornblende, Retrograde Biotite, Chlorite and Hematite, Quartz, Epidote, Opaques, Sphene (KJ07), Apatite, Zircon inclusions	Medium grained, hornblende very poikilitic with some ilmenite exsolution (epidote cores in KJ07) little recrystallization (more in KJ27), plagioclase strained, zoned with sub-grain development. Epidote with cores and as veinlets (KJ07).	Hornblende gone to chlor- ite (considerable in KJ07) and epidote, plagioclase variably altered to sericite/saussurite/ epidote	KJ14 photo 3.5

ɔtes:
- When hornblende is termed poikilitic and exhibits ilmenite exsolution, it pertains to non-recrystallized grains.
- Recrystallized grains form a polygonal aggregate of fine grains occupying the space of the original grain.
- Alteration of hornblende to biotite/chlorite generally occurs along cleavage planes and grain edges.

TABLE 3.2(B)

Petrographic Descriptions of Fine Grained Melanocratic Diorites

ide & ck Type	Mineralogy	Texture	Alteration	Notes
122 orite 105.1 orite	Hornblende, Plagioclase, Epidote, Opaques, Retrograde Biotite/Chlorite/Hematite, Quartz, Sphene, Apatite	Fine grained, equigranular, hornblende slightly poikilitic and highly recrystallized, intergranular and hedral plagioclase and non-idioblastic epidote. Very slight foliation in KJ05.1 due to hornblende alignment.	Plagioclase 12% altered to sericite/saussurite/ epidote, very little hornblende alteration to chlorite (even less biotite)	
111 orite NS-146 orite	Hornblende, Plagioclase (An_{39} for KJ11), Retrograde Chlorite and Biotite, Sphene, Epidote, Quartz, Apatite, Hematite	Fine grained, equigranular, hornblende with ilmenite exsolution, ~50% recrystallized, plagioclase strained, polygonal with subgrain development. Epidote idioblastic and as veinlets which crosscut. Slight foliation due to hornblende alignment.	Plagioclase 5% altered to sericite/saussurite, hornblende slightly gone to biotite/ chlorite	KJ11 - photo 3.10

TABLE 3.2(C)

Petrographic Descriptions of Biotite-Rich Leucocratic Quartz Diorites

lide & ock Type	Mineralogy	Texture	Alteration	Notes
131 uartz orite	Plagioclase (43), Hornblende (25), Biotite (15), Quartz (10), Epidote (6), Spinel (1), Opaques (<1), Retrograde Hematite (<1), Zircon inclusions (percentages estimated)	Medium grained, hornblende extremely poikilitic 55% recrystallized, plagioclase zoned, strained slight foliation only apparent macroscopically.	Some hornblende altered to biotite. Plagioclase quite gone to epidote with a little saussurite	
)NS-147 uartz orite	Plagioclase (55), Hornblende (25), Quartz (8), Biotite (5), Epidote (3), Opaques (3), Retrograde Hematite (<1) Apatite (<1) (percentages estimated)	Medium to coarse grained, hornblende extremely poikilitic with ilmenite exsolution, 10% recrystallized plagioclase is seriate, slightly poikilitic, strained, zoned; quartz coarse and in recrystallized polygonal aggregates. Epidotes idioblastic and large.	Slight alteration of hornblende to biotite, plagioclase generally only very slightly altered but with patches of heavy alteration to sericite/ saussurite	
130 uartz orite	Plagioclase (53), Biotite (20), Quartz (15), Hornblende (6), Epidote (2.5), Opaques (1.5), Retrograde Hematite (<1), K-feldspar (2), Apatite (<1) (percentages estimated)	Coarse grained, plagioclase strained, Biotite is poikitic, irregularly shaped and in contact in many cases with hornblende.	Plagioclase 20% altered to saussurite/epidote, hornblende slightly gone to biotite	photo 3.11

ıble 3.2(C) - Page 2

ide & ɔck Type	Mineralogy	Texture	Alteration	Notes
)NS-145 ıartz orite	Plagioclase (An_{42})(73), Biotite (13), Hornblende (7), Quartz (5), Epidote (1), Opaques (1), Retrograde Chlorite (<1), K-feldspar (1) (percentages estimated)	Coarse grained, plagioclase euhedral and zoned and slightly poikilitic, hornblende poikilitic and elongate, biotite anastomosing around grains defining foliation; seriate quartz; epidote with allanite cores is associated with biotite.	Plagioclase 5% altered to saussurite, little biotite altered to chlorite	

TABLE 3.2(D)

Petrographic Descriptions of anomalous Dioritic Rocks

ide & ck Type	Mineralogy	Texture	Alteration	Notes
04 artz orite	Plagioclase (An_{58})(42), Hornblende (43), Quartz (10), Opaques (2), Retrograde Biotite (1), Epidote (1), Retrograde Chlorite (<1), Hematite (<1), Apatite (<1). Zircon inclusions (percentages from point count)	Medium to fine grained, hornblende poikilitic elongate, strained with ilmenite exsolution and 5% recrystallized; plagioclase as prophyroclasts partially recrystallized at perimeter and as intergranular recrystallized polygonal matrix with quartz. Strong foliation defined by localization of oriented hornblende and squeezed out plagioclase porphyroclasts (sheared) into bands. Epidote idioblastic and with allanite cores.	Hornblende slightly gone to biotite/chlorite, plagioclase 2% altered to saussurite	
20 rnblende	Hornblende (75), Epidote (10), Plagioclase (6), Opaques (5), Retrograde Chlorite (3), Hematite (<1), Apatite (<1) (percentages estimated)	Very coarse grained, hornblende poikilitic with ilmenite exsolution dominates with intergranular plagioclase and epidote with large opaques.	Hornblende 4% gone to chlorite and little saussurite. Plagioclase 100% altered to sericite (muscovite)/ saussurite/epidote	Photo 3.12
34 artz orite	Plagioclase (88), Quartz (8), Epidote (3), Opaques (<1), Retrograde Hematite (<1)(percentates estimated)	Coarse grained, plagioclase equigranular subhedral to euhedral with irregularly shaped intergranular quartz.	Plagioclase 99% altered to mostly saussurite with patches of sericite/ penninite/epidote	Photo 3.13

TABLE 3.3

Petrographic Descriptions of Gneisses

ide & ock Type	Mineralogy	Texture	Alteration	Notes
102 neiss	Quartz (39), Plagioclase (An_{38})(30), Biotite (19), Muscovite (10), Epidote (1), Retrograde Chlorite (<1), Opaques (<1), Garnet (<1), Zircon inclusions (percentages from point count)	Medium grained, elongated micas with slight preferred orientation, aligned between equigranular quartz and plagioclase; idioblastic epidote within biotite grains.	Biotite 1% altered to chlorite and epidote, plagioclase 5% altered to sericite/epidote	
113 neiss	Biotite (35), Quartz (32), Plagioclase (An_{47})(28), Epidote (2), Opaques (2), Garnet (<1), Retrograde Chlorite (<1), Hematite (<1), zircon inclusions	Medium grained, elongate tabular biotite defining foliation between quartz and plagioclase showing sub-grain development; idioblastic epidote with allanite cores within biotite and fine grained fractured garnets.	Biotite very little gone to chlorite and plagioclase 1% altered to saussurite	Photo 3.20

TABLE 3.4

Petrographic Descriptions of Quartzite

lide & ɔck Type	Mineralogy	Texture	Alteration	Notes
)10 ıartzite	Feldspar (52), Quartz (38), Chlorite (8), Opaques (<1), Epidote (1), Muscovite (<1), Retrograde Hematite (<1) (percentages from point count)	Medium grained feldspar porphyroclasts sheared into a foliation and surrounded by a fine grained granoblastic quartz matrix. Chlorite/muscovite form anastomosing foliation around grains. Chlorite and epidote veinlets.	Feldspar 30% altered to sericite/saussurite/ epidote	
)21 ıartzite ;82-579 ıartzite	Quartz, Feldspar, Muscovite, Biotite, Hematite, Epidote, Opaques, Garnet (MR82-579 only)	Quartz and poikilitic porphyroclasts in quartz and feldspar granoblastic matrix. Micas aligned with fractures to define slight foliation.	Feldspars altered to saussurite porphyroclasts (MR82-579 only) gone to muscovite along cleavage planes creating distinct inclusions	

TABLE 3.5

Petrographic Descriptions of Other Rock Types

ide & ck Type	Mineralogy	Texture	Alteration	Notes
12 gmatite	K-feldspar (microcline)(55), Plagioclase (30), Muscovite (8), Quartz (5), Epidote (1), Hematite (<1) (percentages from point count)	Very coarse grained, microcline poikilitic, plagioclase (some grains show myromictic texture) muscovite strained, well fractured.	Plagioclase 50% altered to sericite/ saussurite/epidote	Photo 3.21
15 gmatite	Plagioclase (58), Quartz (38), Epidote (2), Hornblende (1), Retrograde Biotite (1), (percentages from point count)	Seriate coarse to medium grained, plagioclase poikilitic and zoned, patch of hornblende not well developed, some allanite cores in epidote.	Plagioclase 15% altered to mostly saussurite, hornblende highly altered to biotite/ chlorite	
29 lcanic	Feldspar (62), Hornblende (30), Opaques (5), Retrograde Chlorite (3), Retrograde Hematite stain throughout (percentages from point count)	Porphyritic with medium grained fractured poikilitic euhedral hornblende phenocrysts in very fine grained matrix of feldspar, acicular hornblende and tiny opaques.	Matrix 95% altered to hematite, phenocrysts 20% to hematite and chlorite	Photo 3.22
33 lcanic	Plagioclase (with quartz) (68), Retrograde chlorite (18), Hornblende (10), Opaques (2), Epidote (1), Retrograde Hematite (<1), (percentages estimated)	Porphyritic with medium grained, zoned, subhedral to euhedral plagioclase and seriate sub to euhedral hornblende phenocrysts in a fine grained matrix of acicular hornblende and equigranular, rounded quartz and plagioclase.	Hornblende highly altered to chlorite (with biotite traces) and plagioclase 80% altered to sericite/ saussurite/epidote	Photo 3.23

ble 3.5 - Page 2

ide & ck Type	Mineralogy	Texture	Alteration	Notes
32B lite	Plagioclase (43), Quartz (31), K-feldspar (18), Muscovite (3), Retrograde Chlorite (3), Epidote (1), (percentages from point count)	Medium to fine grained, equi-granular, anhedral plagioclase slightly coarser and poikilitic; chlorite in fractures.	Plagioclase 95% altered to mainly saussurite, others only very slightly altered	Photo 3.24

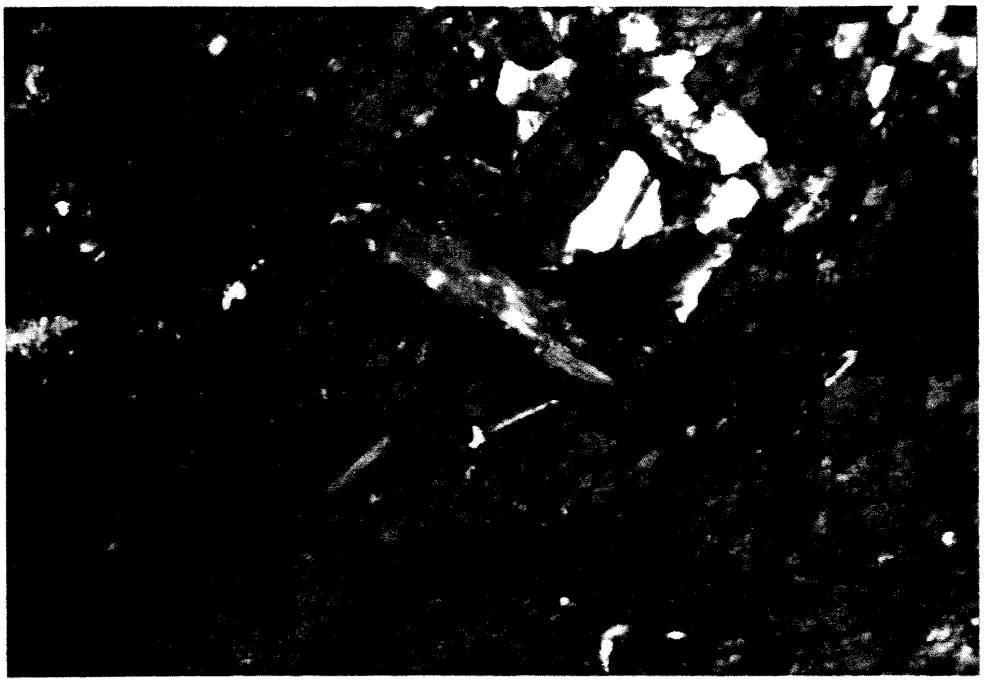

Photo 3.1 Igneous hornblende grain showing ilmenite exsolution and large mica inclusions (KJ23).This grain analysed by microprobe. (Crossed Nicols-XN).

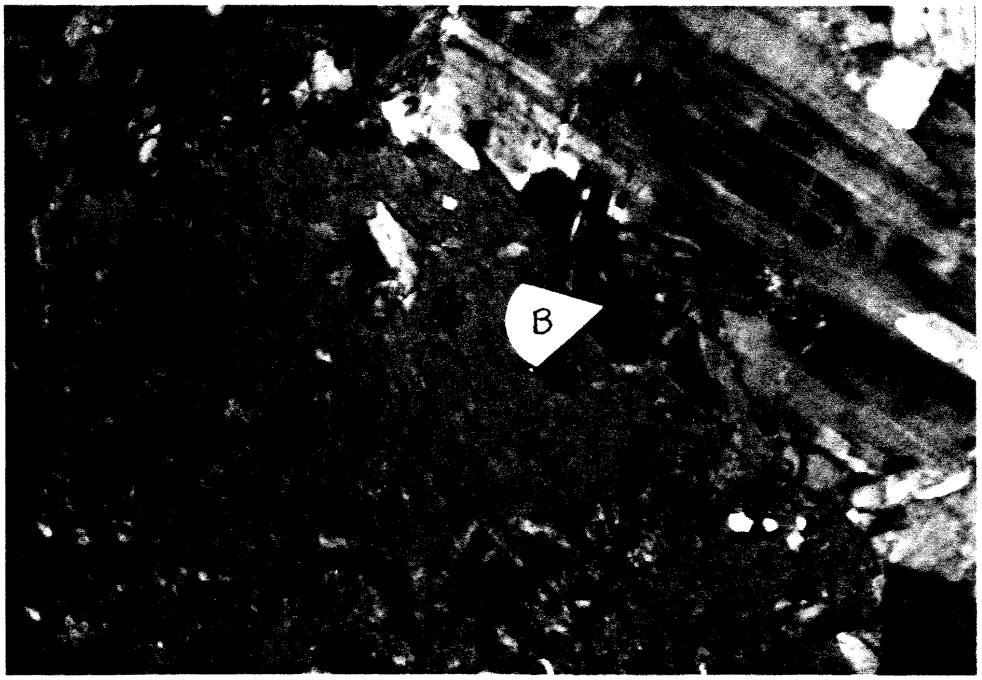

Photo 3.2 Probable igneous hornblende with some alteration to biotite (B) and strained plagioclase (GONS-149).(XN)

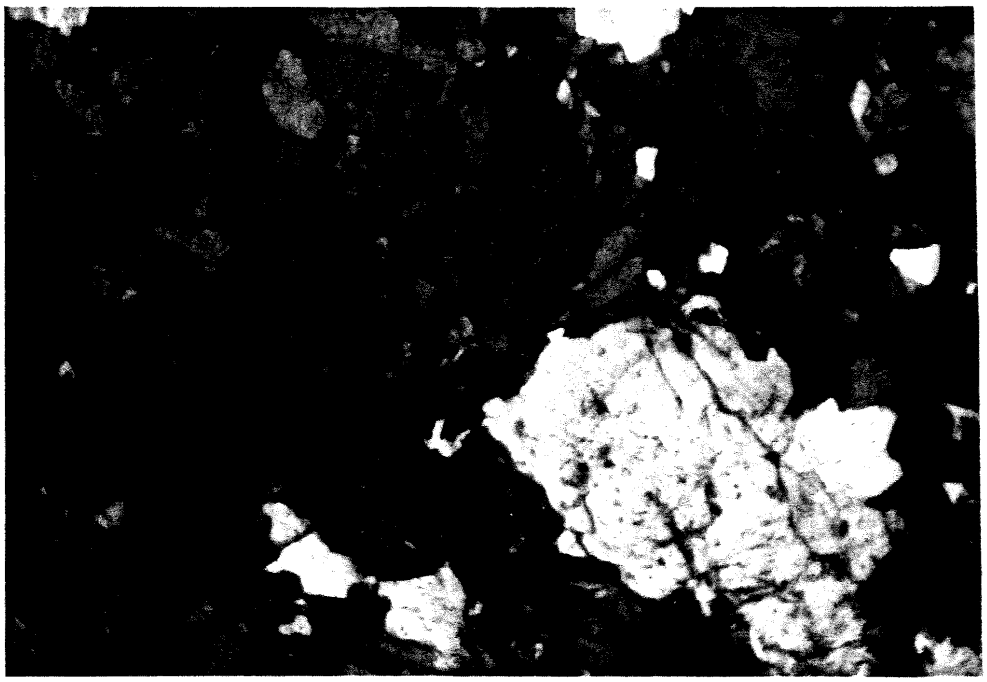

Photo 3.3 Recrystallized hornblende (coloured) and larger plagioclase grains (KJ19).(XN).

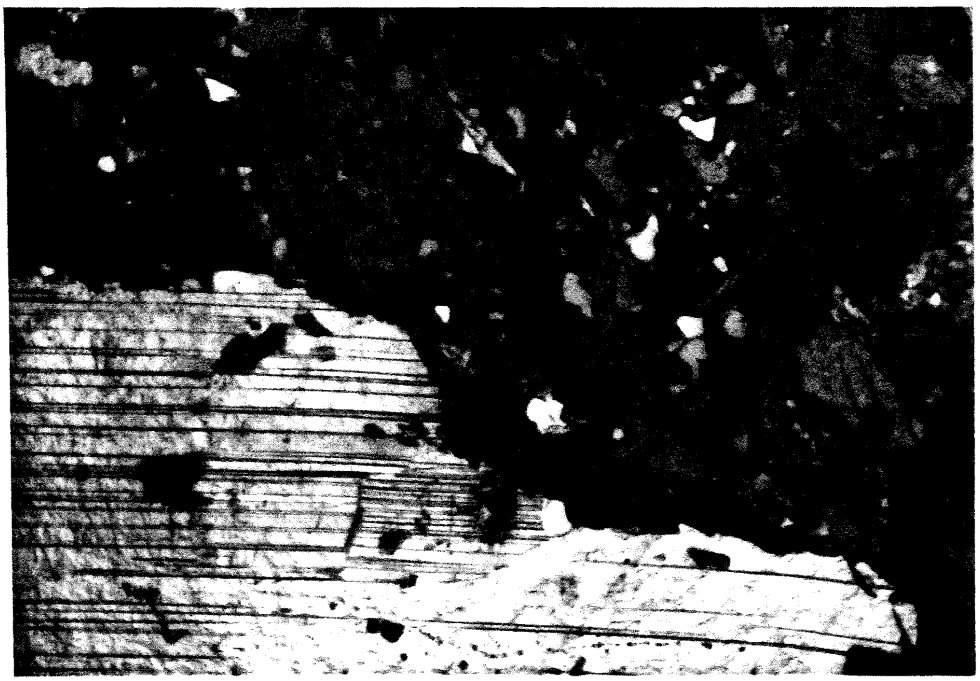

Photo 3.4 Recrystallized hornblende with unrecrystallized plagioclase grain. This slide used for microprobe analysis.(GONS-148).(XN).

Photo 3.5 Large plagioclase grain showing zoning with recrystallized plagioclase (RP) and hornblende altered to chlorite (Ch).(KJ14).(XN).

Photo 3.6 Plagioclase, recrystallized and not, with hornblende showing ilmenite exsolution (KJ08). Analysed by microprobe. (XN).

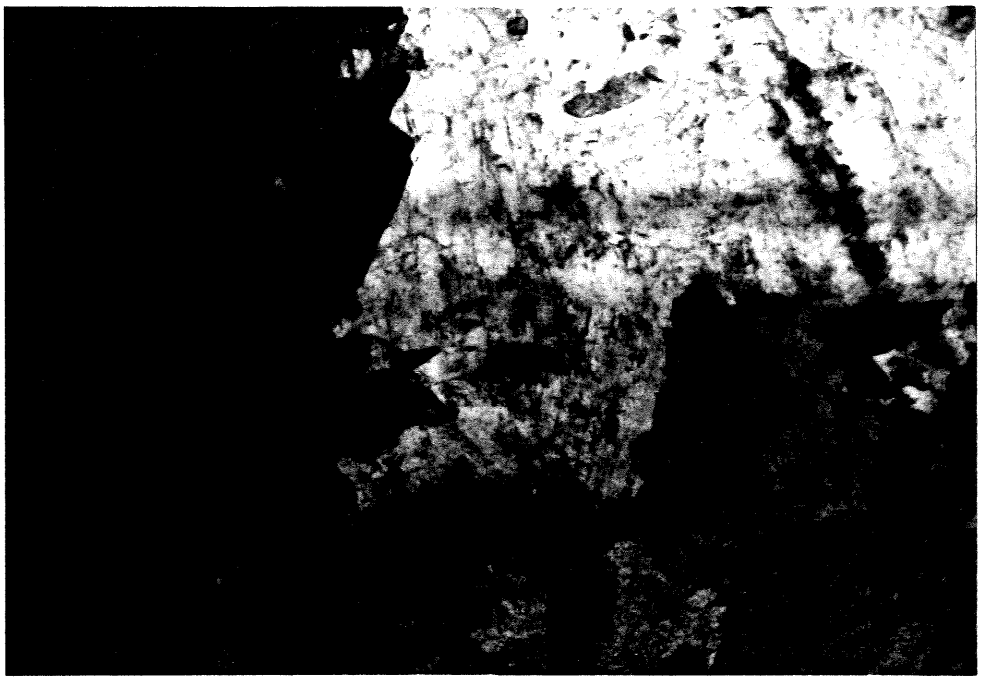

Photo 3.7 Plane polarized light (PPL) view of hornblende and plagioclase, both showing partial recrystallization (KJ03B).

Photo 3.7b Same view as Photo 3.7 in crossed nicols (KJ03B).

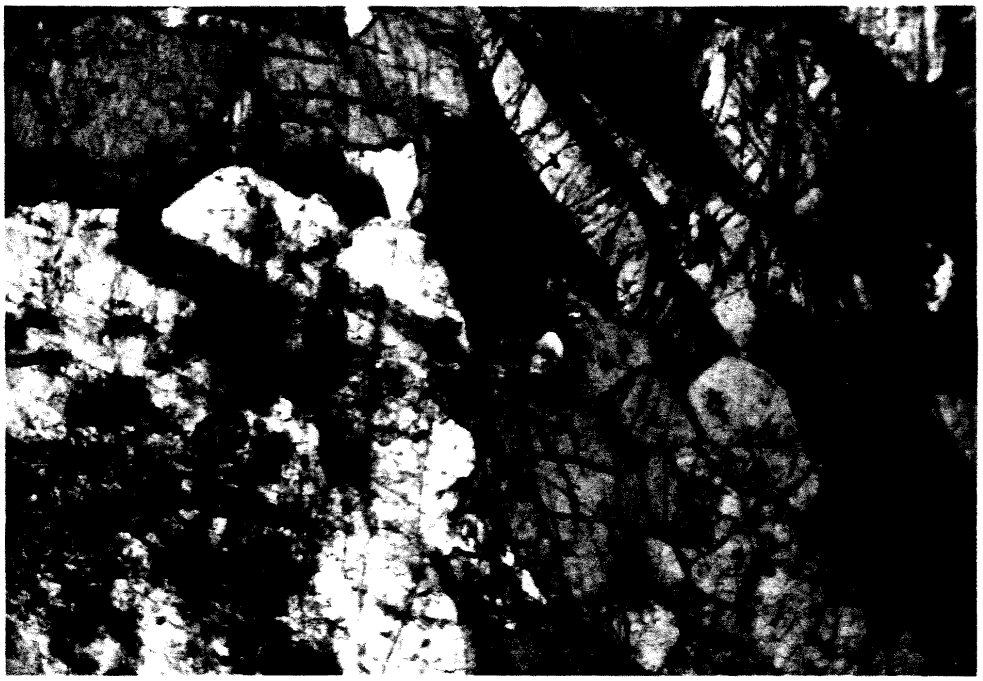

Photo 3.8 Plagioclase showing alteration to sericite and saussurite with recrystallized hornblende (MR81-481).Analysed by microprobe. (XN).

Photo 3.9 Plagioclase highly altered to sericite and epidote. Epidote also as grains (EG) and in a veinlet (EV). Hornblende also present. Epidote here microprobed(KJ23). (XN).

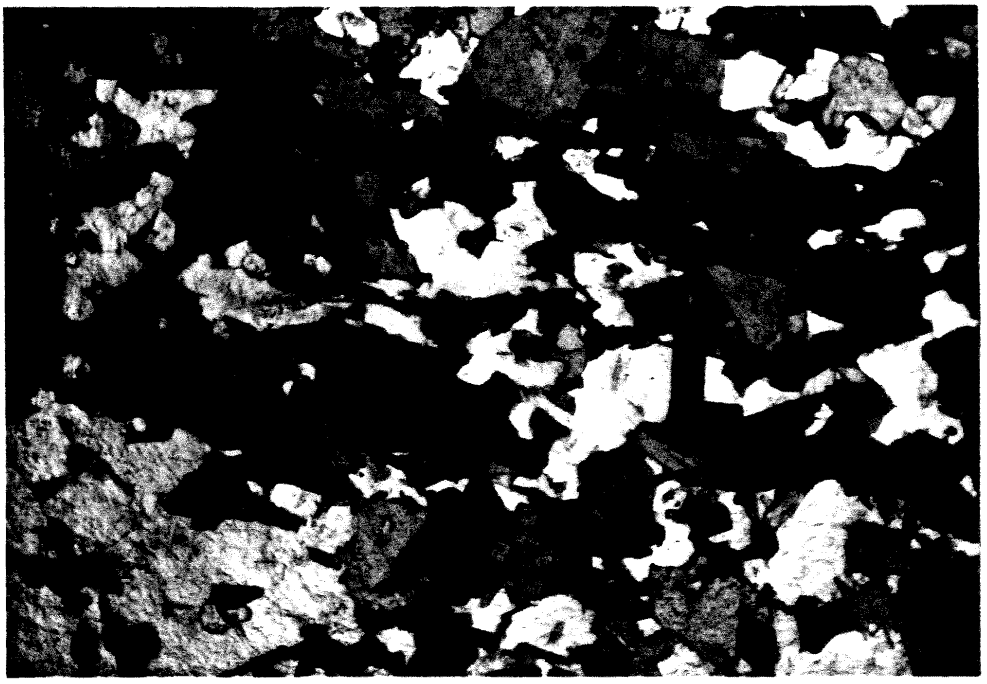

Photo 3.10 Fine grained melanocratic diorite (KJ11).(PPL).

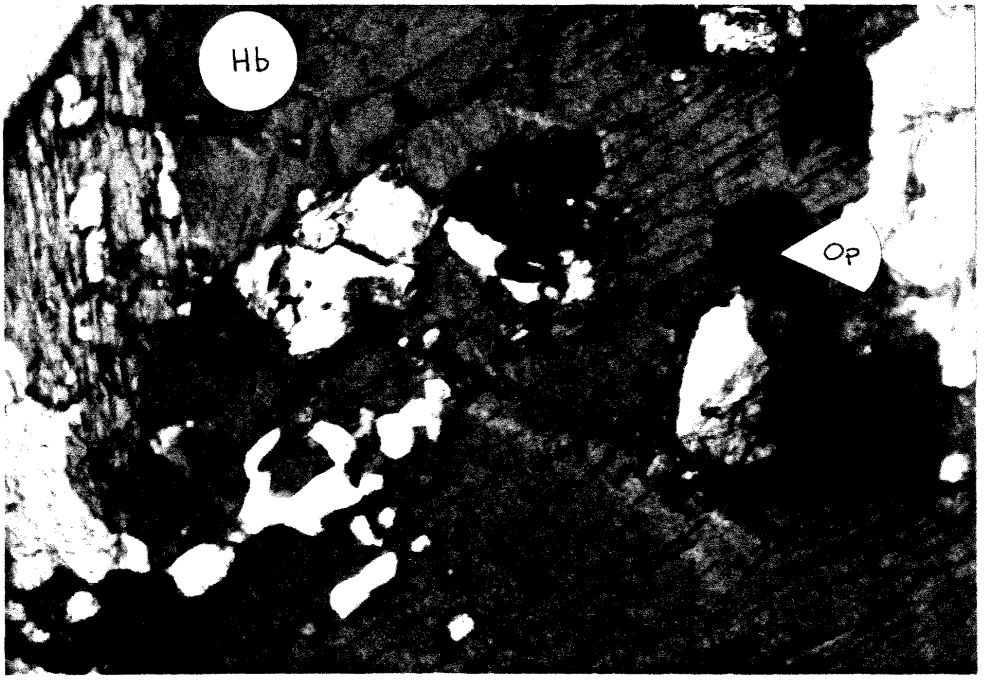

Photo 3.11 Igneous biotite with a kink and included opaques (Op),partially replaced by hornblende (Hb) (KJ30). Analysed by microprobe. (PPL).

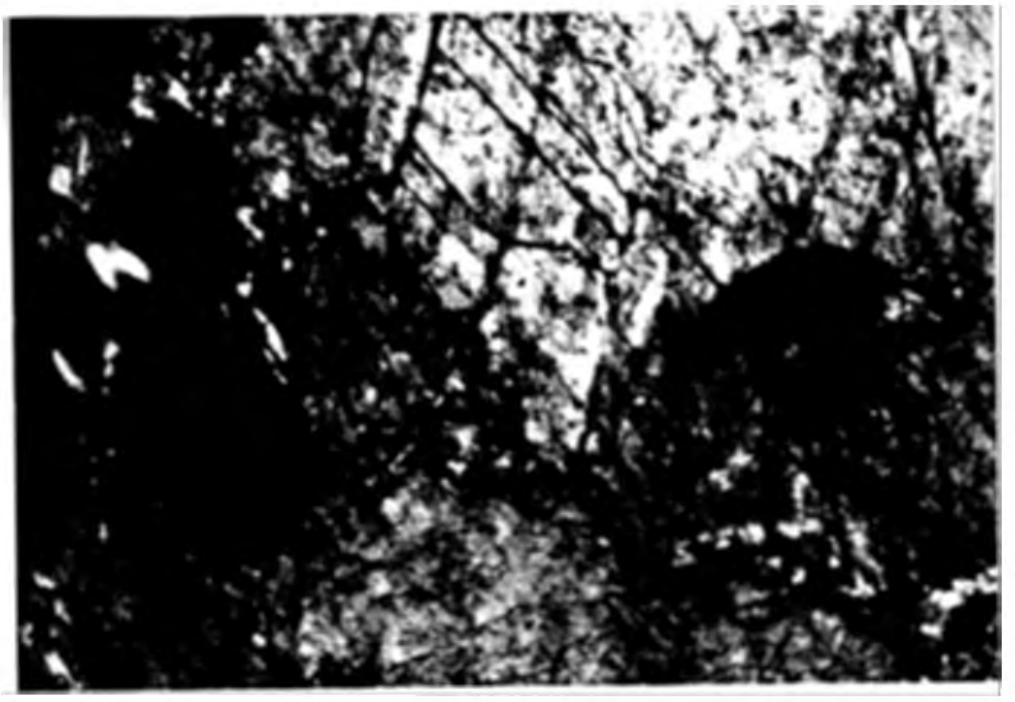

Photo 3.12 Very coarse grained hornblende (igneous) with opaques (KJ20).(XN).

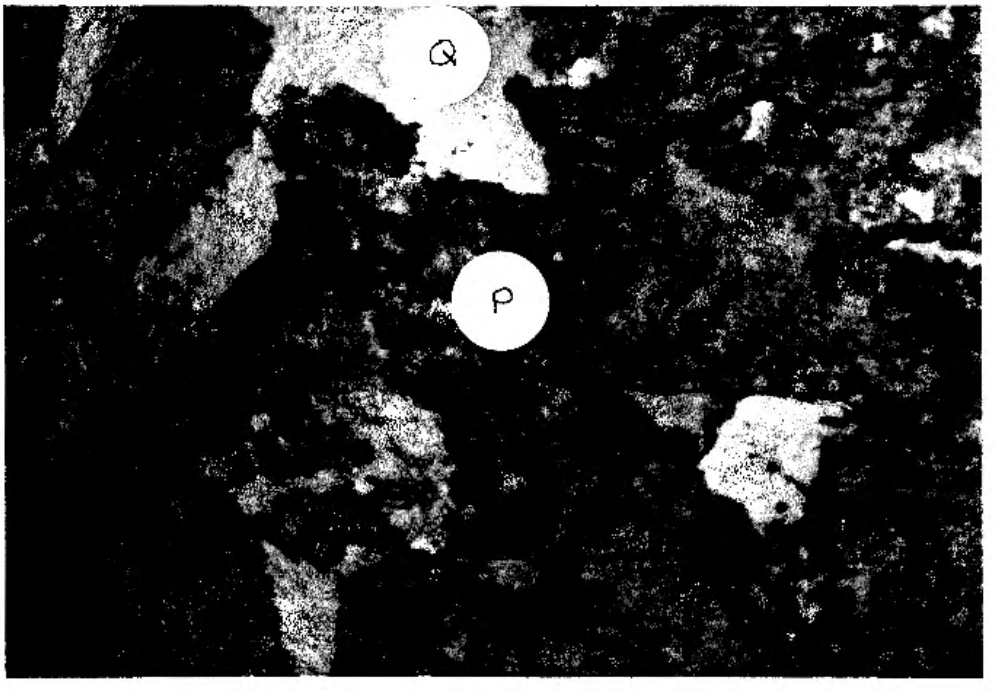

Photo 3.13 Slide entirely extremely altered plagioclase (P) and clean quartz (Q)(KJ34).(PPL).

Photo 3.14 Medium grained phase near contact of KJ09. Plagioclase, hornblende opaque mineralogy. (PPL).

Photo 3.15 Fine grained phase near contact of KJ09 having same mineralogy as above but with flow foliation (PPL).

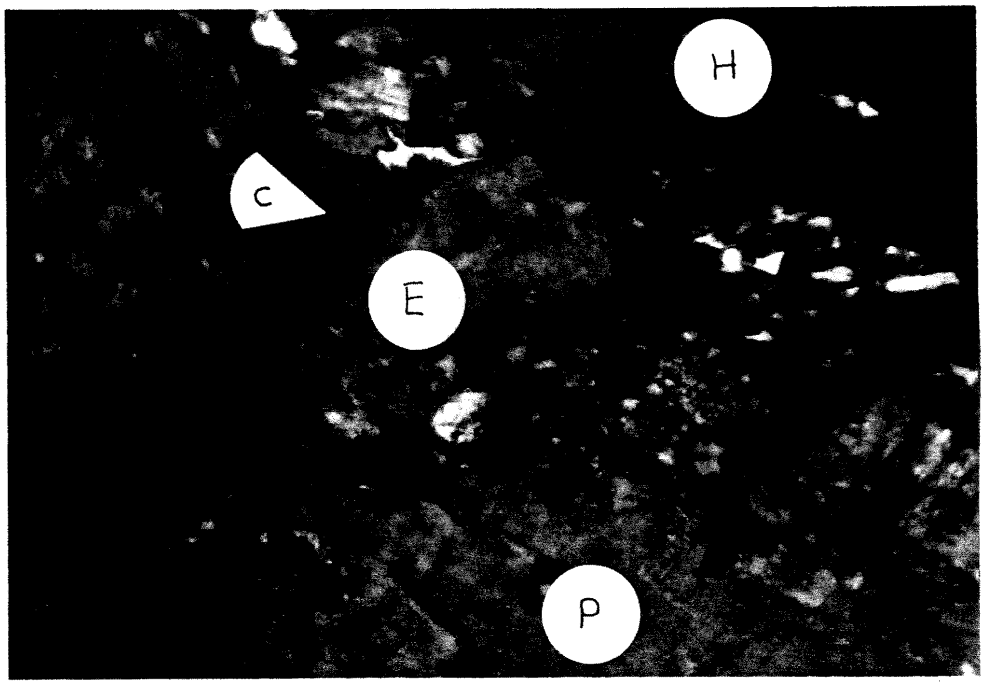

Photo 3.16 Coarse grained hornblende (H), plagioclase (P), and epidote (E) with various alterations (chlorite (C)) (KJ24.2).(XN).

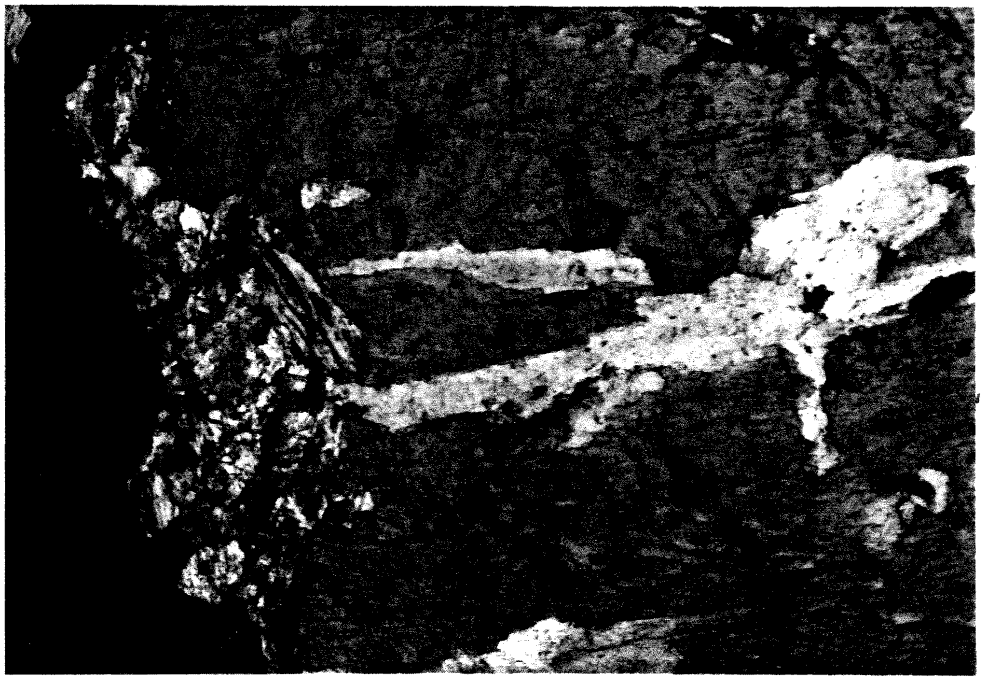

Photo 3.17 Coarse grained hornblende of Zone A, elongated perpendicular to the contact in KJ26. (PPL).

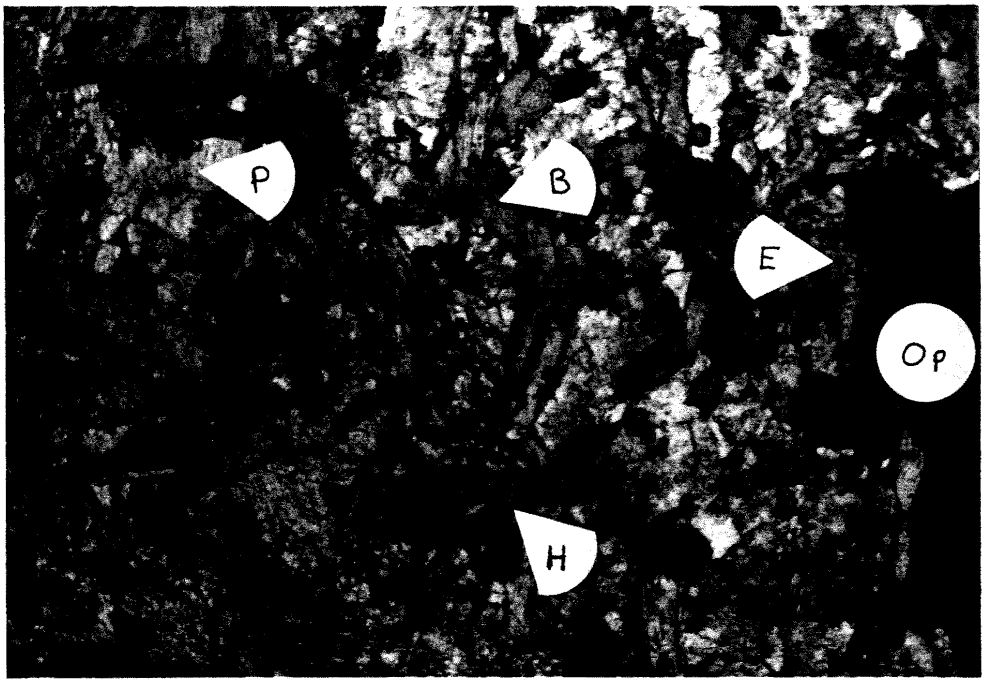

Photo 3.18 Large opaque (Op) , biotite (B) , hornblende (H) , epidote (E) , and plagioclase (P) of Zone B of KJ26. (PPL).

Photo 3.1 Zone C of KJ26 with the same mineralogy as Zone B, but coarser grained. (PPL).

Photo 3.20 Gneiss showing elongate biotite (B) and idioblastic epidote with allanite core (E) in quartz-feldspar matrix (KJ13). (XN).

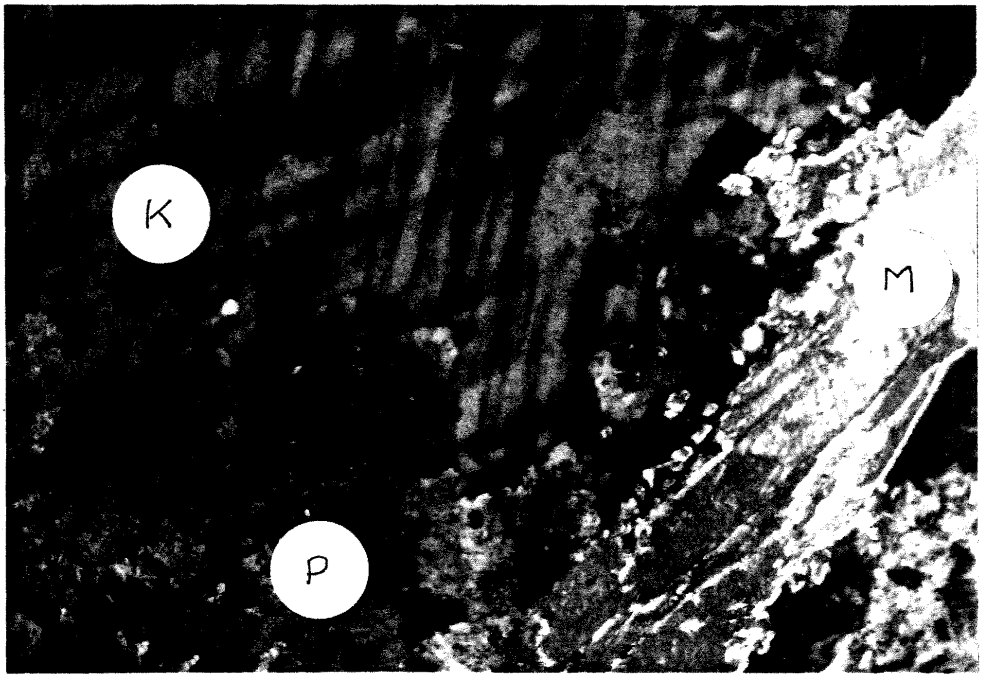

Photo 3.21 Felsic pegmatite with large grains of potassium feldspar (K), muscovite (M), and highly altered plagioclase (P) (KJ12). (XN).

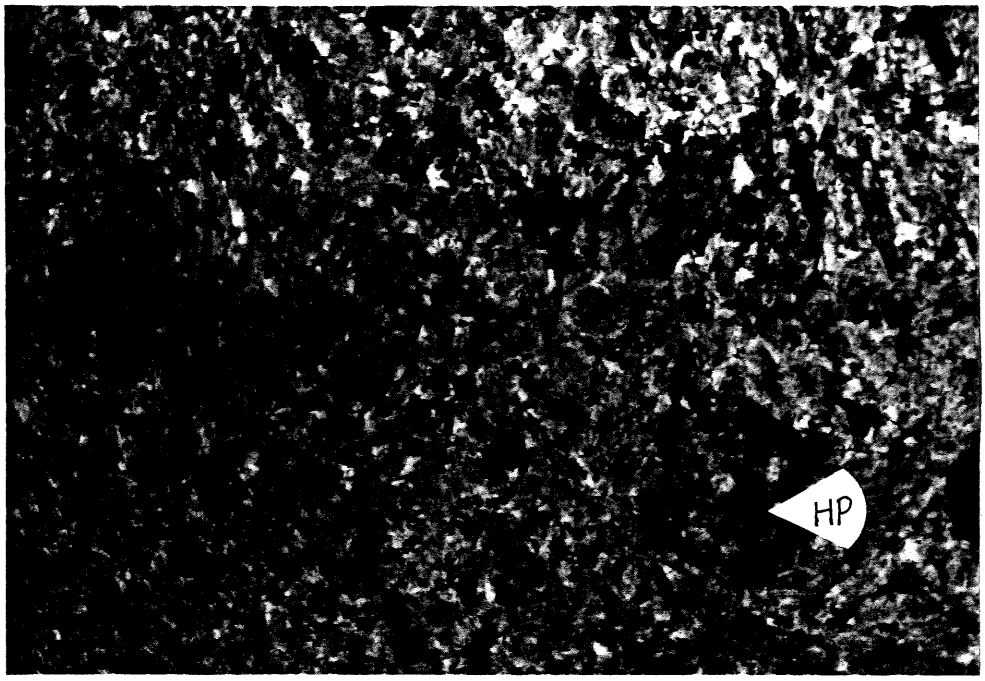

Photo 3.22 Volcanic rock with euhedral hornblende phenocrysts (HP) in a plagioclase-hornblende matrix highly hematite stained (KJ29). (PPL).

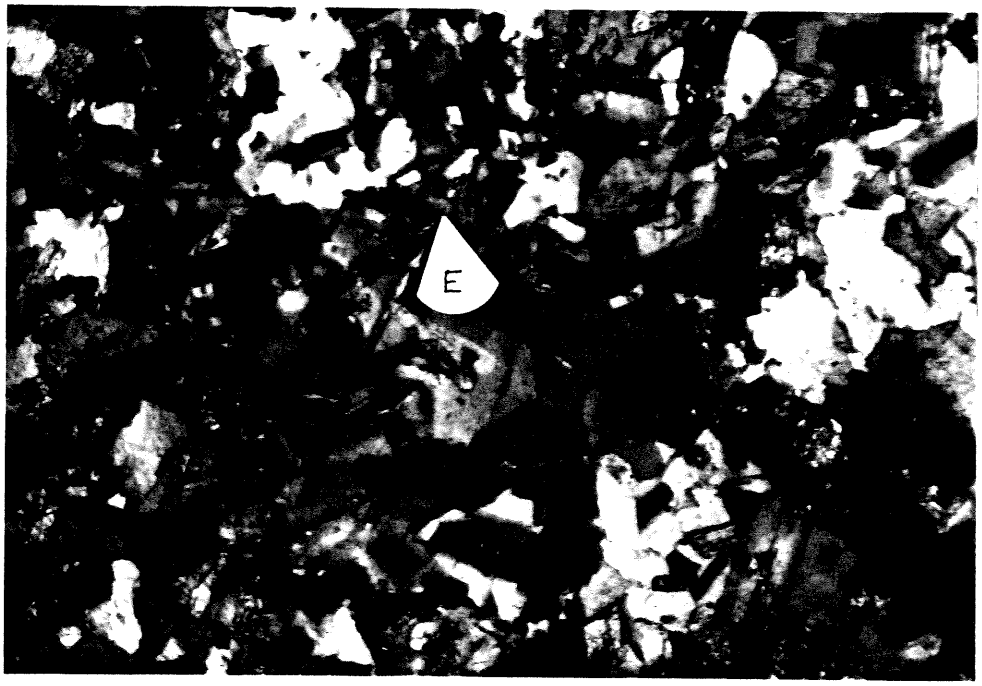

Photo 3.23 Volcanic rock coarser grained than above with relatively minor alteration (epidote (E))(KJ33). (XN).

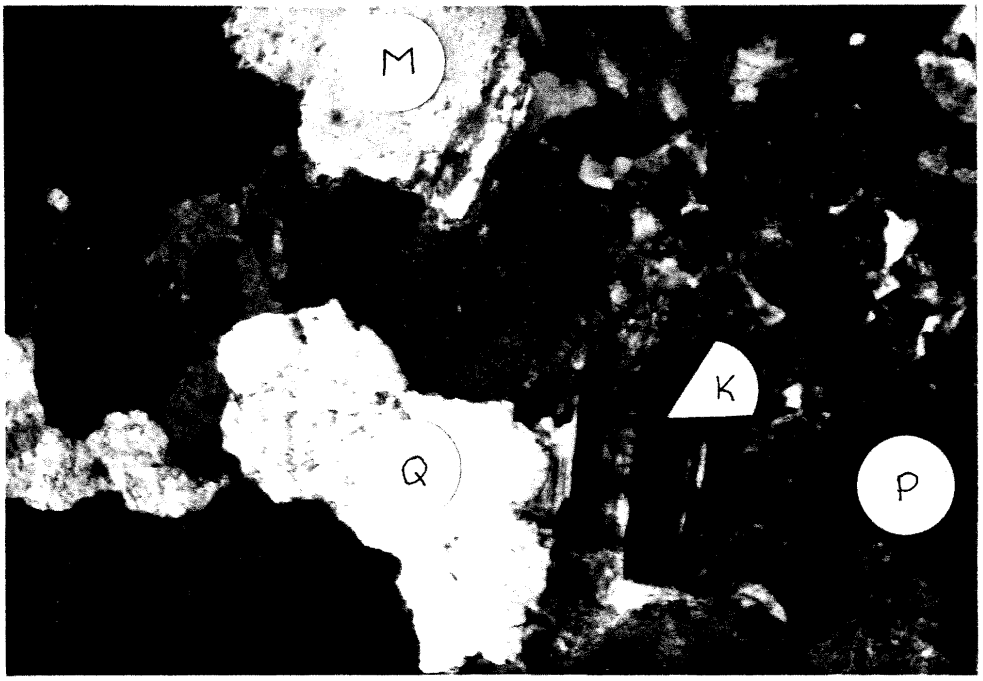

Photo 3.24 Aplite with muscovite (M), quartz (Q), potassium feldspar (K), and highly altered plagioclase (P) (KJ32B). (XN).

CHAPTER 4

MICROPROBE ANALYSES

Introduction

Seven polished thin sections were prepared for electron microprobe analysis of feldspar, hornblende, biotite and epidote. A table listing the seven sections, the minerals analyzed from each and the sample locations appears in Table 4.1. In choosing the slides, even distribution over the area and lack of alteration were desired. Rock samples varied in grain size and mafic proportion and petrographic descriptions are given in the previous chapter. Following is a mineral by mineral examination with emphasis on variations with respect to degree of differentiation and metamorphism.

Feldspar

A total of 37 feldspar analyses were performed and like results from same slides were averaged, giving 24 analyses. All were plagioclase analyses, except two from KJ30 which were of alkali feldspar. Table 4.2 presents the averaged data. Grains are generally medium to coarse, less altered than average for the area, and rather igneous looking, with twinning and little or no sub-grain development. Some were subhedral to euhedral. Only a few analysed grains were determined to be recrystallized, being smaller, non-twinned and of a more granoblastic texture (Photos 3.4, 3.6).

Slide #	Fdspar	Hblde	Biot	Epid	Opaq	Approx. Location
KJ08	*	*		*	*	John MacLeod Brook
KJ16	*	*				North Kathy Road
KJ20		*				West Mariana Road
KJ23	*	*		*		West Mariana Road
KJ30	*	*	*	*	*	East Mariana Road
GONS148	*	*	*		*	East Kathy Road
MR81-481	*	*			*	West Kathy Road

Table 4.1 Minerals analysed from each slide and locations

Figure 4.1 demonstrates the variation in plagioclase compositions within each slide. Tie lines are drawn connecting analyses from the same grain with "C" representing "core" and "R" representing "rim". Analysis points from recrystallized grains are shown as open circles while igneous relict analysis points are shown as closed circles.

Most analyses show compositions from An_{34} to An_{64} (andesine to labradorite). However, GONS-148 is clearly much more calcic, with plagioclase compositions from An_{74} to An_{92} (bytownite to anorthite). This unusually high calcium content in plagioclase is hard to explain. Epidote, which would take calcium from plagioclase, during prograde metamorphic reactions, as it forms, is almost absent in GONS-148, while other sections have considerably more. However, this discrepancy is not sufficient to fully explain the large calcium enrichment. A low An content might suggest a more differentiated rock and KJ30, postulated as such, shows some low An values.

It is apparent from Figure 4.1 that zoning occurs in two directions. Six tie line relationships show sodic rims, while three show calcic rims. The plagioclase phase diagram dictates that igneous zoning will result in an increase in sodium towards the rim. Conversely, increasing metamorphic grade will result in more calcic plagioclase. If recrystallization has occurred, grains will show only metamorphic zoning with calcic rims. However, if plagioclase grains are igneous relicts, zoning may be purely igneous or may have effects of both types of zoning. The degree to which metamorphic zoning overprints igneous zoning determines the apparent direction of zoning

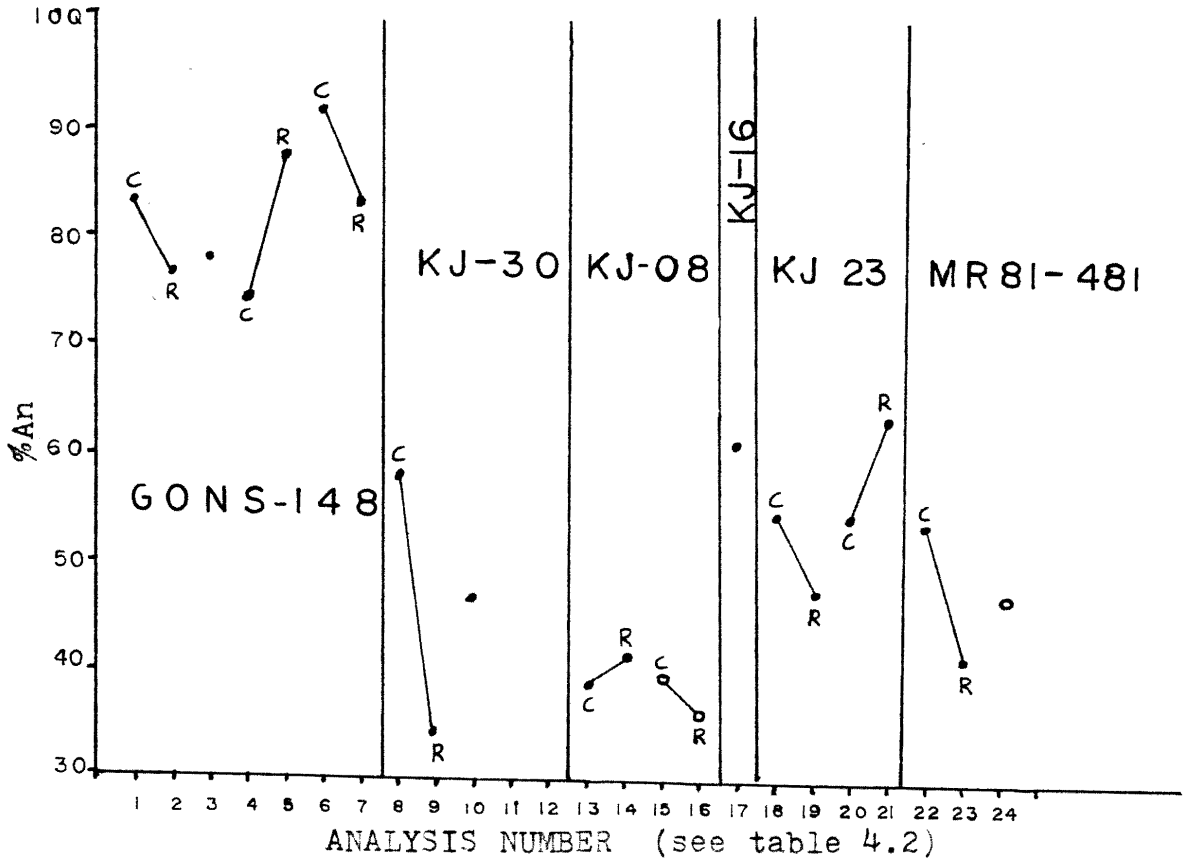

Figure 4.1 Anorthite contents of microprobed plagioclase with tie lines showing zoning (C-core,R-rim). Open circles represent recrystallized grains. Analyses 11 and 12 are alkali feldspars and don't apply here.

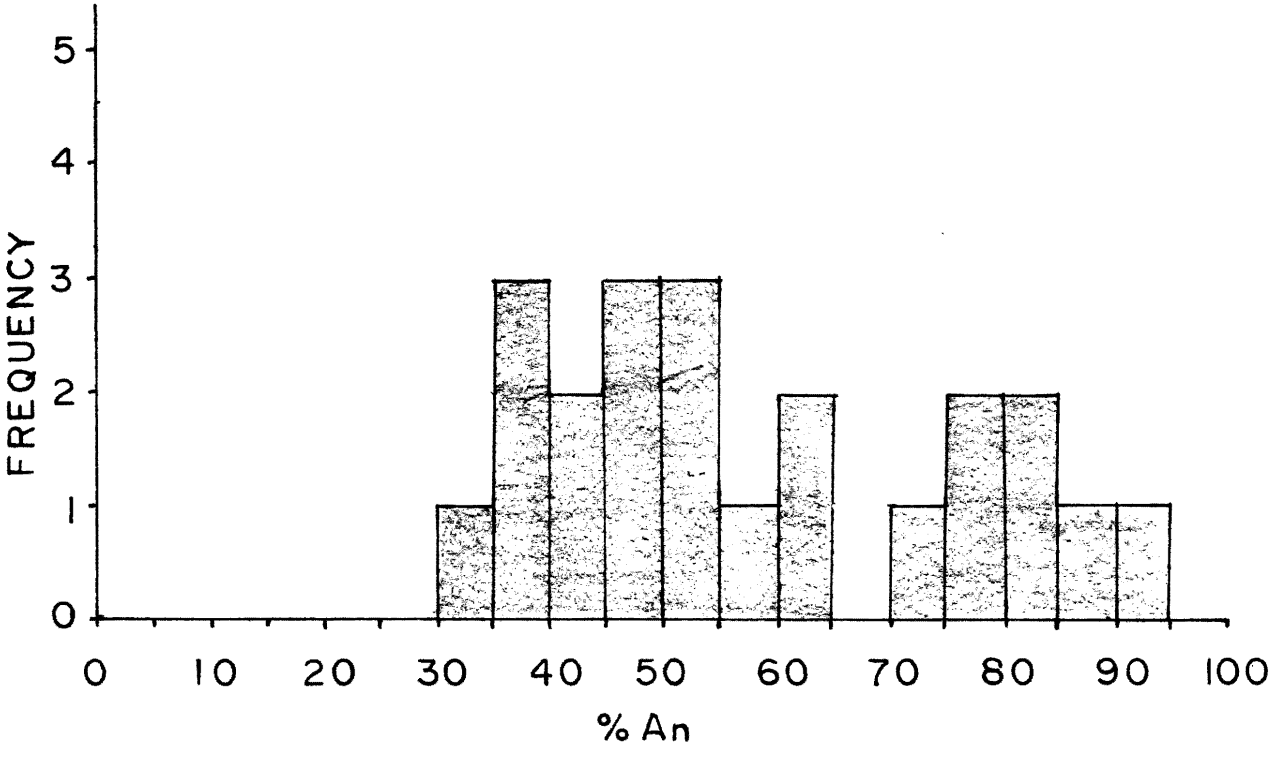

Figure 4.2 Histogram for plagioclase anorthite contents with a 5% interval.

seen in the microprobe data. Presumably, prograde metamorphic processes would procede from grain rims toward the cores, resulting in the zoning effect but this depends on the reactions occurring.

The effects of retrograde metamorphism can also overprint the pre-existing zoning characteristic. This would increase the sodium content similarly. It is quite possible that any combination of igneous, prograde and retrograde zoning may be responsible for the observations, as mineralogical and textural evidence of all three exists in all slides. To fully understand the zoning, a fine grained traverse across each grain is desirable, and all that has been done here is to analyse cores and rims. Therefore, only the resultant zoning can be observed.

There does not seem to be a relationship between zoning direction and texture since both directions were observed in three of the five sections in which zoning was delineated. In fact, in KJ08, a recrystallized grain shows apparent igneous (or retrograde) zoning when prograde zoning would be expected. This suggests that metamorphism was not complete and may have been quite variable spatially and in time.

It should be noted that the separation in composition between core and rim is not necessarily a function solely of the zoning process, but may be due simply to size of the grain or orientation of the analysed cross section. Separations are smaller in KJ08 than others, and this is due, at least in part, to the fact that the grains analysed are much smaller than ones in other slides.

Slide KJ30 contained alkali feldspar and a core and rim analysis was performed on one grain. The orthoclase content increases from Or_{84} to Or_{96} towards the rim, opposite to the direction expected from igneous zoning according to the phase diagram. Although the grain appears like an igneous relict, the zoning may be a metamorphic overprint zoning. The complete analysis appears with plagioclase analyses in Table 4.2. The presence of alkali-feldspar in KJ30, which is also biotite-rich, supports its interpretation as a more differentiated form of diorite. Greater proportions of alkalis (in potassium feldspar and biotite) is a sign of higher degrees of differentiation.

Hornblende

Of 44 hornblende analyses, 24 results were extracted following averaging. The data appears in Table 4.3. Grains, either relict igneous or recrystallized, were analysed from each of seven polished sections. An "R" after any analysis number indicates the grain is considered to be recrystallized. Primary hornblende grains are generally relatively free of alteration, unstrained, but show ilmenite exsolution (Photos 3.1, 3.12). Recrystallized grains are in the form of fine grained polygonal aggregates, totally or partially overgrowing relict grains (Photos 3.4, 3.8).

As an attempt to further classify the hornblendes, Mg/(Mg+Fe) ratios were plotted against Si on a classification diagram proposed by Leake (1978)(Figure 4.3). This diagram is for calcic amphiboles which have greater than 1.34 Ca plus Na X-site atoms per structural formula

	1	2	3	4	5	6
IO2	46.49	48.64	48.36	48.75	46.03	44.76
IO2	0.00	0.00	.02	0.00	0.00	0.00
2O3	33.59	32.05	32.39	32.16	33.43	34.76
2O3	0.00	.03	.02	.05	0.00	0.00
2O3	0.00	0.00	0.00	0.00	0.00	0.00
CO	0.00	.05	.04	.06	.16	.07
NO	0.00	0.00	.03	0.00	0.00	0.00
GO	0.00	0.00	0.00	0.00	0.00	0.00
AO	17.08	15.72	16.12	15.53	17.46	19.05
A2O	1.83	2.04	2.02	2.02	1.39	.87
2O	.02	0.00	.07	.06	0.00	.07
OM	99.22	99.30	99.25	99.52	98.47	99.63

SI	0.696	*	0.993	*	0.902	*	0.967	*	0.596	*	0.211	*
TI	0.000	*	0.000	*	.003	*	0.000	*	0.000	*	0.000	*
AL	7.251	*	6.954	*	7.026	*	6.973	*	7.356	*	7.606	*
FE 3+	0.000	*	0.000	*	0.000	*	0.000	*	0.000	*	0.000	*
FE	0.000	*	.008	*	.006	*	.012	*	.025	*	.011	*
MN	0.000	*	0.000	*	.005	*	0.000	*	0.000	*	0.000	*
MG	0.000	15.948	0.000	15.954	0.000	15.941	0.000	15.954	0.000	15.977	0.000	15.920
CA	3.387	*	3.101	*	3.179	*	3.061	*	3.493	*	3.740	*
NA	.072	*	.942	*	.899	*	1.041	*	.503	*	.213	*
K	.005	4.066	0.000	4.044	.016	4.095	.014	4.116	0.000	3.997	.017	4.120
O	32.000	*	32.000	*	32.000	*	32.000	*	32.000	*	32.000	*

UR	.116	0.000	.401	.342	0.000	.402
AB	16.590	23.307	21.982	25.300	14.292	7.599
AN	83.293	76.693	77.636	74.358	87.408	91.999
QZ	92.739	90.514	90.672	89.469	94.469	96.185
NE	7.193	9.486	9.161	10.390	5.531	3.623
KS	.050	0.000	.167	.140	0.000	.192
F/M	0.000	0.000	0.000	0.000	0.000	0.000
F/FM	0.000	0.000	0.000	0.000	0.000	0.000

1	XXXX	PLAG-1/2 CORES
2	XXXX	PLAG-1/2 RIMS
3	XXXX	PLAG-3
4	XXXX	GDNS-143-PLAG 4 CORE
5	XXXX	GDNS-143-PLAG 4 RIM
6	XXXX	GDNS-146-PLAG 5 CORE

Table 4.2 Microprobe data for plagioclase (Analyses 1-6).

7	8		9	10	11	12
47.38	53.36	SIO2	54.09	56.35	63.28	63.46
0.00	0.00	TIO2	0.00	0.00	0.00	0.00
32.66	29.07	A203	25.07	26.08	18.50	18.35
0.00	0.00	C203	0.00	0.00	0.00	0.00
0.00	0.00	F203	0.00	0.00	0.00	0.00
.04	.06	FEO	0.00	.12	0.00	0.00
0.00	0.00	MNO	0.00	0.00	0.00	0.00
0.00	0.00	MGO	0.00	0.00	0.00	0.00
16.54	12.15	CAO	7.20	9.62	0.00	0.00
1.89	4.87	NA2O	7.49	6.12	1.78	.47
0.00	.05	K2O	.08	.12	13.73	15.40
98.51	99.56	SUM	98.93	98.41	97.29	97.72
3.810 *	9.705 *	SI	10.651 *	10.690 *	11.920 *	11.969 *
0.000 *	0.000 *	TI	0.000 *	0.000 *	0.000 *	0.000 *
7.156 *	6.230 *	AL	5.325 *	5.612 *	4.169 *	4.076 *
0.000 *	0.000 *	FE3+	0.000 *	0.000 *	0.000 *	0.000 *
.006 *	.009 *	FE	0.000 *	.018 *	0.000 *	0.000 *
0.000 *	0.000 *	MN	0.000 *	0.000 *	0.000 *	0.000 *
0.000 15.972	0.000 15.944	MG	0.000 15.976	0.000 15.921	0.000 16.030	0.000 16.047
3.295 *	2.368 *	CA	1.390 *	1.882 *	0.000 *	0.000 *
.881 *	1.717 *	NA	2.618 *	2.167 *	.621 *	.165 *
0.000 3.977	.012 4.097	K	.018 4.026	.028 4.077	3.301 3.952	3.719 3.884
2.000 *	32.000 *	O	32.000 *	32.000 *	32.000 *	32.000 *
0.000	.283	OR	.457	.686	83.538	92.783
17.135	41.921	AB	65.009	53.148	16.462	4.237
82.865	57.796	AN	34.534	46.167	0.000	0.000
92.821	84.879	QZ	80.161	82.421	72.116	75.201
7.179	15.019	NE	19.700	17.355	4.097	1.630
0.000	.101	KS	.138	.224	23.786	23.461
0.000	0.000	F/M	0.000	0.000	0.000	0.000
0.000	0.000	F/FM	0.000	0.000	0.000	0.000

7 XXXX	GONS-148-PLAG 5 RIM
8 XXXX	KJ30-PLAG 1 CORE
9 XXXX	KJ30-PLAG 1 RIM
10 XXXX	KJ30-PLAG 2
11 XXXX	KJ30-KSPAR 1 CORE
12 XXXX	KJ30-KSPAR 1 RIM

Table 4.2 (continued) Microprobe data for plagioclase (Analyses 7-12)

13	14	15	16		17	18
57.67	55.96	57.93	59.28	SIO2	52.63	54.22
0.00	0.00	.02	0.00	TIO2	0.00	0.00
26.11	25.43	26.20	25.27	A203	29.73	28.33
0.00	0.00	.02	0.00	C203	.02	0.00
0.00	0.00	0.00	0.00	F203	0.00	0.00
.31	1.08	.14	.06	FEO	.01	0.00
0.00	0.00	0.00	0.00	MNO	0.00	0.00
0.00	0.00	0.00	0.00	MGO	0.00	0.00
8.17	8.10	8.30	7.36	CAO	12.71	11.56
7.08	6.52	6.85	7.43	NA2O	4.32	5.20
.12	0.00	.10	.02	K2O	.04	.05
99.46	97.09	99.62	99.42	SUM	99.44	99.28

.399	*	10.364	*	10.415	*	10.634	*	SI	9.587	*	9.807	*	
.000	*	0.000	*	.003	*	0.000	*	TI	0.000	*	0.000	*	
.548	*	5.550	*	5.551	*	5.341	*	AL	6.382	*	5.681	*	
.000	*	0.000	*	0.000	*	0.000	*	FE3+	0.000	*	0.000	*	
.047	*	.167	*	.021	*	.009	*	FE	.002	*	0.000	*	
.000	*	0.000	*	0.000	*	0.000	*	MN	0.000	*	0.000	*	
.000	15.994	0.000	16.081	0.000	15.940	0.000	15.984	MG	0.000	15.979	0.000	15.945	
.578	*	1.607	*	1.599	*	1.415	*	CA	2.481	*	2.217	*	
.475	*	4.341	*	2.388	*	2.584	*	NA	1.529	*	1.933	*	
.028	4.061	0.000	3.948	.041	4.028	.005	4.003	K	.009	4.016	.014	4.064	
.000	*	32.000	*	32.000	*	32.000	*	O	32.000	*	32.000	*	
	.076		0.000		1.025		.114	UR		.231		.342	
	00.049		59.293		59.281		64.550	AB		37.995		42.107	
	38.675		40.707		39.694		35.335	AN		61.774		54.551	
	80.001		81.573		81.068		80.422	OZ		80.199		34.231	
	19.183		18.427		18.590		19.543	NE		19.719		19.651	
	.214		0.000		.321		.035	KS		.084		.119	
	0.000		0.000		0.000		0.000	F/M		0.000		0.000	
	0.000		0.000		0.000		0.000	F/FM		0.000		0.000	

13 XXXX	KJ08-PLAG 1 CORE
14 XXXX	KJ08-PLAG 1 RIM
15 XXXX	KJ08-PLAG 2R/3RV CORES
16 XXXX	KJ08-PLAG 2R/3R RIM
17 XXXX	KJ16-PLAG 1/2/3
18 XXXX	KJ23-PLAG 1 CORE

Table 4.2 (continued) Microprobe data for plagioclase (Analyses 13-18).

	19	20	21	22	23	24
O2	56.26	55.09	52.30	55.05	57.01	56.61
O2	0.00	0.00	0.00	0.00	0.00	0.00
O3	27.56	28.04	30.29	28.27	26.23	27.22
O3	.06	.05	0.00	0.00	.07	.02
O3	0.00	0.00	0.00	0.00	0.00	0.00
O	.11	0.00	0.00	0.00	.38	.02
O	0.00	0.00	0.00	0.00	0.00	0.00
O	0.00	0.00	0.00	0.00	.07	0.00
O	9.88	11.45	13.00	10.96	8.49	9.75
2O	6.06	5.18	4.18	5.36	6.78	6.10
O	.12	.15	0.00	0.00	.16	.04
M	100.31	100.71	99.83	99.64	99.12	99.74
I	10.140 *	9.873 *	9.506 *	9.951 *	10.331 *	10.191 *
I	0.000 *	0.000 *	0.000 *	0.000 *	0.000 *	0.000 *
L	5.822 *	6.090 *	6.480 *	6.022 *	5.601 *	5.774 *
E3+	0.000 *	0.000 *	0.000 *	0.000 *	0.000 *	0.000 *
E	.016 *	0.000 *	0.000 *	0.000 *	.058 *	.003 *
N	0.000 *	0.000 *	0.000 *	0.000 *	0.000 *	0.000 *
G	0.000 15.976	0.000 15.963	0.000 15.986	0.000 15.973	.019 16.008	0.000 15.969
A	1.898 *	2.199 *	2.529 *	2.123 *	1.648 *	1.881 *
A	2.113 *	1.800 *	1.471 *	1.879 *	2.382 *	2.129 *
	.027 4.038	.034 4.033	0.000 4.000	0.000 4.001	.037 4.067	.009 4.019
	32.000 *	32.000 *	32.000 *	32.000 *	32.000 *	32.000 *
OR	.679	.850	0.000	0.000	.909	.229
AB	52.329	44.032	36.783	46.949	58.565	52.978
AN	46.991	54.518	63.217	53.051	40.526	46.794
QZ	82.508	84.033	86.597	84.120	81.027	82.657
NE	17.209	15.674	13.403	15.880	18.683	17.268
KS	.223	.293	0.000	0.000	.290	.074
F/M	0.000	0.000	0.000	0.000	3.046	0.000
F/FM	0.000	0.000	0.000	0.000	.753	0.000

19 XXXX	KJ23-PLAG 1 RIM
20 XXXX	KJ23-PLAG 2 CORE
21 XXXX	KJ23-PLAG 2 RIM
22 XXXX	MR81-481-PLAG 1/2 CORES
23 XXXX	MR81-481-PLAG 1 RIM
24 XXXX	MR81-481-PLAG 3R

Table 4.2 (continued) Microprobe data for plagioclase (Analyses 19-24).

PLE	1 KJ20-AMPH 1/2 MIN	INT	MAX	2 KJ20-AMPH 3 MIN	INT	MAX	3 KJ23-AMPH 1 MIN	INT	MAX	4 KJ23-AMPH 2/3 MIN	INT	MAX
2	44.58	44.28	44.23	50.95	50.95	50.95	43.87	43.87	43.87	44.41	44.41	44.41
03	11.63	11.63	11.63	6.19	6.19	6.19	11.27	11.27	11.27	12.03	12.03	12.03
03	1.80	4.45	7.10	1.50	3.15	4.80	1.60	3.35	5.90	3.10	5.25	7.40
5	0.00	0.00	0.00	0.00	0.00	0.00	0.00	0.00	0.00	0.00	0.00	0.00
	12.87	10.49	8.10	10.08	8.60	7.11	12.12	11.28	11.43	14.45	12.56	10.68
	12.30	12.30	12.30	15.86	15.86	15.86	10.35	10.35	10.35	10.75	10.75	10.75
	.16	.16	.16	.12	.12	.12	.21	.21	.21	.19	.19	.19
2	1.22	1.22	1.22	.66	.66	.65	2.14	2.14	2.14	.70	.70	.70
	11.65	11.65	11.65	12.20	12.20	12.20	11.71	11.71	11.71	11.89	11.89	11.89
0	1.45	1.45	1.45	.43	.43	.43	.61	.61	.61	1.07	1.07	1.07
	.22	.22	.22	0.00	0.00	0.00	.42	.42	.42	.65	.65	.65
	0.00	0.00	0.00	0.00	0.00	0.00	0.00	0.00	0.00	0.00	0.00	0.00
	0.00	0.00	0.00	0.00	0.00	0.00	0.00	0.00	0.00	0.00	0.00	0.00
AL	97.88	98.15	98.41	97.99	98.16	98.32	97.70	97.91	98.11	99.24	99.46	99.67
	0.00	0.00	0.00	0.00	0.00	0.00	0.00	0.00	0.00	0.00	0.00	0.00
AL	97.88	98.15	98.41	97.99	98.16	98.32	97.70	97.91	98.11	99.24	99.46	99.67
SI	6.537	6.496	6.455	7.270	7.242	7.214	6.520	6.487	6.455	6.502	6.468	6.435
AL	1.463	1.504	1.545	.730	.758	.786	1.480	1.513	1.545	1.498	1.532	1.565
FE3	0.000	0.000	0.000	0.000	0.000	0.000	0.000	0.000	0.000	0.000	0.000	0.000
AL	.547	.493	.439	.311	.279	.247	.494	.451	.409	.577	.533	.489
FE3	.199	.489	.779	.161	.357	.512	.202	.429	.654	.342	.576	.808
TI	.135	.134	.133	.071	.071	.070	.239	.238	.237	.077	.077	.076
FE2	1.431	1.214	.981	1.084	.953	.823	1.773	1.601	1.407	1.658	1.480	1.282
MN	0.000	0.000	.018	0.000	0.000	0.000	0.000	0.000	.043	0.000	0.000	.022
MG	2.888	2.671	2.454	3.373	3.360	3.347	2.293	2.281	2.270	2.346	2.334	2.322
MG	0.000	0.000	0.000	0.000	0.000	0.000	0.000	0.000	0.000	0.000	0.000	0.000
FE2	.147	.084	0.000	.119	.069	.019	.106	.041	0.000	.111	.044	0.000
MN	.020	.020	.002	.015	.014	.014	.026	.026	.003	.024	.023	.001
CA	1.830	1.819	1.807	1.865	1.858	1.851	1.865	1.855	1.846	1.865	1.855	1.846
NA	.003	.097	.191	.001	.059	.116	.003	.077	.151	.000	.077	.153
CA	0.000	0.000	0.000	0.000	0.000	0.000	0.000	0.000	0.000	0.000	0.000	0.000
NA	.410	.312	.216	.118	.060	.002	.230	.155	.080	.304	.225	.146
K	.041	.041	.041	0.000	0.000	0.000	.080	.079	.079	.121	.121	.120
OH	0.000	0.000	0.000	0.000	0.000	0.000	0.000	0.000	0.000	0.000	0.000	0.000
F	0.000	0.000	0.000	0.000	0.000	0.000	0.000	0.000	0.000	0.000	0.000	0.000
GEN	23.000	23.000	23.000	23.000	23.000	23.000	23.000	23.000	23.000	23.000	23.000	23.000
Z	8.000	8.000	8.000	8.000	8.000	8.000	8.000	8.000	8.000	8.000	8.000	8.000
Y	5.000	5.000	5.000	5.000	5.000	5.000	5.000	5.000	5.000	5.000	5.000	5.000
M4	2.000	2.000	2.000	2.000	2.000	2.000	2.000	2.000	2.000	2.000	2.000	2.000
W	.451	.353	.257	.118	.060	.002	.310	.234	.159	.425	.346	.268
W	.003	.097	.191	.001	.059	.116	.003	.077	.151	.000	.077	.153
Y	1.015	1.249	1.480	.614	.757	.900	1.173	1.326	1.537	1.073	1.203	1.450
Z	1.463	1.504	1.545	.730	.758	.786	1.480	1.513	1.545	1.498	1.532	1.565
X	.451	.353	.257	.118	.060	.002	.310	.234	.159	.425	.346	.268
RATIO	.599	.599	.599	.710	.710	.710	.521	.521	.521	.524	.524	.523
TI	0.000	0.000	0.000	0.000	0.000	0.000	0.000	0.000	0.000	0.000	0.000	0.000
CA	0.000	0.000	0.000	0.000	0.000	0.000	0.000	0.000	0.000	0.000	0.000	0.000
RATIO	.112	.277	.441	.118	.246	.378	.097	.207	.317	.162	.274	.387

Table 4.3 Microprobe data for hornblende (Analyses 1-4).

5 KJ23-AMPH 4R/5R/6R IN	INT	MAX	SAMPLE	6 KJ30-AMPH 1/2/3 MIN	INT	MAX	7 KJ30-AMPH 4 MIN	INT	MAX	8 KJ30-AMPH 5 MIN	INT	MAX
.12	43.12	43.12	SIO2	44.32	44.32	44.32	42.12	42.12	42.12	45.23	45.23	45.23
.96	12.96	12.96	AL203	9.63	9.63	9.63	11.40	11.40	11.40	9.11	9.11	9.11
.80	5.40	7.00	FE203	2.90	4.30	5.70	4.40	5.40	6.40	3.70	3.22	6.80
.00	0.00	0.00	P205	0.00	0.00	0.00	0.00	0.00	0.00	0.00	0.00	0.00
.12	12.68	11.24	FEO	15.12	13.86	12.60	15.21	14.31	13.41	14.30	12.91	11.51
.91	9.91	9.91	MGO	10.47	10.47	10.47	9.24	9.24	9.24	11.11	11.11	11.11
.19	.19	.19	MNO	.36	.35	.35	.37	.37	.37	.47	.47	.47
.49	.49	.49	TIO2	1.23	1.23	1.23	.44	.44	.44	.69	.69	.69
.92	11.92	11.92	CAO	11.88	11.88	11.88	11.88	11.88	11.88	11.97	11.97	11.97
.14	1.14	1.14	NA2O	.80	.80	.80	1.05	1.05	1.05	.75	.75	.75
.49	.49	.49	K2O	.95	.95	.95	1.28	1.28	1.28	.80	.80	.80
.00	0.00	0.00	F	0.00	0.00	0.00	0.00	0.00	0.00	0.00	0.00	0.00
.00	0.00	0.00	H2O	0.00	0.00	0.00	0.00	0.00	0.00	0.00	0.00	0.00
.14	98.30	98.46	TOTAL	97.66	97.80	97.94	97.39	97.49	97.59	98.43	98.59	98.74
.00	0.00	0.00	O=F	0.00	0.00	0.100	0.00	0.00	0.00	0.00	0.00	0.00
.14	98.30	98.46	TOTAL	97.66	97.80	97.94	97.39	97.49	97.59	98.43	98.59	98.74
394	6.369	6.344	Z SI	6.643	6.620	6.597	6.399	6.383	6.367	6.740	6.715	6.690
606	1.631	1.656	AL	1.357	1.380	1.403	1.601	1.617	1.633	1.260	1.285	1.310
000	0.000	0.000	FE3	0.000	0.000	0.000	0.000	0.000	0.000	0.000	0.000	0.000
659	.625	.592	Y AL	.344	.315	.287	.440	.419	.398	.330	.298	.267
425	.001	.776	FE3	.328	.484	.639	.504	.617	.729	.413	.568	.723
055	.054	.054	TI	.139	.138	.138	.050	.050	.050	.077	.077	.077
672	1.538	1.383	FE2	1.851	1.731	1.569	1.914	1.814	1.695	1.729	1.592	1.424
000	0.000	.022	MN	0.000	.001	.045	0.000	.014	.046	0.000	.008	.055
190	2.182	2.173	MG	2.339	2.331	2.323	2.092	2.087	2.082	2.451	2.442	2.433
000	0.000	0.000	M4 MG	0.000	0.000	0.000	0.000	0.000	0.000	0.000	0.000	0.000
079	.029	0.000	FE2	.044	0.000	0.000	.019	0.000	0.000	.041	0.000	0.000
024	.024	.002	MN	.046	.043	.001	.048	.034	.002	.059	.051	.003
894	1.886	1.879	CA	1.908	1.901	1.895	1.934	1.929	1.924	1.899	1.891	1.884
003	.061	.119	NA	.003	.054	.105	.000	.037	.074	.001	.057	.113
000	0.000	0.000	X CA	0.000	0.000	0.000	0.000	0.000	0.000	0.000	0.000	0.000
324	.265	.206	NA	.230	.178	.126	.309	.271	.233	.214	.157	.101
093	.092	.092	K	.182	.181	.180	.248	.247	.247	.151	.151	.150
000	0.000	0.000	OH	0.000	0.000	0.000	0.000	0.000	0.000	0.000	0.000	0.000
000	0.000	0.000	F	0.000	0.000	0.000	0.000	0.000	0.000	0.000	0.000	0.000
000	23.000	23.000	OXYGEN	23.000	23.000	23.000	23.000	23.000	23.000	23.000	23.000	23.000
000	8.000	8.000	SUM Z	8.000	8.000	8.000	8.000	8.000	8.000	8.000	8.000	8.000
000	5.000	5.000	SUM Y	5.000	5.000	5.000	5.000	5.000	5.000	5.000	5.000	5.000
000	2.000	2.000	SUM M4	2.000	2.000	2.000	2.000	2.000	2.000	2.000	2.000	2.000
417	.356	.298	SUM W	.412	.359	.306	.557	.519	.480	.365	.308	.251
003	.061	.119	W	.003	.054	.105	.000	.037	.074	.001	.057	.113
192	1.335	1.476	Y	.948	1.075	1.201	1.044	1.136	1.227	.896	1.035	1.173
606	1.631	1.656	Z	1.357	1.380	1.403	1.601	1.617	1.633	1.260	1.285	1.310
417	.358	.298	X	.412	.359	.306	.557	.519	.480	.365	.308	.251
499	.499	.499	MG RATIO	.508	.508	.508	.457	.457	.457	.522	.522	.522
000	0.000	0.000	TI	0.000	0.000	0.000	0.000	0.000	0.000	0.000	0.000	0.000
000	0.000	0.000	CA	0.000	0.000	0.000	0.000	0.000	0.000	0.000	0.000	0.000
195	.277	.359	FE RATIO	.147	.218	.290	.207	.254	.301	.189	.268	.347

Table 4.3 (continued) Microprobe data for hornblende (Analyses 5-8).

9 KJ30-AMPH 6			10 KJ16-AMPH 1R/2R/3R/4R/6R			SAMPLE	11 KJ16-AMPH 5R			12 KJ08-AMPH 1R/2R		
LN	INT	MAX	MIN	INT	MAX		MIN	INT	MAX	MIN	INT	MAX
.26	43.56	43.56	46.46	46.46	46.46	SIO2	47.90	47.90	47.90	44.54	44.54	44.54
.53	10.53	10.53	10.67	10.67	10.67	AL203	11.19	11.19	11.19	13.34	13.34	13.34
.80	5.20	6.60	2.40	3.70	5.00	FE203	0.00	1.45	2.90	1.20	4.40	7.60
.00	0.00	0.00	0.00	0.00	0.00	P205	0.00	0.00	0.00	0.00	0.00	0.00
.50	14.24	12.98	12.21	11.04	9.87	FEO	13.38	12.08	10.77	14.57	11.69	8.81
.00	10.00	10.00	12.37	12.37	12.37	MGO	12.32	12.32	12.32	10.94	10.94	10.94
.47	.47	.47	.18	.18	.18	MNO	.15	.15	.15	.04	.04	.04
.97	.97	.97	.42	.42	.42	TIO2	.65	.65	.65	.14	.14	.14
.96	11.96	11.96	12.29	12.29	12.29	CAO	11.69	11.69	11.69	11.39	11.39	11.39
.05	1.05	1.05	.81	.81	.81	NA2O	.70	.70	.70	1.48	1.48	1.48
.17	1.17	1.17	.44	.44	.44	K2O	1.06	1.06	1.06	.06	.06	.06
.00	0.00	0.00	0.00	0.00	0.00	F	0.00	0.00	0.00	0.00	0.00	0.00
.00	0.00	0.00	0.00	0.00	0.00	H2O	0.00	0.00	0.00	0.00	0.00	0.00
.01	99.15	99.29	98.25	98.38	98.51	TOTAL	99.04	99.19	99.33	97.70	98.02	98.34
.00	0.00	0.00	0.00	0.00	0.00	O-F	0.00	0.00	0.00	0.00	0.00	0.00
.01	99.15	99.29	98.25	98.38	98.51	TOTAL	99.04	99.19	99.33	97.70	98.02	98.34
196	6.469	6.447	6.756	6.735	6.714	Z SI	6.880	6.857	6.834	6.549	6.498	6.449
508	1.531	1.553	1.244	1.265	1.286	AL	1.120	1.143	1.166	1.451	1.502	1.551
000	0.000	0.000	0.000	0.000	0.000	FE3	0.000	0.000	0.000	0.000	0.000	0.000
341	.313	.284	.585	.558	.532	Y AL	.775	.745	.715	.860	.792	.725
427	.582	.736	.263	.404	.545	FE3	0.000	.139	.312	.193	.464	.829
109	.108	.108	.046	.046	.046	TI	.070	.070	.070	.015	.015	.015
902	1.769	1.607	1.425	1.319	1.193	FE2	1.517	1.400	1.283	1.594	1.329	1.067
000	.015	.059	0.000	0.000	.020	MN	0.000	0.000	0.000	0.000	0.000	.002
224	2.214	2.206	2.681	2.673	2.665	MG	2.638	2.529	2.420	2.397	2.379	2.361
000	0.000	0.000	0.000	0.000	0.000	M4 MG	0.000	0.000	0.000	0.000	0.000	0.000
030	0.000	0.000	.060	.020	0.000	FE2	.090	.046	.002	.198	.097	0.000
059	.045	.000	.022	.022	.002	MN	.018	.018	.018	.003	.003	.003
910	1.903	1.897	1.915	1.909	1.903	CA	1.799	1.793	1.787	1.794	1.781	1.767
001	.052	.103	.003	.049	.095	NA	.092	.143	.193	.063	.116	.230
000	0.000	0.000	0.000	0.000	0.000	X CA	0.000	0.000	0.000	0.000	0.000	0.000
302	.250	.198	.225	.178	.132	NA	.102	.051	.000	.419	.301	.183
222	.222	.221	.082	.081	.081	K	.194	.194	.193	.011	.011	.011
000	0.000	0.000	0.000	0.000	0.000	OH	0.000	0.000	0.000	0.000	0.000	0.000
000	0.000	0.000	0.000	0.000	0.000	F	0.000	0.000	0.000	0.000	0.000	0.000
000	23.000	23.000	23.000	23.000	23.000	OXYGEN	23.000	23.000	23.000	23.000	23.000	23.000
000	8.000	8.000	8.000	8.000	8.000	SUM Z	8.000	8.000	8.000	8.000	8.000	8.000
000	5.000	5.000	5.000	5.000	5.000	SUM Y	5.000	5.000	5.000	5.000	5.000	5.000
000	2.000	2.000	2.000	2.000	2.000	SUM M4	2.000	2.000	2.000	2.000	2.000	2.000
524	.472	.419	.307	.260	.213	SUM W	.297	.245	.193	.430	.312	.195
001	.052	.103	.003	.049	.095	W	.092	.143	.193	.003	.116	.230
985	1.111	1.236	.940	1.054	1.168	Y	.915	1.041	1.166	1.024	1.307	1.589
508	1.531	1.553	1.244	1.265	1.286	Z	1.120	1.143	1.166	1.451	1.502	1.551
524	.472	.419	.307	.260	.213	X	.297	.245	.193	.430	.312	.195
479	.479	.479	.602	.602	.602	MG RATIO	.819	.819	.819	.554	.554	.554
000	0.000	0.000	0.000	0.000	0.000	TI	0.000	0.000	0.000	0.000	0.000	0.000
000	0.000	0.000	0.000	0.000	0.000	CA	0.000	0.000	0.000	0.000	0.000	0.000
181	.248	.314	.150	.232	.313	FE RATIO	0.000	.098	.195	.069	.253	.437

Table 4.3 (continued) Microprobe data for hornblende (Analyses 9-12).

	13 KJ08-AMPH 3R/4R			14 KJ08-AMPH 6			15 KJ08-AMPH 5			SAMPLE	16 GONS-145-AMPH 1		
	MIN	INT	MAX	MIN	INT	MAX	MIN	INT	MAX		MIN	INT	MAX
73	48.73	48.73	48.73	43.70	43.70	43.70	45.47	45.47	45.47	SIO2	43.04	43.04	43.04
94	8.54	8.54	14.36	14.36	14.36	11.17	11.17	11.17	AL2O3	15.27	15.27	15.27	
10	4.55	8.00	2.40	6.05	9.70	2.50	5.95	9.40	FE2O3	3.20	3.33	3.60	
00	0.00	0.00	0.00	0.00	0.00	0.00	0.00	0.00	P2O5	0.00	0.00	0.00	
29	10.19	7.08	14.12	10.84	7.55	13.04	9.94	6.83	FEO	13.93	11.77	9.61	
78	13.78	13.78	10.68	10.68	10.68	12.74	12.74	12.74	MGO	9.56	9.56	9.56	
21	.21	.21	.13	.13	.13	.05	.05	.05	MNO	.18	.18	.18	
49	.49	.49	.31	.31	.31	.57	.57	.57	TIO2	.30	.30	.30	
57	11.57	11.57	11.30	11.30	11.30	10.47	10.47	10.47	CAO	11.76	11.76	11.76	
00	1.00	1.00	1.40	1.40	1.40	.89	.89	.89	NA2O	1.04	1.04	1.04	
16	.16	.16	.14	.14	.14	.29	.29	.29	K2O	.18	.18	.18	
00	0.00	0.00	0.00	0.00	0.00	0.00	0.00	0.00	F	0.00	0.00	0.00	
00	0.00	0.00	0.00	0.00	0.00	0.00	0.00	0.00	H2O	0.00	0.00	0.00	
37	99.22	99.56	98.54	98.91	99.27	97.19	97.54	97.88	TOTAL	98.46	98.70	98.94	
00	0.00	0.00	0.00	0.00	0.00	0.00	0.00	0.00	O-F	0.00	0.00	0.00	
37	99.22	99.56	98.54	98.91	99.27	97.19	97.54	97.88	TOTAL	98.46	98.70	98.94	
12	6.925	6.900	6.387	6.332	6.277	6.679	6.624	6.570	Z SI	6.308	6.272	6.235	
38	1.045	1.100	1.613	1.668	1.723	1.321	1.376	1.430	AL	1.692	1.728	1.764	
00	0.000	0.000	0.000	0.000	0.000	0.000	0.000	0.000	FE3	0.000	0.000	0.000	
50	.392	.325	.861	.784	.708	.613	.542	.472	Y AL	.946	.893	.844	
69	.489	.854	.264	.661	1.050	.277	.653	1.024	FE3	.353	.614	.877	
53	.053	.052	.034	.034	.033	.063	.062	.062	TI	.033	.033	.033	
12	1.134	.839	1.514	1.215	.907	1.258	.976	.699	FE2	1.379	1.301	1.166	
00	0.000	.023	0.000	0.000	.014	0.000	0.000	0.000	MN	0.000	0.000	.020	
26	2.932	2.908	2.327	2.307	2.287	2.789	2.766	2.744	MG	2.089	2.077	2.065	
00	0.000	0.000	0.000	0.000	0.000	0.000	0.000	0.000	M4 MG	0.000	0.000	0.000	
18	.081	0.000	.212	.098	0.000	.344	.235	.127	FE2	.129	.054	0.000	
26	.025	.002	.016	.016	.002	.006	.006	.006	MN	.022	.022	.022	
54	1.759	1.755	1.770	1.754	1.739	1.648	1.634	1.621	CA	1.847	1.835	1.822	
53	.124	.243	.002	.132	.259	.002	.125	.246	NA	.002	.002	.173	
00	0.000	0.000	0.000	0.000	0.000	0.000	0.000	0.000	X CA	0.000	0.000	0.000	
76	.153	.032	.395	.262	.131	.252	.127	.003	NA	.297	.210	.123	
29	.029	.029	.026	.026	.026	.054	.054	.053	K	.034	.033	.033	
00	0.000	0.000	0.000	0.000	0.000	0.000	0.000	0.000	OH	0.000	0.000	0.000	
00	0.000	0.000	0.000	0.000	0.000	0.000	0.000	0.000	F	0.000	0.000	0.000	
00	23.000	23.000	23.000	23.000	23.000	23.000	23.000	23.000	OXYGEN	23.000	23.000	23.000	
00	8.000	8.000	8.000	8.000	8.000	8.000	8.000	8.000	SUM Z	8.000	8.000	8.000	
00	5.000	5.000	5.000	5.000	5.000	5.000	5.000	5.000	SUM Y	5.000	5.000	5.000	
00	2.000	2.000	2.000	2.000	2.000	2.000	2.000	2.000	SUM M4	2.000	2.000	2.000	
05	.182	.061	.421	.288	.156	.306	.180	.057	SUM W	.327	.240	.153	
03	.124	.243	.002	.132	.259	.002	.125	.246	W	.002	.030	.172	
86	.987	1.282	1.194	1.512	1.825	1.016	1.320	1.620	Y	1.356	1.572	1.783	
18	1.045	1.100	1.613	1.668	1.723	1.321	1.376	1.430	Z	1.692	1.728	1.764	
05	.182	.061	.421	.288	.156	.306	.180	.057	X	.327	.240	.153	
29	.629	.629	.537	.537	.537	.597	.597	.597	MG RATIO	.501	.501	.501	
00	0.000	0.000	0.000	0.000	0.000	0.000	0.000	0.000	TI	0.000	0.000	0.000	
00	0.000	0.000	0.000	0.000	0.000	0.000	0.000	0.000	CA	0.000	0.000	0.000	
59	.287	.504	.133	.335	.536	.147	.350	.554	FE RATIO	.171	.300	.429	

Table 4.3 (Continued) Microprobe data for hornblende (Analyses 13-16).

17			18			19			20			
G-I48-AMPH 2R			GUNS-148-AMPH 3			I48 4R/5R/6R/7R			MRB1-481-AMPH 1			SAMPLE
N	INT	MAX	MIN	INT	MAX	MIN	INT	MAX	MIN	INT	MAX	
48	44.48	44.48	44.80	44.80	44.80	43.32	43.32	43.32	51.37	51.37	51.37	SIO2
27	13.27	13.27	13.31	13.31	13.31	14.62	14.62	14.62	6.54	6.54	6.54	AL2O3
40	5.55	8.70	4.40	5.85	7.30	2.50	5.70	8.90	1.00	3.55	6.10	FE2O3
00	0.00	0.00	0.00	0.00	0.00	0.00	0.00	0.00	0.00	0.00	0.00	P2O5
09	11.66	8.42	12.47	11.17	9.86	14.80	11.92	9.04	10.32	8.03	5.73	FEO
72	10.72	10.72	10.79	10.79	10.79	9.89	9.89	9.89	16.28	16.28	16.28	MGO
26	.26	.26	.23	.23	.23	.28	.28	.28	.12	.12	.12	MNO
46	.46	.46	.35	.35	.35	.49	.49	.49	.36	.36	.36	TIO2
49	11.49	11.49	11.48	11.48	11.48	11.45	11.45	11.45	11.94	11.94	11.94	CAO
09	1.09	1.09	.38	.38	.38	1.22	1.22	1.22	.66	.66	.66	NA2O
19	.19	.19	.12	.12	.12	.37	.37	.37	0.00	0.00	0.00	K2O
00	0.00	0.00	0.00	0.00	0.00	0.00	0.00	0.00	0.00	0.00	0.00	F
00	0.00	0.00	0.00	0.00	0.00	0.00	0.00	0.00	0.00	0.00	0.00	H2O
45	98.77	99.08	98.33	98.48	98.62	98.94	99.26	99.58	98.59	98.85	99.10	TOTAL
00	0.00	0.00	0.00	0.00	0.00	0.00	0.00	0.00	0.00	0.00	0.00	O=F
45	98.77	99.08	98.33	98.48	98.62	98.94	99.26	99.58	98.59	98.85	99.10	TOTAL
04	6.452	6.407	6.510	6.496	6.473	6.343	6.294	6.246	7.275	7.232	7.190	Z SI
96	1.545	1.593	1.482	1.504	1.527	1.657	1.706	1.754	.725	.768	.810	AL
00	0.000	0.000	0.000	0.000	0.000	0.000	0.000	0.000	0.000	0.000	0.000	FE3
61	.725	.660	.800	.770	.740	.865	.798	.731	.367	.317	.269	Y AL
64	.007	.944	.482	.639	.792	.276	.624	.967	.107	.377	.643	FE3
51	.050	.050	.038	.038	.038	.054	.054	.053	.038	.038	.038	TI
58	1.249	1.014	1.339	1.221	1.103	1.647	1.383	1.090	1.052	.852	.654	FE2
00	0.000	.030	0.000	0.000	0.000	0.000	0.000	.033	0.000	0.000	0.000	MN
36	2.319	2.302	2.340	2.332	2.324	2.158	2.142	2.126	3.437	3.416	3.396	MG
00	0.000	0.000	0.000	0.000	0.000	0.000	0.000	0.000	0.000	0.000	0.000	M4 MG
65	.067	0.000	.179	.133	.088	.166	.066	0.000	.171	.093	.017	FE2
32	.032	.002	.028	.028	.028	.035	.034	.001	.014	.014	.014	MN
00	1.787	1.773	1.790	1.783	1.777	1.796	1.782	1.769	1.812	1.801	1.791	CA
02	.115	.225	.004	.055	.106	.004	.118	.230	.003	.091	.178	NA
00	0.000	0.000	0.000	0.000	0.000	0.000	0.000	0.000	0.000	0.000	0.000	X CA
07	.192	.079	.104	.052	.000	.343	.226	.111	.178	.089	.001	NA
35	.035	.035	.022	.022	.022	.069	.069	.068	0.000	0.000	0.000	K
00	0.000	0.000	0.000	0.000	0.000	0.000	0.000	0.000	0.000	0.000	0.000	OH
00	0.000	0.000	0.000	0.000	0.000	0.000	0.000	0.000	0.000	0.000	0.000	F
00	23.000	23.000	23.000	23.000	23.000	23.000	23.000	23.000	23.000	23.000	23.000	OXYGEN
00	8.000	8.000	8.000	8.000	8.000	8.000	8.000	8.000	8.000	8.000	8.000	SUM Z
00	5.000	5.000	5.000	5.000	5.000	5.000	5.000	5.000	5.000	5.000	5.000	SUM Y
00	2.000	2.000	2.000	2.000	2.000	2.000	2.000	2.000	2.000	2.000	2.000	SUM M4
42	.227	.114	.126	.074	.022	.412	.295	.179	.178	.089	.001	SUM W
02	.115	.225	.004	.055	.106	.004	.118	.230	.003	.091	.178	W
56	1.432	1.704	1.359	1.486	1.611	1.249	1.529	1.804	.550	.770	.988	Y
96	1.545	1.593	1.482	1.504	1.527	1.657	1.706	1.754	.725	.768	.810	Z
42	.227	.114	.126	.074	.022	.412	.295	.179	.178	.089	.001	X
36	.536	.536	.536	.536	.536	.504	.504	.504	.719	.719	.719	MG RATIO
00	0.000	0.000	0.000	0.000	0.000	0.000	0.000	0.000	0.000	0.000	0.000	TI
00	0.000	0.000	0.000	0.000	0.000	0.000	0.000	0.000	0.000	0.000	0.000	CA
33	.308	.482	.241	.321	.400	.132	.301	.470	.080	.285	.490	FE RATIO

Table 4.3 (continued) Microprobe data for hornblende (Analyses 17-20).

MPLE	481-A 2R/4R/5R			481-A 3/7/9/10			481-AMPH 6R			481-AMPH 8R		
	MIN	INT	MAX	MIN	INT	MAX	MIN	INT	MAX	MIN	INT	MAX
02	49.13	49.13	49.13	47.76	47.78	47.78	46.10	46.10	46.10	50.24	50.24	50.24
203	8.76	8.76	8.76	10.36	10.36	10.36	11.70	11.70	11.70	7.19	7.19	7.19
203	1.10	4.30	7.50	.90	4.10	7.30	.90	4.30	7.70	1.40	3.70	6.00
05	0.00	0.00	0.00	0.00	0.00	0.00	0.00	0.00	0.00	0.00	0.00	0.00
0	10.82	7.9x	5.06	12.04	x.16	8.28	12.49	9.43	6.37	10.44	8.37	6.30
0	15.14	15.14	15.14	13.97	13.97	13.97	13.12	13.12	13.12	15.61	15.61	15.61
0	.06	.06	.06	.11	.11	.11	.08	.08	.08	.05	.05	.05
02	.34	.34	.34	.60	.60	.60	.60	.60	.60	.31	.31	.31
0	11.74	11.74	11.74	11.73	11.73	11.73	11.51	11.51	11.51	11.72	11.72	11.72
20	.95	.95	.95	1.11	1.11	1.11	1.34	1.34	1.34	.59	.59	.59
0	.06	.06	.06	.14	.14	.14	.13	.13	.13	0.00	0.00	0.00
	0.00	0.00	0.00	0.00	0.00	0.00	0.00	0.00	0.00	0.00	0.00	0.00
0	0.00	0.00	0.00	0.00	0.00	0.00	0.00	0.00	0.00	0.00	0.00	0.00
TAL	98.10	98.42	98.74	98.74	99.06	99.38	97.97	98.31	98.65	97.55	97.78	98.01
F	0.00	0.00	0.00	0.00	0.00	0.00	0.00	0.00	0.00	0.00	0.00	0.00
TAL	98.10	98.42	98.74	98.74	99.06	99.38	97.97	98.31	98.65	97.55	97.78	98.01
SI	7.031	6.979	6.927	6.846	6.795	6.745	6.686	6.632	6.579	7.204	7.165	7.126
AL	.969	1.021	1.073	1.154	1.205	1.255	1.314	1.368	1.421	.796	.835	.874
FE3	0.000	0.000	0.000	0.000	0.000	0.000	0.000	0.000	0.000	0.000	0.000	0.000
AL	.509	.446	.383	.596	.532	.468	.686	.616	.547	.419	.373	.328
FE3	.119	.460	.797	.097	.439	.777	.098	.466	.826	.151	.398	.641
TI	.037	.036	.036	.065	.064	.064	.065	.065	.064	.033	.033	.033
FE2	1.106	.852	.597	1.258	1.003	.742	1.314	1.040	.760	1.061	.878	.697
MN	0.000	0.000	.006	0.000	0.000	.010	0.000	0.000	.009	0.000	0.000	0.000
MG	3.230	3.206	3.182	2.984	2.961	2.939	2.836	2.813	2.791	3.336	3.318	3.300
MG	0.000	0.000	0.000	0.000	0.000	0.000	0.000	0.000	0.000	0.000	0.000	0.000
E.2	.189	.091	0.000	.184	.086	0.000	.201	.095	0.000	.191	.121	.051
MN	.007	.007	.002	.013	.013	.003	.010	.010	.001	.006	.006	.006
CA	1.800	1.787	1.774	1.801	1.787	1.774	1.789	1.774	1.760	1.800	1.791	1.781
NA	.003	.113	.223	.001	.113	.223	.001	.121	.239	.002	.083	.162
CA	0.000	0.000	0.000	0.000	0.000	0.000	0.000	0.000	0.000	0.000	0.000	0.000
NA	.260	.147	.035	.307	.193	.081	.376	.253	.132	.162	.081	.000
K	.011	.011	.011	.026	.025	.025	.024	.024	.024	0.000	0.000	0.000
OH	0.000	0.000	0.000	0.000	0.000	0.000	0.000	0.000	0.000	0.000	0.000	0.000
F	0.000	0.000	0.000	0.000	0.000	0.000	0.000	0.000	0.000	0.000	0.000	0.000
(GEN	23.000	23.000	23.000	23.000	23.000	23.000	23.000	23.000	23.000	23.000	23.000	23.000
1 Z	8.000	8.000	8.000	8.000	8.000	8.000	8.000	8.000	8.000	8.000	8.000	8.000
1 Y	5.000	5.000	5.000	5.000	5.000	5.000	5.000	5.000	5.000	5.000	5.000	5.000
1 M4	2.000	2.000	2.000	2.000	2.000	2.000	2.000	2.000	2.000	2.000	2.000	2.000
1 W	.271	.158	.046	.333	.218	.106	.400	.277	.155	.162	.081	.000
W	.003	.115	.225	.001	.113	.223	.001	.121	.239	.002	.083	.162
Y	.701	.978	1.252	.822	1.099	1.372	.915	1.212	1.504	.637	.837	1.036
Z	.969	1.021	1.073	1.154	1.205	1.255	1.314	1.368	1.421	.796	.835	.874
X	.271	.158	.046	.333	.218	.106	.400	.277	.155	.162	.081	.000
RATIO	.694	.694	.694	.658	.658	.657	.636	.636	.636	.703	.703	.703
TI	0.000	0.000	0.000	0.000	0.000	0.000	0.000	0.000	0.000	0.000	0.000	0.000
CA	0.000	0.000	0.000	0.000	0.000	0.000	0.000	0.000	0.000	0.000	0.000	0.000
RATIO	.084	.328	.572	.063	.287	.512	.061	.291	.521	.108	.285	.462

Table 4.3 (continued) Microprobe data for hornblende (Analyses 21-24).

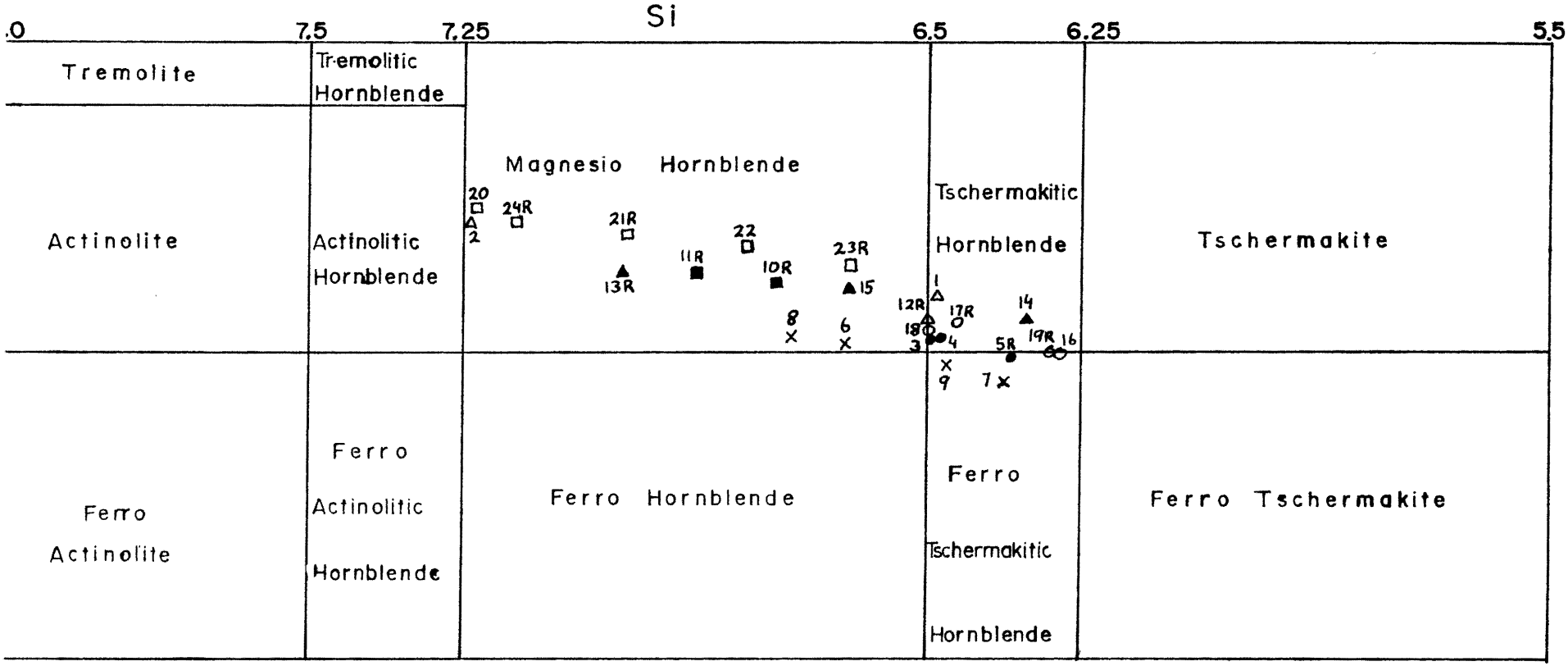

Figure 4.3 Plot of silicon versus magnesium ratio (atoms per unit formula) for Ti and A-site elements both less than 0.50, after Leake (1978). "R"-recrystallized. Numbers refer to hornblende analyses (Table 4.3).

unit, with Na alone less than 0.67. Use of this diagram also requires that Ti <0.50 and A-site Na+K <0.50. All thesis hornblendes plot as magnesio-hornblende or tschermakitic-hornblende (analysis 9 from KJ30 is a ferro-tschermatritic hornblende) with the exception of analysis 7 from KJ30. Since its A-site alkalis are greater than 0.5 it is subject to a different plot not reproduced here, and is termed a ferroan pargasitic hornblende. Analyses 7 and 9 and others from KJ30 are all low in magnesium relative to iron, a trend expected from more differentiated rocks. Recrystallized hornblende analyses are well scattered within the region of plotted points and no chemical separation between primary and recrystallized grains is evident from this plot.

To further examine variation, a plot of tetrahedral aluminium versus the alkalis (sodium plus potassium) is presented as Figure 4.4. Igneous hornblendes tend to plot in regions of greater than 1.8 Al^{IV} and greater than 0.8 (Na+K) while metamorphic hornblendes plot closer to the origin (Jamieson, 1981). By this criterion, all analyses plot as metamorphic, whether recrystllized or not. Values for alkalis are all less than 0.6 and values for tetrahedral aluminium are all less than 1.8. This suggests that if a grain has not recrystallized, it has equilibrated with surrounding recrystallized grains to a less alkaline and aluminous composition. The anomalously alkaline data points 7 and 9 from KJ30 can be explained as a result of the sample being more differentiated than others. While other points from KJ30 are also more alkaline than average, all fall clearly within the ranges cited for metamorphic rocks. Another anomalous point is

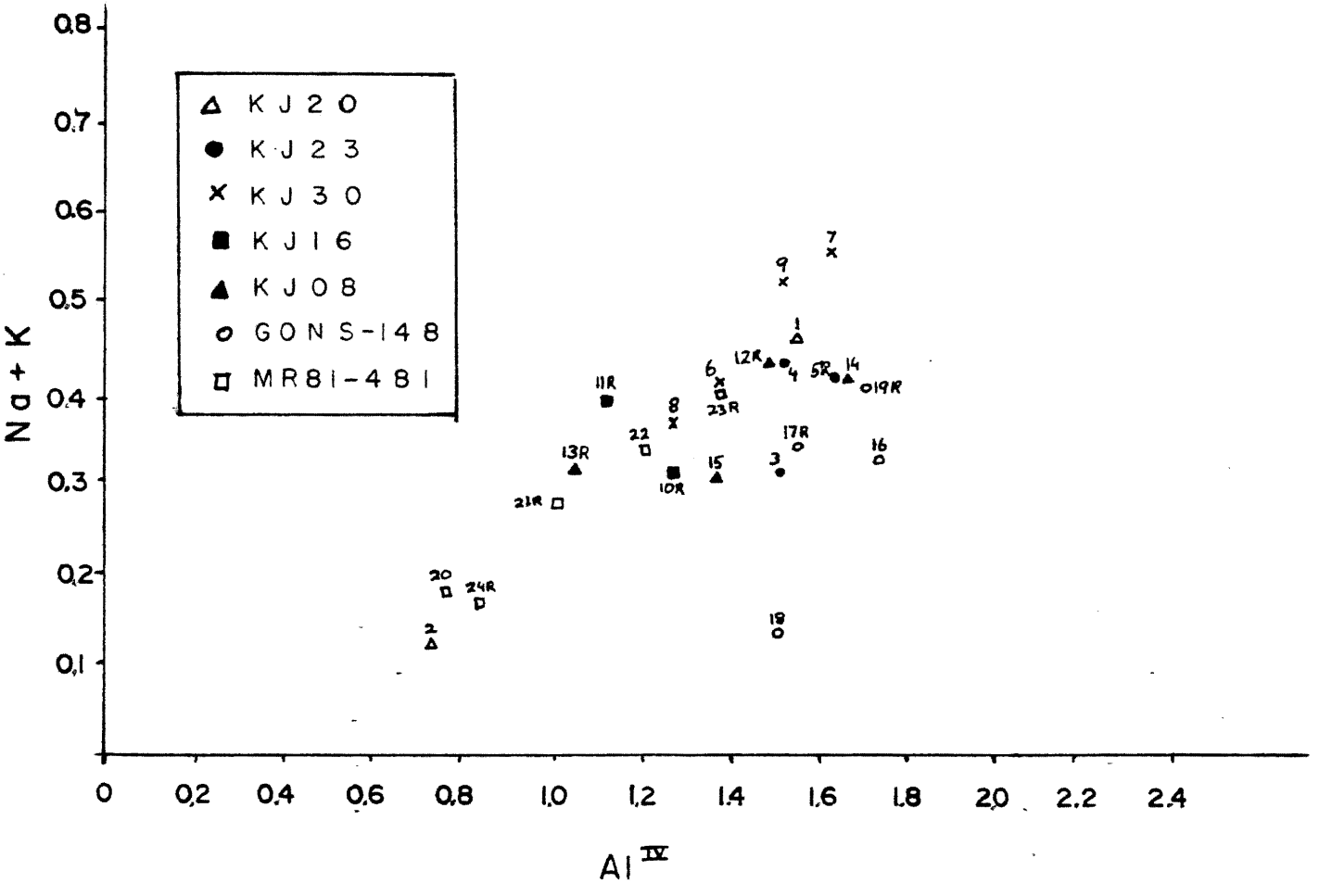

Figure 4.4 Plot of tetrahedral aluminium versus alkalis. Numbers refer to analysis numbers for hornblende (Table 4.3)."R"-recrystallized.

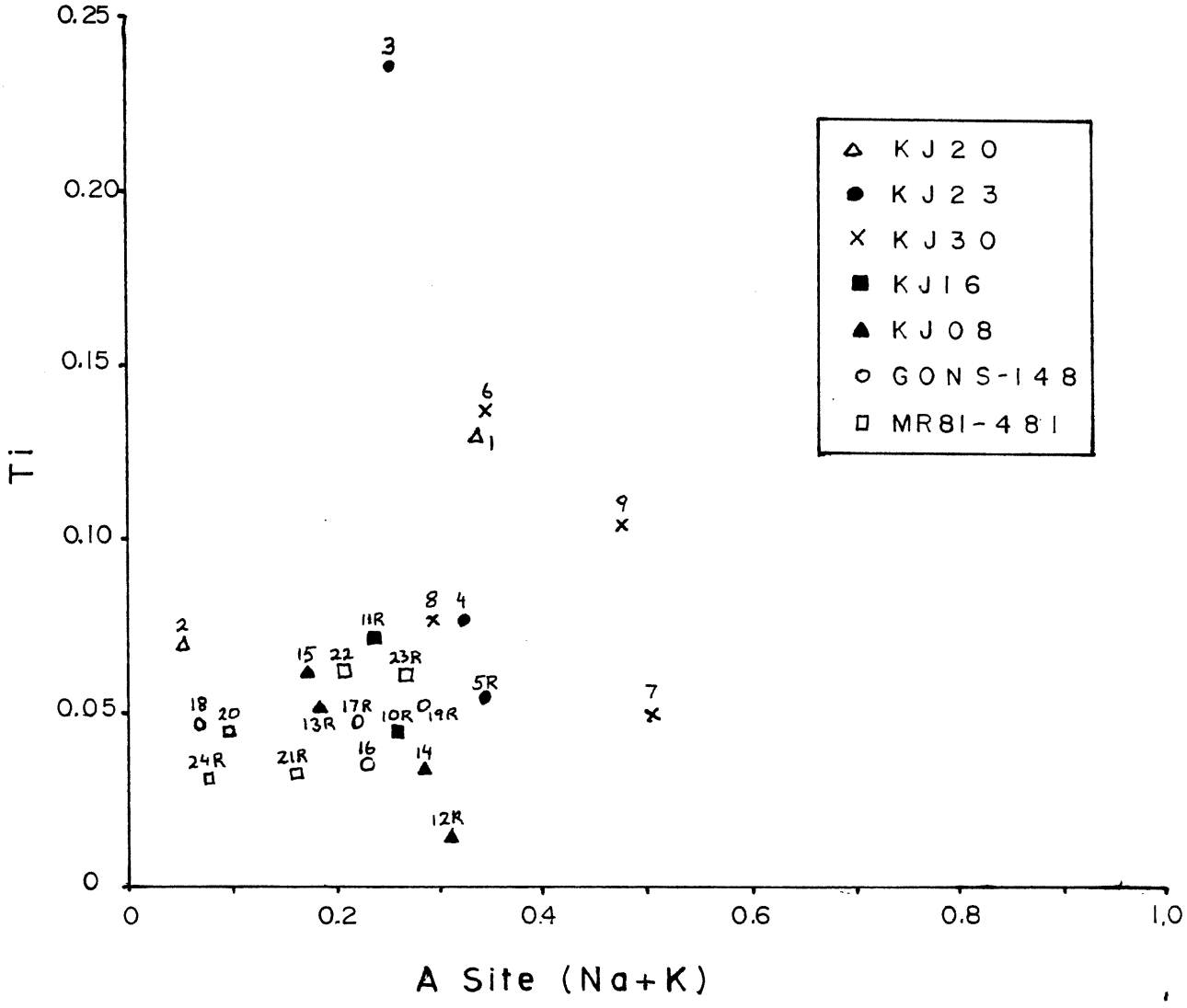

Figure 4.5 Plot of A-site alkalis versus titanium (atoms per unit formula) for hornblende analyses (Table 4.3)."R"-recrystallized.

analysis 18 from GONS-148 which is very low in alkalis while being near average in aluminium content. It is not as easy to explain because other analyses from GONS-148 do not show the same trend. However, the fact that the GONS-148 plagioclase compositions are so low in sodium may indicate possible bulk compositional control for this analysis. Also, hornblende is more altered to biotite in GONS-148 than other polished sections and this may have caused extraction of potassium from hornblende to create the biotite. Analyses 2, 20 and 24R are somewhat anomalous, being low on both axes, but no explanation for these has been postulated, as they are not all from the same sample, and nothing unusual is apparent about the grains from which they came.

Figure 4.5 shows alkalis plotted against titanium. Igneous hornblendes tend to plot greater than 0.25 titanium and 0.7 A-site alkalis, while metamorphic hornblendes plot below those values. Again, all points are plotted in the metamorphic range. Analysis 3 is anomalously high in titanium, near the igneous range, but no unusual grain characteristics are apparent. However, considerable ilmenite exsolution in KJ23 may be a factor, even though other grains from this slide have a lower titanium content (Photo 3.1).

Structural formulae are constructed from microprobe data and Table 4.4 contains individual results. The ideal formula is:

$$A_{0-1}X_2Y_5Z_8O_{22}(OH)_2$$

with A = (Na,K), X = (Ca,Fe^{+2},Mn,Na), Y = (Mg,Fe^{+2},Al,Fe^{+3},Ti), Z = (Si+Al). The formulae all fall within the ranges expressed by:

$$(Na_{.051-.312}K_{.000-.247})(Ca_{1.634-1.929}Fe^{+2}_{.000-.235}Mn_{.005-.051}Na_{.037-.143})(Mg_{2.077-3.416}Fe^{+2}_{.852-1.814}Al_{.274-.985}Fe^{+3}_{.156-.661}Ti_{.015-.238})(Si_{6.272-7.242}Al_{.758-1.728})O_{22}(OH)_2.$$

TABLE 4.4

HORNBLENDE STRUCTURAL FORMULAS

1. KJ23-AMPH1/2 $(Na_{.312}K_{.041})(Ca_{1.819}Fe^{+2}_{.064}Mn_{.020}Na_{.097})(Mg_{2.671}Fe^{+2}_{1.214}Al_{.493}Fe^{+3}_{.489}Ti_{.134})(Si_{6.496}Al_{1.504})O_{22}(OH)_2$

2. KJ23-AMPH3 $(Na_{.060})(Ca_{1.858}Fe^{+2}_{.069}Mn_{.014}Na_{.059})(Mg_{3.360}Fe^{+2}_{.953}Al_{.279}Fe^{+3}_{.337}Ti_{.071})(Si_{7.242}Al_{.758})O_{22}(OH)_2$

3. KJ23-AMPH1 $(Na_{.155}K_{.079})(Ca_{1.855}Fe^{+2}_{.041}Mn_{.026}Na_{.077})(Mg_{2.281}Fe^{+2}_{1.601}Al_{.451}Fe^{+3}_{.429}Ti_{.238})(Si_{6.487}Al_{1.513})O_{22}(OH)_2$

4. KJ23-AMPH2/3 $(Na_{.225}K_{.121})(Ca_{1.855}Fe^{+2}_{.044}Mn_{.023}Na_{.077})(Mg_{2.344}Fe^{+2}_{1.480}Al_{.533}Fe^{+3}_{.576}Ti_{.077})(Si_{6.468}Al_{1.532})O_{22}(OH)_2$

5. KJ23-AMPH4R/5R $(Na_{.265}K_{.092})(Ca_{1.886}Fe^{+2}_{.029}Mn_{.024}Na_{.061})(Mg_{2.182}Fe^{+2}_{1.538}Al_{.625}Fe^{+3}_{.601}Ti_{.054})(Si_{6.369}Al_{1.631})O_{22}(OH)_2$

6. KJ30-AMPH1/2/3 $(Na_{.178}K_{.181})(Ca_{1.901}Mn_{.045}Na_{.054})(Mg_{2.331}Fe^{+2}_{1.731}Al_{.315}Fe^{+3}_{.484}Ti_{.138})(Si_{6.620}Al_{1.380})O_{22}(OH)_2$

7. KJ30-AMPH4 $(Na_{.271}K_{.247})(Ca_{1.929}Mn_{.034}Na_{.037})(Mg_{2.087}Fe^{+2}_{1.814}Al_{.419}Fe^{+3}_{.619}Ti_{.050})(Si_{6.383}Al_{1.617})O_{22}(OH)_2$

8. KJ30-AMPH5 $(Na_{.157}K_{.151})(Ca_{1.891}Mn_{.051}Na_{.057})(Mg_{2.442}Fe^{+2}_{1.592}Al_{.298}Fe^{+3}_{.583}Ti_{.077})(Si_{6.715}Al_{1.285})O_{22}(OH)_2$

9. KJ30-AMPH6 $(Na_{.250}K_{.222})(Ca_{1.903}Mn_{.045}Na_{.052})(Mg_{2.214}Fe^{+2}_{1.769}Ap_{.313}Fe^{+3}_{.582}Ti_{.108})(Si_{6.469}Al_{1.531})O_{22}(OH)_2$

10. KJ16-AMPH 1R/2R/3R/4R/6R $(Na_{.178}K_{.081})(Ca_{1.909}Fe^{+2}_{.020}Mn_{.022}Na_{.049})(Mg_{2.673}Fe^{+2}_{1.319}Al_{.558}Fe^{+3}_{.404}Ti_{.046})(Si_{6.735}Al_{1.265})O_{22}(OH)_2$

11. KJ16-AMPH 5R $(Na_{.051}K_{.194})(Ca_{1.793}Fe^{+2}_{.096}Mn_{.018}Na_{.143})(Mg_{2.629}Fe^{+2}_{1.400}Al_{.745}Fe^{+3}_{.156}Ti_{.070})(Si_{6.857}Al_{1.143})O_{22}(OH)_2$

12. KJ08-AMPH 1R/2R $(Na_{.301}K_{.011})(Ca_{1.781}Fe^{+2}_{.097}Mn_{.005}Na_{.118})(Mg_{2.379}Fe^{+2}_{1.329}Al_{.792}Fe^{+3}_{.484}Ti_{.015})(Si_{6.498}Al_{1.502})O_{22}(OH)_2$

13. KJ08-AMPH 3R/4 $(Na_{.153}K_{.029})(Ca_{1.769}Fe^{+2}_{.081}Mn_{.025}Na_{.124})(Mg_{2.932}Fe^{+2}_{1.134}Al_{.392}Fe^{+3}_{.489}Ti_{.053})(Si_{6.955}Al_{1.045})O_{22}(OH)_2$

14. KJ08-AMPH 6 $(Na_{.262}K_{.026})(Ca_{1.754}Fe^{+2}_{.098}Mn_{.016}Na_{.132})(Mg_{2.307}Fe^{+2}_{1.215}Al_{.784}Fe^{+3}_{.661}Ti_{.039})(Si_{6.332}Al_{1.668})O_{22}(OH)_2$

15. KJ08-AMPH 5 $(Na_{.127}K_{.054})(Ca_{1.634}Fe^{+2}_{.235}Mn_{.006}Na_{.125})(Mg_{2.766}Fe^{+2}_{.976}Al_{.542}Fe^{+3}_{.653}Ti_{.062})(Si_{6.624}Al_{1.376})O_{22}(OH)_2$

16. GONS-148-AMPH 1 $(Na_{.206}K_{.033})(Ca_{1.836}Fe^{+2}_{.054}Mn_{.022}Na_{.088})(Mg_{2.077}Fe^{+2}_{1.381}Al_{.895}Fe^{+3}_{.615}Ti_{.033})(Si_{6.272}Al_{1.728})O_{22}(OH)_2$

17. GONS-148-AMPH 2 $(Na_{.192}K_{.035})(Ca_{1.787}Fe^{+2}_{.067}Mn_{.032}Na_{.115})(Mg_{2.319}Fe^{+2}_{1.299}Al_{.725}Fe^{+3}_{.607}Ti_{.050})(Si_{6.455}Al_{1.545})O_{22}(OH)_2$

18. GONS-148-AMPH 3 $(Na_{.052}K_{.022})(Ca_{1.783}Fe^{+2}_{.133}Mn_{.028}Na_{.055})(Mg_{2.332}Fe^{+2}_{1.221}Al_{.770}Fe^{+3}_{.639}Ti_{.038})(Si_{6.496}Al_{k,504})O_{22}(OH)_2$

19. GONS-148-AMPH 4 $(Na_{.226}K_{.069})(Ca_{1.782}Fe^{+2}_{.066}Mn_{.034}Na_{.118})(Mg_{2.142}Fe^{+2}_{1.383}Al_{.798}Fe^{+3}_{.624}Ti_{.054})(Si_{6.294}Al_{1.706})O_{22}(OH)_2$

20. MR81-481-AMPH 1 $(Na_{.089})(Ca_{1.801}Fe^{+2}_{.093}Mn_{.014}Na_{.098})(Mg_{3.416}Fe^{+2}_{.852}Al_{.317}Fe^{+3}_{.377}Ti_{.038})(Si_{7.232}Al_{.768})O_{22}(OH)_2$

21. MR81-481-AMPH 2R/4R/5R $(Na_{.147}K_{.011})(Ca_{1.789}Fe^{+2}_{.091}Mn_{.007}Na_{.175})(Mg_{3.206}Fe^{+2}_{.852}Al_{.446}Fe^{+3}_{.460}Ti_{.036})(Si_{6.979}Al_{1.021})O_{22}(OH)_2$

22. MR81-481-AMPH 3/7/9/10 $(Na_{.193}K_{.025})(Ca_{1.787}Fe^{+2}_{.086}Mn_{.013}Na_{.113})(Mg_{2.961}Fe^{+2}_{1.003}Al_{.532}Fe^{+3}_{.439}Ti_{.064})(Si_{6.795}Al_{1.205})O_{22}(OH)_2$

23. MR81-481-AMPH 6R $(Na_{.253}K_{.024})(Ca_{1.774}Fe^{+2}_{.095}Mn_{.010}Na_{.121})(Mg_{2.813}Fe^{+2}_{1.040}Al_{.616}Fe^{+3}_{.466}Ti_{.065})(Si_{6.632}Al_{1.368})O_{22}(OH)_2$

24. MR81-481-AMPH 8R $(Na_{.081})(Ca_{1.791}Fe^{+2}_{.121}Mn_{.006}Na_{.083})(Mg_{3.318}Fe^{+2}_{.878}Al_{.373}Fe^{+3}_{.398}Ti_{.033})(Si_{7.165}Al_{.835})O_{22}(OH)_2$

Biotite

Only 10 analyses were done for biotite, on two slides, KJ30 and GONS-148. The former has plentiful medium grained biotite (est. 20%) in primary and well developed secondary grains from hornblende (Photo 3.11). Grains are slightly strained and closely associated with large opaques. The latter showed only slivers of retrograde biotite within cleavage planes and on edges of hornblende grains. Most analyses for KJ30 were almost identical, whether considered primary or secondary, and were averaged. Four analyses resulted after averaging. Their complete microprobe analyses appear in Table 4.5 and here an "R" represents "retrograde" rather than "recrystallized".

A comparison between well developed biotite from KJ30 and poorly developed retrograde biotite from GONS-148 reveals a higher magnesium content and lower potassium content in the latter. Since it is poorly developed as an alteration from hornblende, it has a chemical nature closer to that of hornblende than does the well developed biotite. Hornblende is higher in magnesium and lower in potassium than biotite.

The ideal structural formula for biotite is:

$$A_2X_{6-4}Y_{0-2}Z_8O_{20}(OH)_4$$

with A = (K,Na,Ca), X = (Mg,Fe+2,Mn), Y = (Fe+3,Al,Ti), Z = (Si,Al). Individual structural formulae appear in Table 4.5a.

Epidote

Analysis was performed on 15 epidote grains and 10 analyses results are presented here after averaging. Grains analysed are

	1		2		3		4	
SIO2	37.60		37.65		35.27		37.8[illegible]	
TIO2	1.75		2.20		1.22		1.48	
A2O3	16.49		16.53		16.96		16.37	
C2O3	0.00		0.00		0.00		0.00	
F2O3	0.00		0.00		0.00		0.00	
FEO	17.64		15.24		18.05		15.2[illegible]	
MNO	.35		.02		.03		.35	
MGO	12.97		12.20		16.03		14.2[illegible]	
CAO	.05		0.00		.37		.18	
NA2O	.01		0.00		0.00		0.00	
K2O	9.27		9.69		8.22		7.8[illegible]	
H2O	4.02		4.02		3.91		4.07	
SUM	100.35		100.73		99.36		99.2[illegible]	
SI	5.628	*	5.610	*	5.099	*	5.564	*
AL	2.372	8.000	2.390	8.000	2.901	8.000	2.436	8.000
AL	.522	*	.514	*	.523	*	.749	*
TI	.196	*	.247	*	.141	*	.164	*
CR	0.000	*	0.000	*	0.000	*	0.000	*
FE3+	0.000	*	0.000	*	0.000	*	0.000	*
FE	2.197	*	2.674	*	2.333	*	2.670	*
MN	.044	*	.003	*	.004	*	.007	*
MG	2.879	5.637	2.711	5.744	3.682	6.692	3.125	5.919
CA	.008	*	0.000	*	.001	*	.028	*
NA	.003	*	0.000	*	0.000	*	0.000	*
K	1.761	1.771	1.881	1.881	.956	.749	1.437	1.476
H	4.000	4.000	4.000	4.000	4.000	4.000	4.000	4.000
O	24.000	*	24.000	*	24.000	*	24.000	*
	PHLO	56.229		54.354		61.243		62.4[illegible]
	ANN	42.908		45.[illegible]		38.692		37.3[illegible]
	MN	.862		.051		.065		.1[illegible]
	MARG	.420		0.000		0.113		1.[illegible]
	PARA	.163		0.000		0.000		0.[illegible]
	MUSC	99.367		100.000		91.887		98.1[illegible]
	F/M	.776		.840		.833		.801
	F/FM	.436		.436		.3[illegible]		.[illegible]

1 XXXX KJ30-B10 1/2/3/4R/5R 3 XXXX GDNS-1[illegible]-B10 1R/2R
2 XXXX KJ30-B10 6 4 XXXX GDNS-1[illegible]-B10 3R/4R

Table 4.5 Microprobe data for biotite. (R-recrystallized)

TABLE 4.5a

BIOTITE STRUCTURAL FORMULAE

1. KJ30-BIO 1/2/3/4R/5R $(K_{1.761}Na_{.003}Ca_{.008})(Mg_{2.879}Fe_{2.879}Mn_{.044})(Al_{.522}Ti_{.196})(Si_{5.628}Al_{2.372})O_{20}(OH)_4$

2. KJ30-BIO 6 $(K_{1.881})(Mg_{2.711}Fe_{2.274}Mn_{.003})(Al_{.514}Ti_{.247})(Si_{5.610}Al_{2.390})O_{20}(OH)_4$

3. GONS-148-BIO 1R/2R $(K_{.088}Ca_{.061})(Mg_{3.662}Fe_{2.313}Mn_{.004})(Al_{.523}Ti_{.141})(Si_{5.099}Al_{2.901})O_{20}(OH)_4$

4. GONS-148-BIO 3R/4R $(K_{1.467}Ca_{.028})(Mg_{3.125}Fe_{1.870}Mn_{.007})(Al_{.749}Ti_{.164})(Si_{5.564}Al_{2.436})O_{20}(OH)_4$

either well developed products of metamorphism or within veins cutting the fabric. Analyses from two subparallel purely epidote veinlets in KJ23 are marked "V" and "VV" (Photo 3.9).

Full epidote microprobe analyses appear in Table 4.6. In Figure 4.6, aluminium is plotted against ferric iron, the two elements that share the Y-site in the structural formula (see below). There does not seem to be a marked separation of prograde and veinlet epidote compositions, indicating that if there ever was, it has been eliminated through equilibration. Analysis 2 from KJ30 is clearly more iron-rich than others, since more differentiated samples will have bulk compositions with higher iron contents.

The ideal epidote group formula is:

$Ca_2Y_3Si_3O_{12}(OH)$

where Y = (Al, Fe^{+3}, Mn). Individual structural formulae appear in Table 4.7. True epidote has two aluminium and one ferric iron in the Y-site while clinozoisite has three aluminiums. These analyses have a ratio in between the two end numbers, but is close to epidote.

Opaques

Four analyses from four slides were performed on large opaques. The microprobe computer system is not set up to separate ferric and ferrous iron so three of the four analyses, which gave FeO proportions higher than 90% but totals less than 93% cannot be recalculated to give structural formulae. These must have considerable ferric iron then, and are magnetites ($Fe^{+2}Fe^{+3}{}_2O_4$).

	1	2	3	4	5	6	7	8	9	10
SiO	37.72	37.67	37.99	38.07	38.08	38.23	38.36	37.93	38.15	38.06
TiO	-	-	0.14	0.12	0.05	-	-	-	-	-
Al O	24.38	23.66	25.27	25.61	24.23	26.08	24.67	25.02	24.58	25.94
Fe O	11.09	12.34	10.40	9.96	11.37	10.20	11.23	10.20	11.08	10.14
MnO	0.07	0.10	0.06	0.18	-	0.49	0.08	-	-	0.06
CaO	23.40	23.52	23.88	23.20	23.86	22.85	23.90	23.85	23.40	23.72
Sum	96.66	97.29	97.74	97.14	97.59	97.85	98.24	97.01	97.21	97.93
Si	3.018	3.010	3.000	3.014	3.023	3.006	3.021	3.016	3.030	2.994
Ti	-	-	0.009	0.007	0.003	-	-	-	-	-
Al	2.299	2.229	2.353	2.390	2.268	2.417	2.290	2.345	2.301	2.405
Fe	0.669	0.753	0.620	0.595	0.681	0.605	0.667	0.612	0.664	0.602
Mn	0.005	0.007	0.004	0.012	-	0.033	0.005	-	-	0.004
Ca	2.006	2.014	2.020	1.968	2.030	1.925	2.016	2.032	1.991	1.999
O	13.00	13.00	13.00	13.00	13.00	13.00	13.00	13.00	13.00	13.00

1 KJ08-Ep 2/3
2 KJ30-Ep 1/2/3/4/5
3 KJ23-Ep 1V
4 KJ23-Ep 2V
5 KJ23-Ep 3VV
6 KJ23-Ep 4VV
7 KJ23-Ep 5
8 KJ23-Ep 6
9 KJ23-Ep 7
10 KJ23-Ep 8

Table 4.6 Microprobe data for epidote (10 Analyses).

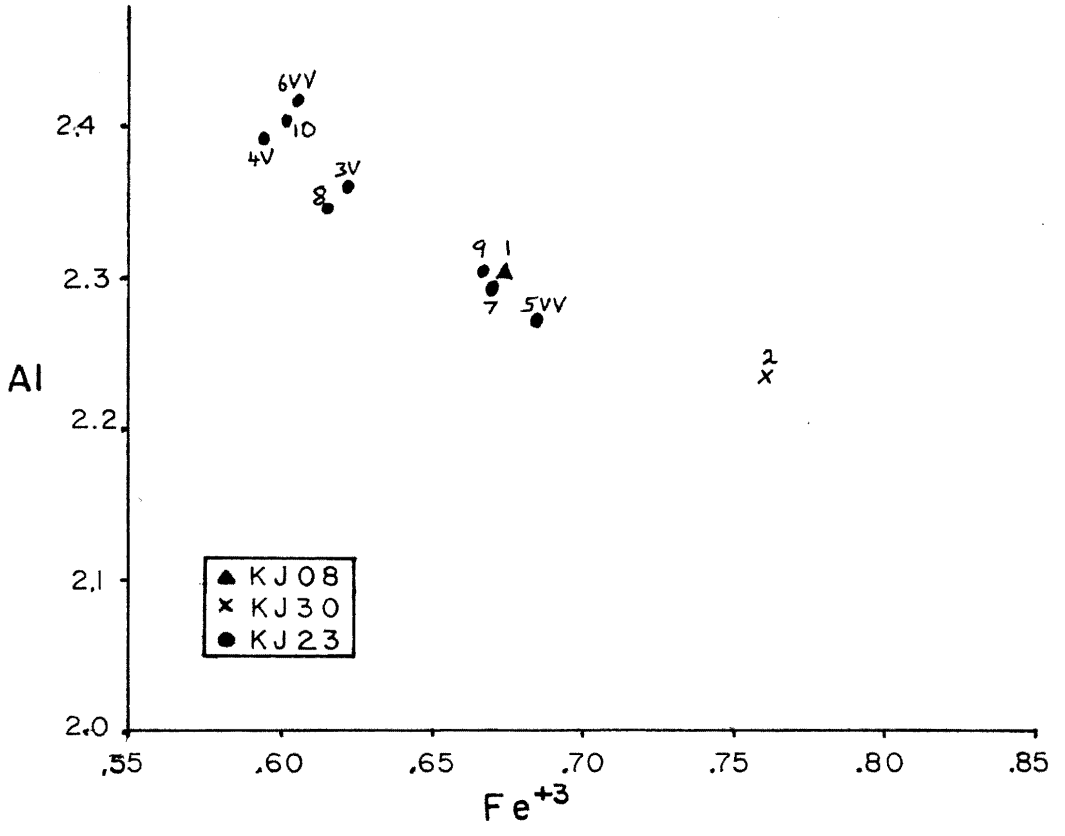

Figure 4.6 Plot of ferric iron versus aluminium (atoms per unit formula) for epidote analyses (Table 4.6). "V"-first vein, "VV"-second vein.

TABLE 4.7

EPIDOTE STRUCTURAL FORMULAE

1.	KJ08-EP2/3	$Ca_{2.006}(Al_{2.299}Fe_{0.669}Mn_{0.005})Si_{3.018}O_{12}(OH)$
2.	KJ30-EP 1/2/3/4/5	$Ca_{2.014}(Al_{2.229}Fe_{0.753}Mn_{0.007})Si_{3.010}O_{12}(OH)$
3.	KJ23-EP 1V	$Ca_{2.030}(Al_{2.353}Fe_{0.620}Mn_{0.004}Ti_{o.009})Si_{3.000})_{12}(OH)$
4.	KJ23-EP 2V	$Ca_{1.968}(Al_{2.390}Fe_{0.595}Mn_{0.012}Ti_{0.007})Si_{3.014}O_{12}(OH)$
5.	KJ23-EP 3VV	$Ca_{2.030}(Al_{2.268}Fe_{0.681}Ti_{0.003})Si_{3.023}O_{12}(OH)$
6.	KJ23-EP 4VV	$Ca_{1.925}(Al_{2.417}Fe_{0.605}Mn_{0.033})Si_{3.006}O_{12}(OH)$
7.	KJ23-EP 5	$Ca_{2.016}(Al_{2.290}Fe_{0.667}Mn_{.005})Si_{3.021}O_{12}(OH)$
8.	KJ23-EP 6	$Ca_{2.032}(Al_{2.345}Fe_{0.612})Si_{3.016}O_{12}(OH)$
9.	KJ23-EP 7	$Ca_{3.030}(Al_{2.301}Fe_{0.664})Si_{3.030}O_{12}(OH)$
10.	KJ23-EP 8	$Ca_{1.999}(Al_{2.405}Fe_{0.602}Mn_{0.004})Si_{2.994}O_{12}(OH)$

The analysis from KJ08 showed the opaque to be ilmenite and the analysis and structural formula appear in Table 4.8. The few number of analyses done here disallows any conclusions as to all opaques in the diorites or even any one sample, but it is clear that at least two different opaques are present.

Comparison with Other Data

Microprobe analyses previously acquired by Jamieson (1983) were made available for comparison. Sample BLD-Z, from the Baddeck Lakes Diorite, was analysed for plagioclase, hornblende and biotite.

Three zoned, unrecrystallized, plagioclase grains were analysed three to seven times in progression from core to rim. In all cases, zoning went from calcic andesine to more sodic andesine or to oligoclase. The whole compositional range is from An_{44} to An_{18}. This zoning appears to be igneous with no sign of metamorphic overprint zoning. The compositional range is more sodic than for the thesis plagioclase analyses, which is a sign for a higher degree of differentiation, as determined in the petrography chapter.

Primary hornblende analyses for BLD-Z were averaged and results plot in the magnesio/hornblende range of the chart in Figure 4.3. However, the Mg/(Mg+Fe) ratios are not as low as those for the differentiated KJ30 as we might expect. On the graphs in Figures 4.4 and 4.5, the BLD-Z hornblendes plot in locations heavily populated by thesis analyses indicating that the former are also chemicially metamorphic rather than igneous. Also, formula values of BLD-Z hornblende elements fall comfortably within compositional ranges cited

TiO	52.22
FeO	43.44
MnO	5.05
MgO	0.11
Sum	100.82
Ti	0.993
Fe	0.919
Mn	0.088
Mg	0.004
O	3.000

Table 4.8 Microprobe data for ilmenite.

$$(Fe_{.919}\ Mn_{.088}\ Mg_{.004})Ti_{.993}O_3$$

for thesis hornblendes. Overall, these hornblendes are very compatible with thesis ones described earlier in this chapter.

A relict biotite grain was analysed for BLD-Z and values for all elements are very close to those of the primary biotite of KJ30. The presence of primary biotite and their high iron values relative to magnesium and high potassium counts, supports the notion that BLD-Z is a highly differentiated form of diorite (tonalite) much like KJ30.

Two other samples have available microprobe analyses and they are worth mentioning because they have been used for geochronology, which will be discussed in the next chapter. MR82-585 and MR82-590 are both located approximately eight kilometers north of the study area.

MR82-585 is a hornblendite and was analysed only for hornblende. Analyses plot in positions compatible with thesis hornblendes in all of Figures 4.3, 4.4 and 4.5. In fact, all elemental proportions are comparable to thesis values and, chemically, there is no reason to suggest that, based on hornblendes, MR82-585 is unrelated to the diorites further south in the study area.

MR82-590 is more granodioritic in appearance and was analysed for plagioclase and biotite. Plagioclase compositions ranged from An_{27} to An_{41} with most being recrystallized grains. One indication of apparent igneous zoning was noticed. The rather sodic overall compositions suggests a more differentiated version than most thesis diorites, but evidence is scanty. However, biotite is recrystallized and exhibits a high iron content relative to magnesium, further supporting this notion.

CHAPTER 5

GEOCHRONOLOGY

Introduction

As a further contribution, the $^{40}Ar/^{39}Ar$ dating technique was performed on prepared biotite and hornblende separates from three samples. For time reasons, samples used were from those previously collected by Jamieson (1979-1983), and were separated in the summer of 1983. MR82-585 and MR82-590 are from a location approximately eight kilometers north of the study area. The former is a hornblendite and the latter is a highly differentiated diorite. MR81-442 is a tonalite from about 3.5 kilometers south of the thesis area, near the Baddeck Lakes region. Samples were chosen mainly on the basis of the amount of clean, unaltered, biotite and/or hornblende.

Separation involved crushing of samples and seiving to the 80 to 120 mesh size, which resulted in mostly monomineralic grains. Magnetite was eliminated carefully by hand magnet and the remainder was passed through the magnetic separater. The voltage was adjusted experimentally until only hornblende and biotite were separated. Biotite was separated by pouring the mixture over a sheet of paper. The flat surfaces of the phyllosilicate biotite stuck to the paper while hornblende rolled off. This was repeated until inspection under binocular microsope revealed that separation was nearly complete. Purities and masses of separates of each sample are listed in Table 5.1.

Sample	Purities		Masses	
	Hbld	Biot	Hbld	Biot
MR81-442	100%	100%	516mg	506mg
MR82-585	98%	-	514mg	-
MR82-590	-	100%	-	105mg

Table 5.1 Purities and masses of mineral separates

Brief petrographic descriptions of hornblende and biotite in the three thin sections, relating to metamorphism, are necessary in order to interpret the obtained results. MR81-442 contains 40% very poikilitic hornblende, 15% recrystallized to non-oriented aggregates. Primary hornblende is partially gone to retrograde biotite but the majority of biotite (10% of slide) is primary-looking, some possibly gone to hornblende by prograde reactions. Biotite occurs mainly in non-oriented aggregates of elongate grains. There is some evidence of recrystallization or well developed sub-grain development (Photo 5.1).

MR82-585 is 94% very coarse hornblende. Grains are very clean but strained and 20% recrystallized, mainly along grain boundaries, to polygonal aggregates exhibiting no preferred orientation. Hematite stained fractures cut the grains throughout (Photo 5.2).

Biotite in MR82-590 is much like that in the differentiated KJ30, occurring as non-oriented elongate grains in clumps or aggregates. Grains are unstrained and well developed, appearing, for the most part, primary. However, some appear retrograde (poorly developed) but without the presence of hornblende anywhere in the slide. Biotite is relatively clean with only very minor chlorite alteration (Photo 5.3).

Where plagioclase exists in these slides, it is mostly primary, showing well developed twinning and zoning. Only MR81-442 has what appears to be recrystallized plagioclase, but only at less than 10%. Well developed retrograde metamorphic epidote occurs in all three samples.

After the separation of hornblende and biotite was completed, separates were sent to McMaster University for irradiation. This is done in a small ractor to produce the artificial isotope ^{39}K which decays to ^{39}Ar, which is measured for the dating calculations. A period of cooling is necessary to allow sufficient decay of ^{39}K to take place.

Background

Argons exists in nature as three isotopes. The most abundant is ^{40}Ar (99.600%) followed by ^{36}Ar (0.337%) and by ^{38}Ar (0.063%). These percentages are considered constant over most of recent geologic time. Radiogenic argon (^{40}Ar) is produced from potassium (^{40}K) by a process of electron capture, usually accompanied by gamma ray emission. The captured electron combines with a proton to form a neutron, reducing the atomic number by one, while maintining the mass number. Over 11% of ^{40}K decay occurs by this process; the remainder is decay to ^{40}Ca by beta emission.

Decay of potassium to argon is continuous, so, assuming potassium bearing minerals are presnt in a rock, once argon is rendered unable to escape (called blocking), the amount will build up over time. Therefore, the blocking age of the rock can be determined using the decay equation once the amount of radiogenic argon is known. However, not all of the argon in any rock will be radiogenic. Atmospheric ^{40}Ar proportions must be removed from the total ^{40}Ar value. This is done by measuring ^{36}Ar present, which is solely

atmospheric, and using the natural $^{40}Ar/^{36}Ar$ ratio to determine the atmospheric ^{40}Ar present.

The age calculated is actually the age since radiogenic argon began to build up in the rock. At this time, the radiogenic "clock" is set. Crystallization from molten rock is not sufficient to set the clock, as argon will still escape at very high temperatures. As the rock cools, it reaches the blocking temperature when argon is trapped in the crystal lattices of potassium bearing minerals, and this is the time calculated by this method. The duration between crystallization and blocking may be on the order of several days or several million years. Also, there may be a considerable time period between when a small proportion of argon is trapped and when all of the argon is trapped. The setting of the clock is by no means instantaneous.

At any time, the radiogenic clock can be reset. A metamorphic event accompanied by heating can raise the temperature above the blocking value allowing all or some of the argon to escape. Deep burial can also raise the temperature high enough for argon loss. Partial argon loss can further complicate the situation since the age will reflect neither the time of original igneous cooling nor the time of metamorphism.

Naturally, it is desirable to use minerals that are capable of retaining argon in their lattices at higher temperatures as well as ones that have high potassium proportions, for dating purposes. Different minerals will retain argon at different temperatures. Hornblende is the most resistant to argon loss with a retention or blocking temperature of $500 \pm 25^{o}C$ (Harrison and McDougall, 1980, and

others). It also is a common mineral in many rocks but contains rarely more than 1% K_2O. Biotite is also common, contains as much as 8% K_2O but has a retention temperature of 300±25°C. A combination of hornblende and biotite calculated ages might provide a good base for interpretation.

Procedure

Irradiation of the separates creates the artificial isotope ^{39}K from ^{40}K which decays to ^{39}Ar. Therefore, the amount of ^{39}Ar in a sample is proportional to the amount of original ^{40}K.

Argon is released from the irradiated sample by a method of step-wise heating and the amount of each isotope of argon is measured after each step.. A hornblende or biotite sample is placed in a lead cased furnace and heated to 200°C. The first step where argon is measured is after heating for an hour from 200°C to 650°C. The gas exsolved is collected in a cold trap (section of tube cooled by liquid nitrogen) and then allowed to diffuse into a line of pyrex glass tubing, and isolated by closing valves. At this point, it is cleaned of CO_2 and other reactive impurity gases by exposing it to a titanium furnace heated to 800°C. The remaining gas is nearly pure argon; though minor amounts of other inert gases may exist. The argon is then admitted to a mass spectrometer by opening a valve and allowed to diffuse to create an equilibrium. The amount of gas in the mass spectrometer will then be a known proportion of the total gas in the system. The mass spectrometer does analysis of the gas for proportions of ^{36}Ar, ^{37}Ar (a minor isotope produced by radiogenic Ca

decay, proportions of which are used to calculate Ca-derived ^{40}Ar proportions to be subtracted), ^{39}Ar and ^{40}Ar.

Proportions and values needed to make determinations are incorporated into the computer program which handles the whole calculation process. Argon isotope values are expressed as ratios of ^{36}Ar and atmospheric ^{40}Ar calculated and removed from total ^{40}Ar to determine radiogenic ^{40}Ar. The age is calculated by computer using the general equation:

$$t = (1/\ ) \ln\left[\frac{^{40}Ar}{^{39}Ar} J+1\right] \qquad = \text{decay constant, radiogenic } ^{40}Ar$$

where "J" is a factor considering the process of neutron flux, creating ^{39}Ar from ^{40}K. An error limit is computed, based on the amount of argon released and the percentage that is atmospheric.

This whole process is repeated, beginning with a heating of the furnace to a higher temperature. After 650°C the temperature steps are about 100°C until 850° or 950° when they are reduced to 50°C. The final step is to 1200°C, where all argon is assumed to be released. This results in ten or eleven steps per sample. An age determination is produced from each step. As step-wise heating procedes, a certain amount of wander may occur which is monitored and corrected, once heating is completed, by linear regression. Standards are then run to calibrate the results and a printout showing the corrected step-wise results and a weighted average is produced. A plot of age (ordinate) versus cumulative gas percentage per step (abscissa) is drawn by the computer. The abscissa is also a measure of increasing temperature steps. Error bars expressing confidence are drawn for each step plateau.

The advantage to stepwise heating is that inference can be given to several episodes of heating which may result in differing amounts of argon loss at different temperature levels. This will result in younger apparent ages. Argon gain, showing an older age, can also be interpreted. Using several minerals could, since they retain argon at different temperatures, theoretically indicate a rate of cooling of the rock body. Interpretation of the results is an important part of Argon-Argon dating.

Results and Interpretation

Numerical step-wise results for each analysed sample, along with the total gas age, a weighted average calculated by computer, are presented in Tables 5.2 to 5.5. An "H" in table headings represents hornblende with a "B" represents biotite. Figures 5.1 to 5.4 show the corresponding plot printouts.

A blue line has been drawn on each plot representing a visual best fit estimate for the age that is being represented. Only intervals that constitute a plateau are considered for this time. Typically, low temperature intervals to the left of plots are lower in radiogenic argon and give young ages. They also have low total argon emissions (signified by short horizontal length of such line segments) and have generally high atmospheric content (Tables 5.2 to 5.3), resulting in high error bars. To aid in line placement, errors have been doubled to 2σ where necessary, giving more confidence in the range (95%, statistically).

TEMP. (°C)	mV Ar39	% Ar39	AGE +/- 1@(MY.)	% ATMOS.	% INT. ISO.
2 0-650	.69	1.22	505.53 +/- 260.41	85.71	.22
6J0-750	.3	.52	14.88 +/- 262.23	98.85	.09
750-850	.4	.7	483.99 +/- 103.95	53.79	.18
850-950	.8	1.4	288.62 +/- 69.31	52.27	.52
9)0-1000	.75	1.31	178.29 +/- 78.59	72.73	.76
1)00-1050	4.75	8.33	415.47 +/- 15.74	58.83	1.04
1050-1100	10	17.54	414.11 +/- 2.64	11.33	.69
1100-1150	13	22.8	419.76 +/- 2.71	4.8	.66
1150-1200	23.8	41.75	421.1 +/- 1.54	22.03	.73
200-1250	2.5	4.38	370.2 +/- 96.58	71.96	.75,

TOTAL GAS AGE = 411.69 MY. +/- 13.26 MY.

Table 5.2 Step-wise results for hornblende from MR82-585.

MJ--442--H SUMMARY

TEMP.(°C)	mV Ar39	% Ar39	AGE +/- 1@(MY.)	% ATMOS.	% INT.ISO.
200-650	1.91	1	356.85 +/- 21.4	72.46	.02
650-750	5.9	3.09	388.82 +/- 13.39	42.87	.01
750-840	3.74	1.95	395.9 +/- 11.48	29.48	.01
840-900	6.89	3.61	399.27 +/- 4.88	28.35	.01
900-950	1.39	.73	365.3 +/- 47.07	32.68	.02
950-1000	1.52	.79	290.99 +/- 11.72	48.08	.03
1000-1050	10.8	5.65	408.97 +/- 3.76	42.77	.22
1050-1100	32.6	17.08	417.84 +/- 2.59	8.3	.34
1100-1150	83.59	43.8	416.36 +/- .73	7.6	.35
1150-1200	39.59	20.75	417.77 +/- 1.71	17.29	.38
1200-1250	2.86	1.49	398.95 +/- 15.44	38.22	.37

TOTAL GAS AGE = 412.44 MY. +/- .86 MY.

Table 5.3 Step-wise results for hornblende from MR81-442.

MR-442-B SUMMARY

TEMP.(°C)	mV Ar39	% Ar39	AGE +/- 1@(MY.)	% ATMOS.	% I	T.ISO.
600-650	20.39	7.34	375.63 +/- 2.04	39.77	0	
650-750	26	9.35	396.91 +/- .83	11.43	0	
750-800	63.2	22.74	403.96 +/- .88	7.67	0	
800-850	6.5	2.33	406.82 +/- 5.61	4.68	0	
850-900	6.89	2.48	408.86 +/- 3.91	4.55	0	
900-950	10	3.59	400.19 +/- 5.24	45.73	.02	
950-1000	27.39	9.82	409.08 +/- 1.97	[illegible]	.1	
1000-1050	19	6.83	402.25 +/- 2.18	4.8	0	
1050-1100	66.99	24.1	405.07 +/- 1.88	3.87	.02	
1100-1150	30.99	11.15	402.82 +/- 1.93	11.93	.01	
1150-1200	.6	.21	846.53 +/- 140.3	76.13	.33	

TOTAL GAS AGE = 402.9 MY. +/- .5σ MY.

Table 5.4 Step-wise results for biotite from MR81-442.

K3-590-B SUMMARY

TMP.(°C)	mV Ar39	% Ar39	AGE +/- 1@(MY.)	% ATMOS.	% INT.ISO.
[illegible]-650	22.59	11.21	412.35 +/- 7.82	10.57	0
0-750	9.89	4.91	427.14 +/- 10.21	7.66	0
[illegible] 850	49	24.3	424.96 +/- 1.58	13.74	0
[illegible]-900	9.19	4.56	409.77 +/- 5.87	17.14	0
[illegible]50	16.19	8.03	421.66 +/- 3.79	12.[illegible]	0
0-1000	11.29	5.6	428.01 +/- 5.7	15.88	0
[illegible]-1050	34.5	17.11	426.42 +/- 1.54	10.37	0
[illegible]-1100	22.3	11.16	421.29 +/- 3.1	9.51	0
0-1150	25	12.4	420.55 +/- 4.32	13.[illegible]	0
[illegible] 1200	1.59	.79	296.12 +/- 87.17	79.7	.03

TAL GAS AGE = 422.29 MY. +/- 1.33 My.

Table 5.5 Step-wise results for biotite from MR82-590.

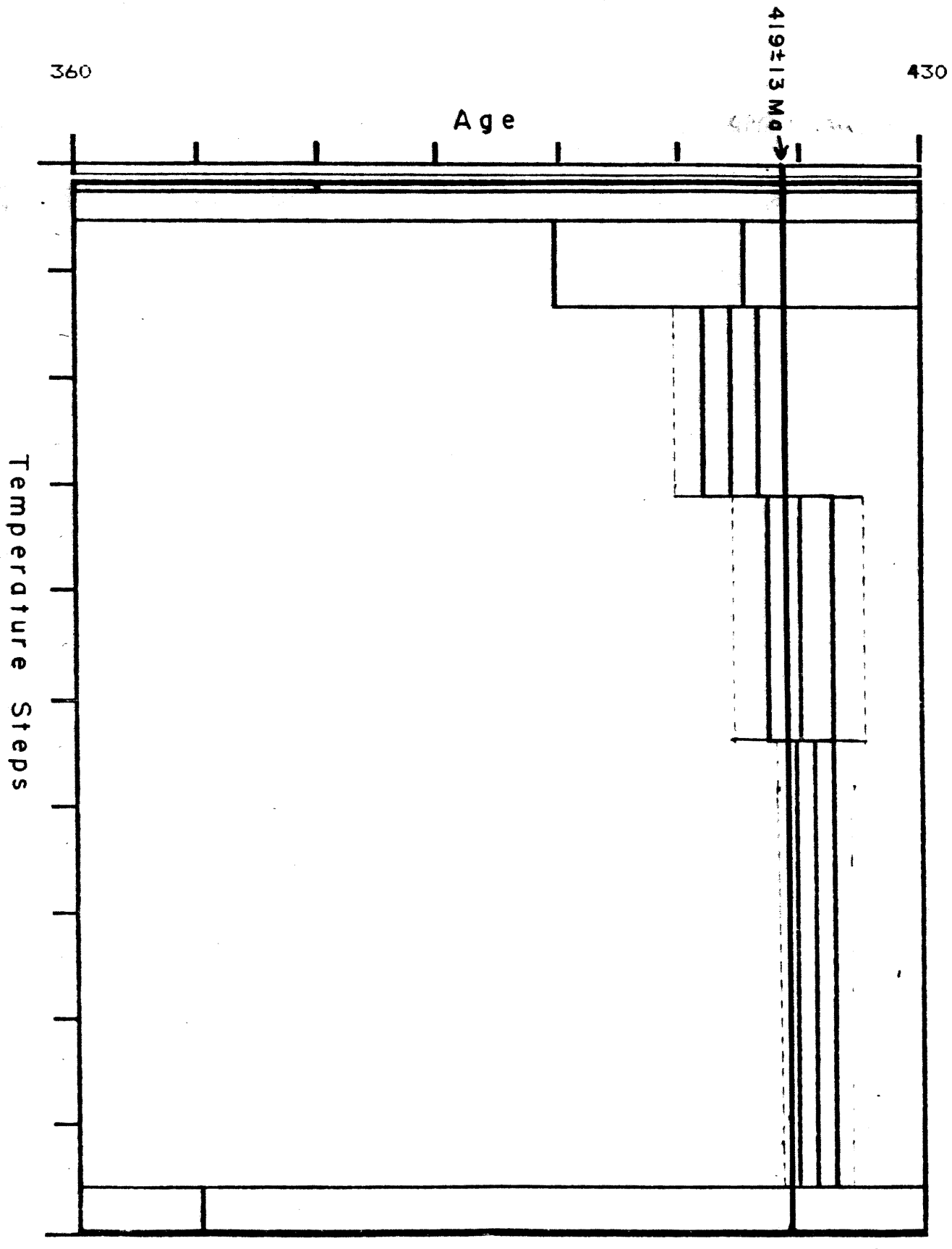

Figure 5.1 Plot of step-wise ages with 1σ (solid) and 2σ (dashed) error bars for hornblende from MR82-585. Blue line indicates an estimated best fit. Data in Table 5.2.

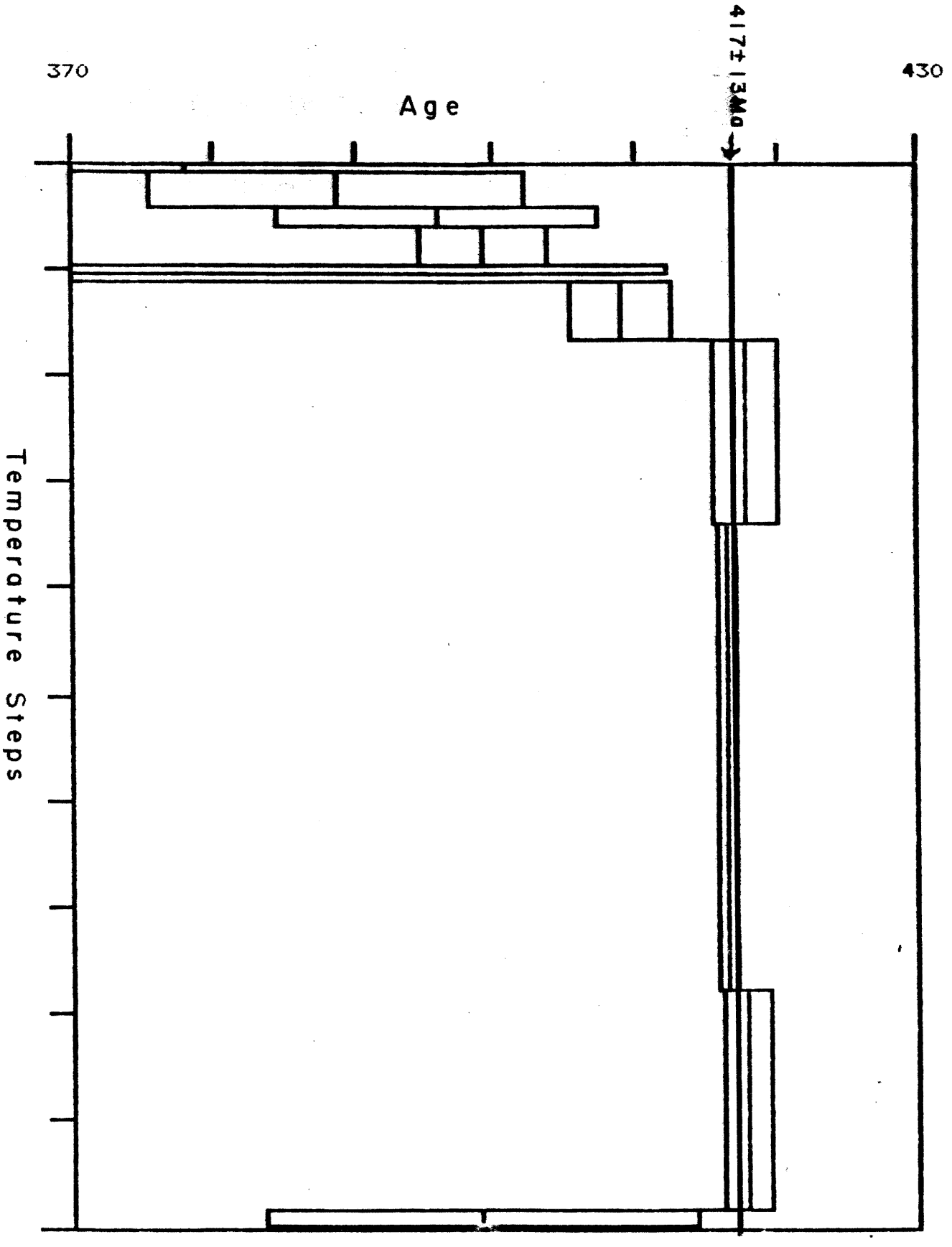

Figure 5.2 Plot of step-wise ages with 1σ error bars for hornblende from [redacted]81-442(Table 5.3). Blue line is best fit.

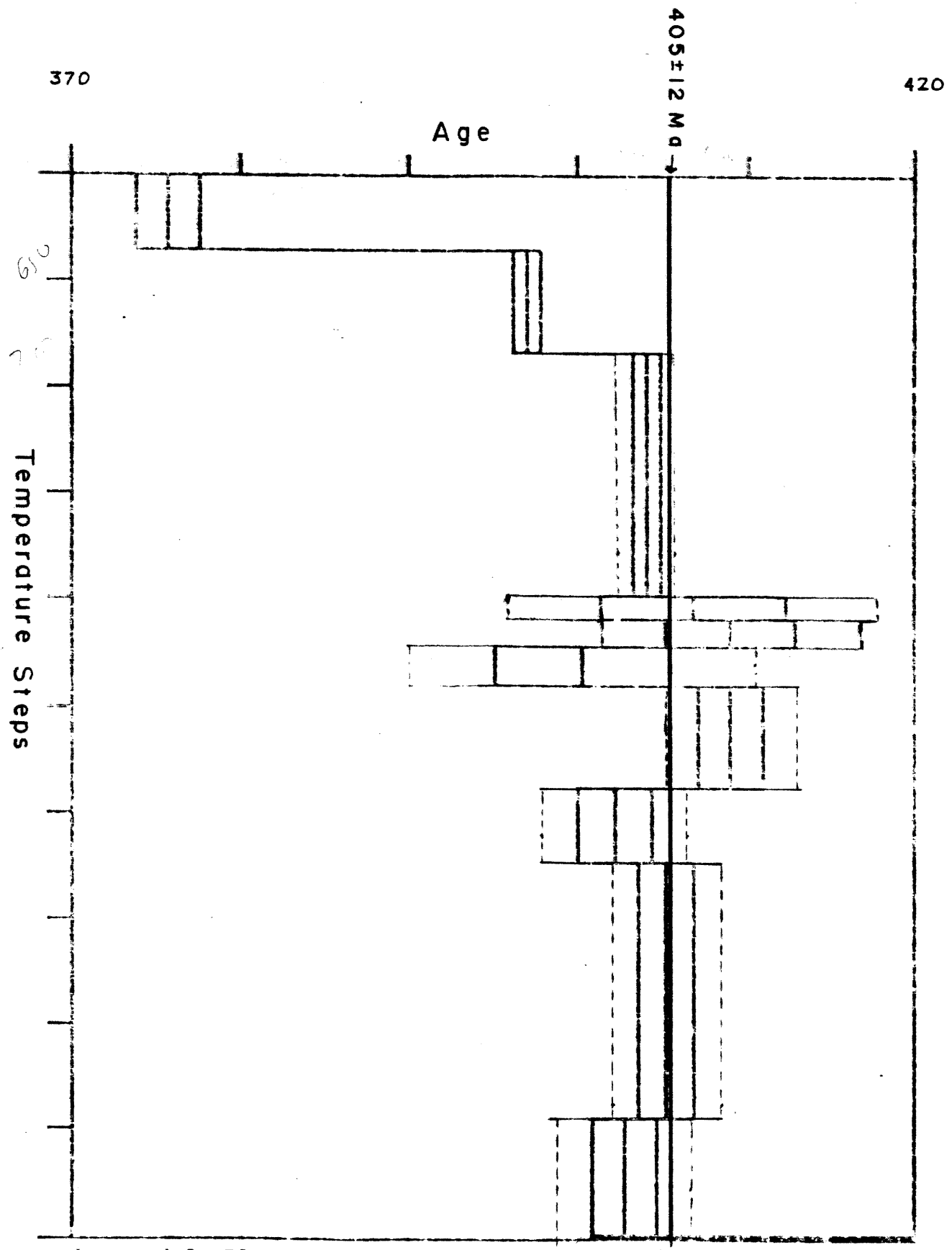

Figure 5.3 Plot of step-wise ages with 1σ (solid) and 2σ (dashed) error bars for biotite from MR81-442 (Table 5.4). Blue line indicates an estimated best fit.

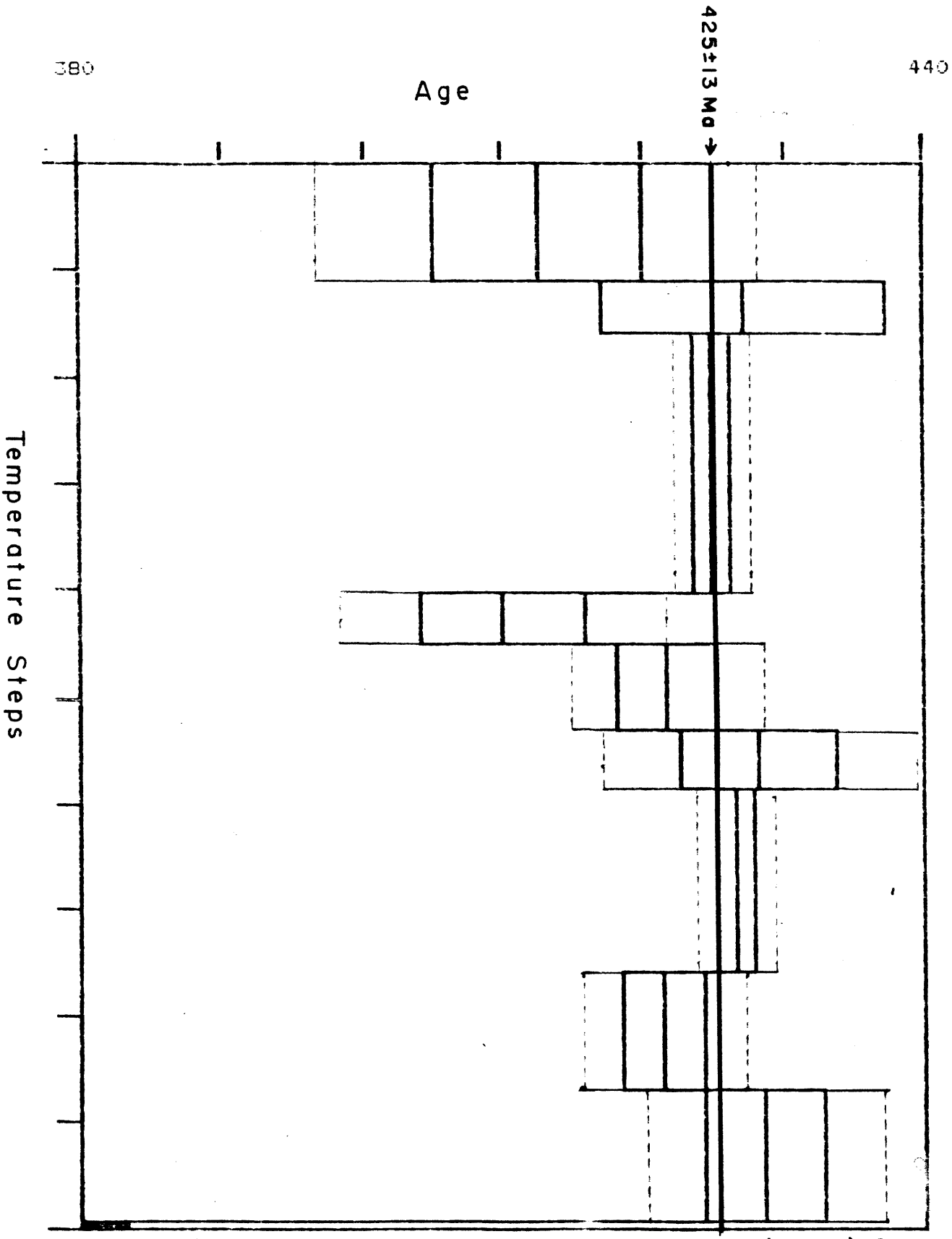

Figure 5.4 Plot of step-wise ages and error bars ($1\sigma, 2\sigma$) for

The ages determined by the best fit lines are indicated and have been quoted with a three percent error range. This is an arbitrary value placed to cover possible between sample error, based on experience with argon dating data (Reynolds, personal communication, 1984).

There is clearly a difference between hornblende and biotite results. Plots of the former show well defined plateaus at 417 million years for MR81-442-H and 419 milion years for MR82-585-H. In both cases, temperature steps from 1050°C to 1200°C make up the plateau. Biotite plots, on the other hand, show more irregularity between steps, and less well defined plateaus. Steps with higher proportions of the total gas content (longer time segments), and lower error bars were given more weight in drawing a best fit line. The difference between plots of the two minerals is due to the fact that hornblende retains argon in its crystal lattice better than biotite and is, therefore, more reliable and less likely to lose gas from minor heating episodes not hot enough to fully reset the clock.

Such a minor episode might be indicated in Figure 5.1 by the step by step increase in apparent ages of the lower heating step from 200°C to 1050°C. A minor episode of heating may have resulted in partial argon loss and as the rock body heats and cools, more of the radiogenic argon that can escape at lower temperatures was released than the argon that can escape at higher temperatures. Therefore, upon laboratory heating, the lower the temperature step, the less radiogenic argon remains as a proportion of the amount that would exist if not for the heating event, and the younger the age

determination. A date for this minor episode, if it occurred, is difficult to predict because of the limits of the plot but indications are that it is near or less than 370 million years ago. The same event may be responsible for the irregular patterns observed in the two biotite plots. Since biotite has a lower blocking temperature, the effect does not show up in a regular step wise pattern.

Taking into account the between sample error and the relative unreliability of biotite values, it seems that ages determined are compatible. It is unlikely that differences in apparent age are real age differences because of the proximity involved. However, the difference between hornblende and biotite ages of MR81-442, although not statistically significant, might be due to the different blocking temperatures of the two minerals suggesting a cooling rate of 200°C in 12 million years, or approximately 17°C per million years. The error involved, however, makes this only conjecture.

The petrography, described earlier in this chapter, revealed that hornblendes from MR82-585 and MR81-442 were partially recrystallized and microprobe data of similar rocks showed that relict hornblende and recrystallized hornblende had equilibrated to metamorphic compositions. Biotite, however, showed no sign of metamorphism in the slides concerned, but other minerals such as plagioclase and epidote did give such indications. It is likely then, that the ages of 405 to 425 million years are cooling ages reset by metamorphism.

Comparison with Other Ages

The ages determined belong to the late Silurian. A comparison with other age data in the Cape Breton highlands reveals that two Acadian dates are quite close (Jamieson, in press). The North River Monzogranite, southwest of the study area, is dated at 401 ± 13 Ma and the Muskrat Brook/Sarach Brook mylonite zone, further south, is dated at 394 ± 28 Ma. These are from Rb-Sr dating which measures reactive cations from the whole rock rather than inert gases from certain minerals. They will be fixed in crystal lattices at higher temperatures thus will tend to give older ages than argon gas. However, the argon-argon dated diorites all gave older ages, and although the error bounds overlap with the Acadian ages, it is unlikely that the metamorphism of the thesis diorite is due to Acadian activity.

Of more likely connection are two Rb-Sr ages of 439 ± 7 and 447 ± 37 for two granitic intrusions twenty kilometers west and slightly north of the diorite and twenty kilometers east and slightly north of the diorite respectively (Figure 1.2). Although not as close spatially as the North River Monzogranite, they have ages, taking into account the dating method differences, that indicate that tectonic events associated with their intrusion, may be responsible for the metamorphic heating and subsequent cooling of the diorites.

In an attempt to explain the possible minor episode of heating, interpreted from Figure 5.1, ages of near 370 Ma were located for the MacMillan Mountain Volcanics (370 ± 20 Ma), volcanics in western Cape Breton (near Cheticamp)(376 ± 12 Ma) and a Carboniferous

megacrystic granite (350 ± 9 Ma)(Figure 1.2). The last of these is relatively close to the study area, only about 15 kilometers in a northwest direction. It is possible that this granite,, or tectonics associated with it or the volcanics mentioned, may be responsible for the possible heating effect.

The Baddeck Lakes Diorites have been dated at 752 ± 26 Ma by Rb-Sr dating (Jamieson, in press). However, this is an igneous age. Since whole rock results are used in Rb-Sr dating, rather than mineral results for Ar-Ar, a metamorphic event must promote diffusion of radiogenic elements on a much larger scale to reset the clock. Therefore, the previous Rb-Sr age cannot be compared with the ages produced here. However, since MR81-442 was taken from an area near the Baddeck Lakes Diorite and is part of the same pluton, its compatibility in age with other samples done here from further north supports the equivalence of diorites from the two regions.

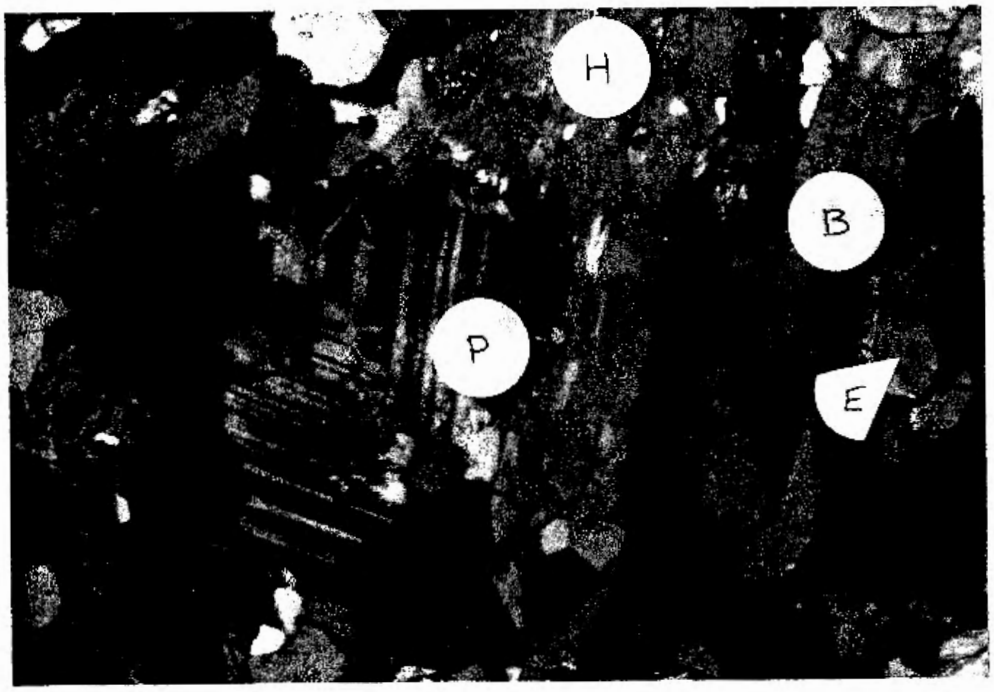

Photo 5.1 Mineralogy and texture of MR81-442 with biotite (B), hornblende (H), plagioclase (P), quartz (Q), and epidote (E).(XN).

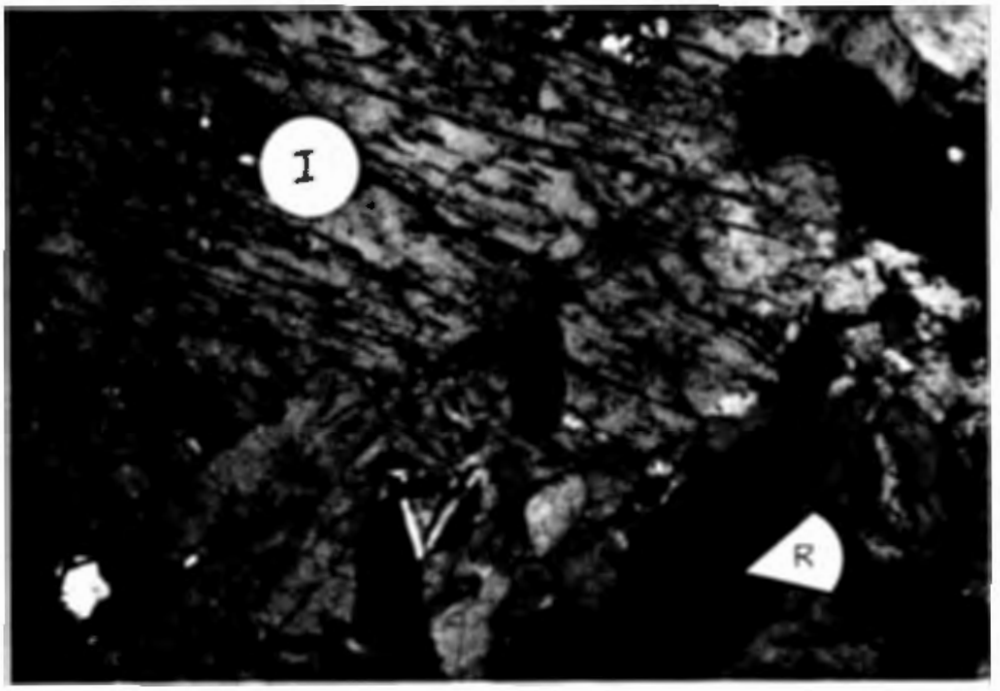

Photo 5.2 Hornblende dominated MR82-585 with igneous (I) and recrystallized (R) grains. (XN).

Photo 5.3 Biotite (B) with epidote (E) in quartz-plagioclase dominated MR82-590. (XN).

CHAPTER 6

CONCLUSIONS

In addition to providing a general description of the geology of the study area, an attempt to draw conclusions answering several specific questions can be made. The nature and relationship of different phases of diorite is more complicated than originally suspected. Field relations and petrography sugest that a fine grained melanocratic diorite intrusion into pre-existing gneiss and quartzite groups was followed by an intrusion of a coarser grained slightly more leucocratic phase of diorite to tonalite. This phase dominated the study area showing considerable variation in modal mineral proportions spatially. Coarse grained, even pegmatitic, dioritic phases (extremely melanocratic or extremely leucocratic) may be related to this intrusion episode or may be later. As intrusion continued, phases became more differentiated. Petrographic and microprobe data confirm the existance of more differentiated phases. One outcrop suggests the subsequent intrusion of diabase into this complex, a phase prominent in tonalites to the south. After an episode of deformation, one or more phases of felsic pegmatite and aplite (unknown relationship) intruded the whole area.

A microscopic and geochemical comparison of these dioritic rocks with mainly tonalites of the Baddeck Lakes region approximately nine kilometers south, showed mineralogical and chemical compatibility allowing for some magmatic differentiation. The Baddeck Lakes tonalites appear to be related to the leucocratic diorites to

tonalites of the study area, but as a more differentiated phase, perhaps equivalent to (or close to) the differentiated phase mentioned previously.

The dioritic rocks of the study area have been metamorphosed, resulting macroscopically in a variable foliation and a shear zone which crosses the area. Both trend slightly west of north. Some mylonitization of diorites has occurred locally in the shear zone. Microscopically, metamorphism is evidenced by replacement of igneous grains and a varying degree of recrystallization. In all cases though, apparently relict igneous grains remain. This is best seen in hornblende. Plagioclase was recrystallized to a lesser degree but microprobe analysis showed zoning in both calcic and sodic directions, even in the same sample. This suggests the presence of both igneous and metamorphic plagioclase. However, plots of element proportions in hornblende, suggest that all grains are chemically metamorphic due to equilibration processes. The presence of metamorphic epidote, and sphene indicate how significant metamorphism is, and with replacement hornblende and plagioclase generally in the andesine range, the diorites to tonalites are considered to be in the lower amphibolite metamorphic facies.

The Argon-Argon geochronologicial techniques for hornblende provided an average age of 418 million years. Determinations for biotite are less reliable and gave ages of both greater and less than this value. Biotite has a lower argon retention temperature and is therefore more easily disturbed. Ignoring the possible disturbance, the difference in hornblende and biotite ages from the same sample

gave a hypothetical cooling rate of 17°C per million years. The age results are interpreted as metamorphic ages because of the degree to which metamorphism has altered the chemistry. Values are too old for Acadian metamorphism to be responsible but granitic plutons located east and west of the study area have compatible ages. Associated tectonism may be responsible for the diorite metamorphism. Plotted argon-argon results indicate that a later episode of heating may have affected the area. Several indications of igneous activity with appropriate ages exist in the southern Highlands and one or more may be, at least partially, responsible.

Several suggestions of further work that would improve knowledge of the region can be proposed. Diabase dykes occur in abundance in the Baddeck Lakes region and further field work to examine their spatial extent is desired. Differentiation in dioritic rocks increases south of the study area and it would be interesting to see how it changes north of the area. Additional geochronological work desired would be Rb-Sr dating of the thesis diorites to compare with the value for the Baddeck Lakes Tonalites and Ar-Ar dating of diorites outside the study are to determine spatial metamorphic influence.

ACKNOWLEDGEMENTS

Thanks are extended to R. MacKay for his assistance with the electron microprobe and in computer manipulation of the data, and to K. Taylor for his operation of the Ar-Ar dating system and his words of explanation. Also appreciated was the help with interpretation of geochronologicial results from Dr. P. Reynolds. Most apprecated was the continuous advice and assistance of Dr. R.A. Jamieson and her guidance during field work.

REFERENCES

Barr, S.M. and Macdonald, A.S., 1982. Geology, petrology, and mineralization of the Cheticamp pluton, northwestern Cape Breton Island, Nova Scotia. GAC-MAC Program with Abstracts, v. 7, p. 38.

Blanchard, M.C., 1982. Geochemistry and petrogenesis of the Fisset Brook Formation, western Cape Breton Island, Nova Scotia. unpublished M.Sc. thesis, Dalhousie University, 225 p.

Cormier, R.F., 1972. Radiometric ages of granitic rocks, Cape Breton Island, Nova Scotia. Can. Journal Earth Sci., v. 9, pp. 1074-1085.

Currie, K.C., Loveridge, W.D. and Sullivan, R.W., 1982. A U-Pb age on zircon from dykes feeding basal rhyolitic flows of the Jumping Brook Complex, northwestern Cape Breton Island, Nova Scotia. Current Research, Part C, Geological Survey of Canada, Paper 82-1C, pp. 125-128.

Donaldson, C.H., 1974. Olivine crystals in harrisitic rocks of the Rhum pluton and Archean spinifex rocks. Geol. Soc. Am. Bull., v. 85, pp. 1721-1726.

Harrison, T.M. and McDougall, I., 1980a. Investigations of an intrusive contact, northwest Nelson, New Zealand: I. Thermal, chronologicial and isotopic constraints. Geochim. Cosmochin. Acta. 44, pp. 1985-2003.

Jamieson, R.A., 1981. The geology of the Crowdis Mountain Volcanics, southern Cape Breton Highlands. Current Research, Part A, Geologicial Survey of Canada, Paper 81-1C, pp. 77-81.

Jamieson, R.A. and Cran, D., 1983. Reconnaissance mapping of the southern Cape Breton Highlands - a preliminary report. Current Research, Part A, Geologicial Survey of Canada, Paper 83-1A, pp. 263-268.

Jamieson, R.A. and Doucet, P., 1983. The Middle River-Crowdis Mountain area, southern Cape Breton Highlands. Current Research, Part A, Geological Survey of Canada, Paper 83-1A, Report 37, pp. 269-275.

Jamieson, R.A., (in press). Timing of Tectonism in the Cape Breton Highlands - New evidence from Rb-Sr geochronology. Can. Journal Earth Sci.

Keppie, J.D. and Smith, P.K., 1978. Compilation of isotopic age data of Nova Scotia. Nova Scotia Department of Mines, Report 78-4.

Keppie, J.D., 1979. Geological map of the province of Nova Scotia. Nova Scotia Department of Mines and Energy.

Leake, B.E., 1978. Nomenclature of Amphiboles. American Mineralogist, v. 63, pp. 1023-1052.

Milligan, G.C., 1970. Geology of the George River Series, Cape Breton. Nova Scotia Department of Mines, Memoir 7, 111 pp.

Olsyewski, W.KJ., Gaudette, M.E., Keppie, J.D. and Donhoe, H.V., 1981. Rb-Sr whole rock age of Kelly's Mountain basement complex, Cape Breton Island. Geologicial Society of America, Abstracts with Programs, v. 13, p. 169.

Wager, L.R. and Brown, G.M., 1968. Layered Igneous Rocks, Oliver and Boyd, Edinburg, 588 pp.

THESIS STUDY AREA

Magnetic North
True North
Grid North

1:25,000
0 1 Km

LEGEND

- Major Logging Rd.
- Side Roads
- Stream
- 500 Contour Line (250m interval)
- Lake or Pond
- Foliation
- Bedding
- Lineation

OUTCROPS

- × Diorite-Tonalite
- + Gneiss
- □ Quartzite
- △ Pegmatite
- ▽ Aplite
- ◇ Volcanic

(Sample numbers indicated where taken, prefix of KJ on numbers 01 to 36)

Kelly Rd.
Kathy Rd.
Miners Rd.
Bateman Brook
N. Kathy Rd.
MR81-480
SHEAR ZONE
MR82-579
MR81-481
GONS-145, 146
GONS-149
GONS-148
GONS-147
SHEAR ZONE
John MacLeods Brook
Middle Branch North River
MR81-482
E. Kathy Rd.
W. Kathy Rd.
SHEAR ZONES
East Branch North River
Mariana Rd.
W. Mariana Rd.
E. Mariana Rd.
Timber Lake Ponds
Bonnie Lake
Timber Lake
Oxford Lakes
Mount McCurdy
Timber Brook
1500
1250
1000
500